

# The Effect of Gravitational Tidal Forces on Renormalized Quantum Fields

---

**Timothy J. Hollowood and Graham M. Shore**

*Department of Physics,  
Swansea University,  
Swansea,  
SA2 8PP, UK.*

*E-mail:* [t.hollowood@swansea.ac.uk](mailto:t.hollowood@swansea.ac.uk), [g.m.shore@swansea.ac.uk](mailto:g.m.shore@swansea.ac.uk)

**ABSTRACT:** The effect of gravitational tidal forces on renormalized quantum fields propagating in curved spacetime is investigated and a generalisation of the optical theorem to curved spacetime is proved. In the case of QED, the interaction of tidal forces with the vacuum polarization cloud of virtual  $e^+e^-$  pairs dressing the renormalized photon has been shown to produce several novel phenomena. In particular, the photon field amplitude can locally increase as well as decrease, corresponding to a negative imaginary part of the refractive index, in apparent violation of unitarity and the optical theorem. Below threshold decays into  $e^+e^-$  pairs may also occur. In this paper, these issues are studied from the point of view of a non-equilibrium initial-value problem, with the field evolution from an initial null surface being calculated for physically distinct initial conditions and for both scalar field theories and QED. It is shown how a generalised version of the optical theorem, valid in curved spacetime, allows a local increase in amplitude while maintaining consistency with unitarity. The picture emerges of the field being dressed and undressed as it propagates through curved spacetime, with the local gravitational tidal forces determining the degree of dressing and hence the amplitude of the renormalized quantum field. These effects are illustrated with many examples, including a description of the undressing of a photon in the vicinity of a black hole singularity.

# 1 Introduction

Investigations of the effect of vacuum polarization on photon propagation in gravitational backgrounds have revealed many unexpected features of far wider importance for quantum field theory in curved spacetime. In particular, the geometry induces a much richer analytic structure for Green functions which, while preserving causality, fundamentally changes the assumptions behind established theorems in S-matrix theory and dispersion relations in flat space quantum field theory [1–5]. A variety of new phenomena associated with the lack of translation invariance also imply that many standard results based around unitarity and the optical theorem must be reassessed in curved spacetime.

In QED, gravitational tidal forces act on the virtual cloud of electron-positron pairs which dress the photon with the result that photons do not simply propagate along classical null geodesics. Rather, the spacetime acts as an optical medium with a non-trivial refractive index  $n(\omega)$  [6–9]. Moreover, as originally found by Drummond and Hathrell [10], the low-frequency phase velocity arising from this effect may be super-luminal, which standard dispersion relations would imply is incompatible with causality.

In a series of papers [1–5], we have developed the theory of photon propagation in QED in curved spacetime and calculated the full frequency dependence of the refractive index in terms of a geometric quantity, the Van Vleck-Morette determinant, which characterises the null geodesic congruence around the classical trajectory. The important role of the Penrose limit [11–13] in identifying the salient features of the background geometry was identified and exploited to develop a rich phenomenology covering photon propagation in a wide class of spacetimes. In particular, it was shown how the curved spacetime geometry induces a novel analytic structure for the Green functions and refractive index which modifies fundamental properties of QFT and S-matrix theory such as hermitian analyticity and the Kramers-Kronig dispersion relation [3]. This improved understanding of analyticity in curved spacetime allows a reconciliation of the apparent paradox between low-frequency super-luminal motion and causality.

While this work resolved the problem of how causality is realised in QFT in curved spacetime, it led to a further apparent paradox, this time with unitarity. It was found that in certain backgrounds, including those associated with black holes, the imaginary part of the refractive index can be negative [3, 4]. This is in marked contrast to a conventional optical medium where  $\text{Im} n(\omega)$  is always positive, corresponding to scattering

of photons from the beam and a reduction in the field amplitude. A negative  $\text{Im } n(\omega)$  would imply gain, with energy pumped in from an external source. In quantum field theory in flat space, the optical theorem relates  $\text{Im } n(\omega)$  to the rate of production of real  $e^+e^-$  pairs and therefore vanishes. Even if we considered an off-shell “photon” which is above the pair production threshold,  $\text{Im } n(\omega)$  would still be manifestly positive. In contrast, in curved spacetime we find examples where  $\text{Im } n(\omega)$  can be negative, or non-vanishing and positive below the  $e^+e^-$  threshold. Clearly, understanding these phenomena and reconciling them with unitarity requires a careful reformulation of the optical theorem in curved spacetime.

For instance, for QED in the weak curvature expansion we find that the refractive index matrix takes the form

$$n_{ij}(u; \omega) = \delta_{ij} - \frac{3\alpha}{180\pi m^2} (13R_{uu}(u)\delta_{ij} - 4R_{iuju}(u)) - \frac{i\alpha\omega}{1260\pi m^4} (25\dot{R}_{uu}(u)\delta_{ij} - 6\dot{R}_{iuju}(u)) + \dots, \quad (1.1)$$

where  $u$  is the affine parameter along the photon ray and  $i, j = 1, 2$  are the two transverse space-like directions along which the polarization vector points.  $R_{iuju}$  are components of the Riemann tensor and  $R_{uu} = R^i{}_{uiu}$ . The first correction in (1.1) is the original Drummond-Hathrell result [10], which can lead to either a sub- or superluminal low-frequency phase velocity. The second term, however, gives a non-vanishing contribution to  $\text{Im } n(\omega)$  and depending on whether the derivatives  $\dot{R}_{iuju}(u)$  are positive or negative along the photon trajectory can lead to an amplification or attenuation of the amplitude.

In this paper, we investigate the realisation of unitarity in photon propagation in curved spacetime from the point-of-view of an initial-value problem. Light-front evolution of renormalized quantum fields from an initial null surface is studied for a variety of field theories and initial conditions and the physical mechanisms responsible for the observed amplification or attenuation of the amplitude are explored. The centrepiece is the formulation of a generalisation of the optical theorem to curved spacetime.

The key point is that in curved spacetime, the fundamental optical theorem relating a decay probability or cross-section and the imaginary part of a Green function must be viewed as a *global* result, integrated along the whole history of the decaying particles. The corresponding *local* identity, which is the standard theorem in flat spacetime, loses the essential positivity needed for the identification with a probability. This vital difference between the local and global identities arises only in curved spacetime because of the lack, in general, of translation invariance along the particle trajectory.

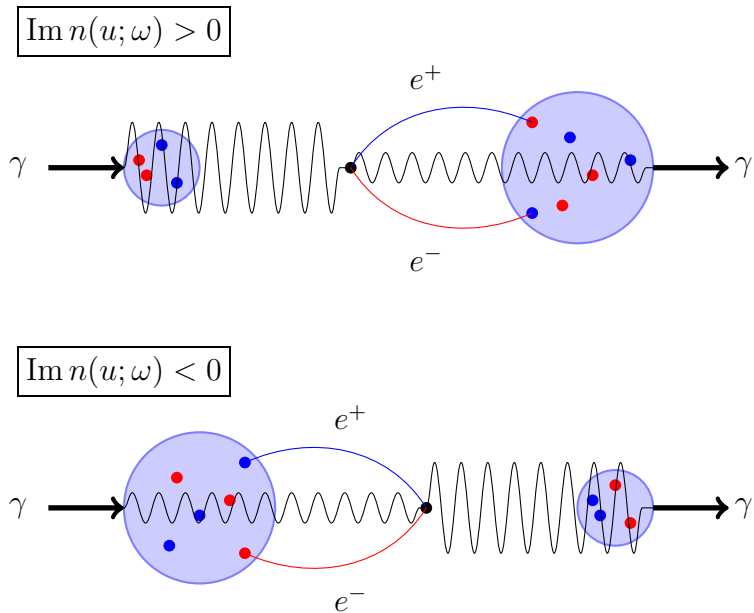


**Figure 1.** Heuristic pictures which illustrate the behaviour of the renormalized photon made up of modes of the bare field (the wave) and virtual cloud of  $e^+e^-$  pairs. In the top diagram there are increasing Riemann tensor components (made precise in (1.1)) along the null coordinate  $u$  of the photon's propagation leading to an increase in virtual  $e^+e^-$  pairs and an attenuation of the photon modes (dressing). In the bottom diagram there are decreasing Riemann tensor components leading to the opposite effect and an amplification of the photon modes (undressing).

As a result, the amplitude of a renormalized quantum field propagating through curved spacetime may be locally amplified, although integrated along its whole past trajectory there must be a net attenuation. This will be interpreted as a real-time dressing and undressing of the field by its cloud of virtual pairs. Locally the curvature can undress the field, resulting a reduced screening and an amplification of the renormalized amplitude. Along its entire trajectory, however, the net dressing must remain positive. A heuristic picture of how dressing or undressing occurs is illustrated in Fig.1.

These ideas are made precise in section 4, where an exact mathematical formulation of the optical theorem in curved spacetime is presented. The general theory is then illustrated with a detailed exploration of the initial value problem and field evolution in a variety of special cases, involving both different quantum field theories and different initial conditions, corresponding to a field in both the bare and dressed state.

The paper is presented as follows. We have already shown in previous work [3, 4] that for massless photon propagation through curved spacetime, the essential features of the curvature are captured by the Penrose plane-wave limit. We therefore restrict ourselves here to the study of quantum field theory in plane-wave backgrounds, although we shall consider both massless and massive theories. We therefore start in section 2 with a brief review of the nature of the Penrose limit and the geometry of plane waves. Section 3 sets up the initial-value problem and describes the different, physically distinct, initial conditions that we will consider. An essential feature is the Schwinger-Keldysh formalism [14–17] formalism for studying real-time, non-equilibrium phenomena in QFT and the relation of the causal field equations to the Feynman vacuum polarization or self-energy is carefully explained. The general solution of the field equations for plane-wave backgrounds is then given and a re-summation technique, the dynamical renormalization group [18], is applied. The interpretation of attenuation and amplification of the amplitude as dressing and undressing of the renormalized field is introduced.

The core of the paper is section 4, where the optical theorem in curved spacetime is presented. The relation of the local and integrated versions of the identity are explained in detail and the issue of unitarity and the positivity of imaginary parts of the Green functions and refractive index is addressed. The realisation of the optical theorem for different classes of initial conditions is also explained.

The remainder of the paper illustrates these ideas for several quantum field theories – massless and massive scalar  $A\phi^2$  theory in both  $d = 4$  and 6 dimensions and QED. This allows us to address some special issues related to renormalization and also to discuss mass thresholds for decaying particles.

First, we study real-time renormalization phenomena in flat spacetime, using a Laplace transform formalism, to develop insights into the initial-value problem and the role of initial conditions. This technique is then applied to QFT in symmetric (i.e. Cahen-Wallach [19]) plane wave spacetimes, which are translation invariant in the light-cone coordinate which serves as the affine parameter along the classical null geodesics. This reveals many interesting phenomena, including in some cases the below-threshold decay of the field  $A$  into  $\phi$  pairs with a rate which is non-perturbative in the curvature. The consistency of all these results with our improved understanding of the optical theorem and the precise nature of the positivity constraint implied by unitarity is checked.

Finally, we consider non-translationally-invariant backgrounds, in particular the

homogeneous plane waves which arise as the Penrose limits of null geodesics in cosmological or black hole spacetimes [4, 12]. In particular, we consider in detail the tidal effects on a renormalized photon field as it approaches a singularity and show explicitly how the photon can become undressed along such a trajectory.

The insights and techniques developed in this paper should also have applications in a wider field. The methods of section 6 have already been used [18] to study real-time relaxation problems in quantum field theory, which are of relevance to inflationary and early-universe cosmology where the non-equilibrium evolution of scalar fields is important (see e.g. [20–22]). Plane waves and Cahen-Wallach spaces are also important as backgrounds in string theory and have an important role in the AdS/CFT correspondence (see e.g. [23–25] and references therein). The study of QFT on plane waves has been pioneered in [26] and some more recent work motivated by string theory appears in [27, 28]. Our work will answer some of the questions regarding the stability of interacting QFT in certain plane wave backgrounds posed in these latter two papers.

## 2 Penrose Limit and QFT on Plane Wave Spacetimes

To begin, we review some essential features of the geometry of plane wave spacetimes and how they arise in connection with photon propagation as Penrose limits. For a complete discussion, see our earlier papers, especially refs.[3, 4]. Some preliminary results on the formulation of QFT on a plane wave background are then described.

### 2.1 Penrose limit and the geometry of plane wave spacetimes

To illustrate how the Penrose limit arises and motivate our specialisation to plane wave spacetimes, consider first an interacting scalar field theory with an  $A\phi^2$  interaction. The  $A$  field (playing the role of the photon in QED) is massless while the  $\phi$  field (the electron) has mass  $m$ . Including the one-loop vacuum polarization, the equation of motion for the  $A$  field in the presence of a source  $J$  is

$$\square A(x) - \int d^4x' \sqrt{g(x')} \Pi(x, x') A(x') = J(x) , \quad (2.1)$$

We will define this precisely in the next section as an initial value problem, using the Schwinger-Keldysh formalism to identify  $\Pi(x, x')$  as the retarded vacuum polarization and  $A(x)$  as the “*in-in*” VEV of the quantum field.

We consider two limits: (i)  $\omega \gg L_{\mathfrak{R}}^{-1}$  and (ii)  $L_{\mathfrak{R}} \gg \lambda_c$ , where  $\omega$  is the frequency of the wave solution for  $A$ ,  $\lambda_c = \frac{1}{m}$  is the Compton wavelength of the “electron”, and  $L_{\mathfrak{R}}$  is a typical curvature scale. The first is the geometric optics condition, which allows the description of the propagation of the free  $A$  field in terms of individual rays (“photon trajectories”) following null geodesics. We then introduce Penrose, or adapted, coordinates  $(u, V, x^a)$ ,  $a = 1, 2$ , in which  $u$  is the affine parameter along the null geodesic,  $V$  is the associated null coordinate, and  $x^a$  are transverse spatial coordinates. The free wave solution is then

$$A(x) = g(x)^{-1/4} e^{i\omega\vartheta(x)} , \quad (2.2)$$

where  $g = -\det g_{\mu\nu}$  and  $k^\mu = \partial^\mu\vartheta(x)$  is the tangent vector to a null congruence  $g(k, k) = 0$ . Along the geodesics  $\vartheta(x) = V$  is constant while the affine parameter  $u$  varies;  $V$  specifies the individual geodesic in the congruence.

In our previous work [1–4], we have shown, using both worldline and conventional QFT methods, how the second limit allows us to simplify the evaluation of the vacuum polarization corrections to (2.2). To leading order in  $\mathfrak{R}/m^2$  (where  $\mathfrak{R} \sim L_{\mathfrak{R}}^{-2}$  is a typical curvature scale), the vacuum polarization is determined by geodesic fluctuations around the photon trajectory; in turn, this is determined entirely by geometric quantities, specifically the Van Vleck-Morette determinant, which describe the geometry of geodesic deviation. But this is precisely the property of the geometry encoded in the Penrose limit, in which the full spacetime metric in a tubular neighbourhood of the chosen null geodesic  $\gamma$  (with  $V = x^a = 0$ ) is approximated by

$$ds^2 = 2du dV + C_{ab}(u) dx^a dx^b . \quad (2.3)$$

Eq.(2.3) describes a gravitational plane wave, in Rosen coordinates. An alternative form, in terms of Brinkmann coordinates, is

$$ds^2 = 2du dv - h_{ij}(u) z^i z^j du^2 + dz^i dz^i , \quad (2.4)$$

where the profile function  $h_{ij}(u) = R^i{}_{uju}(u)$ , the components of the Riemann tensor which occur in the Jacobi equation describing geodesic deviation. An elegant and comprehensive review of the Penrose limit can be found in ref.[12, 13], which explains the scaling by which the plane wave metric (2.4) arises as the leading term in an expansion of the full metric in Fermi null coordinates around  $\gamma$ . The relation with vacuum polarization and photon propagation is described in full detail in our earlier

work, especially ref.[4], which contains a complete review of the geometry and notation used here.<sup>1</sup>

While the relation with geodesic deviation and therefore the motivation for using the Penrose limit is most readily seen in terms of Brinkmann coordinates, the field-theoretic calculations are best expressed using Rosen coordinates. The relation is given in terms of a zweibein  $E^i_a(u)$  for the transverse coordinates in (2.3) and (2.4):

$$C_{ab}(u) = E^i_a(u)\delta_{ij}E^j_b(u) , \quad (2.5)$$

where  $E^i_a$  is obtained by solving the differential equation<sup>2</sup>

$$\ddot{E}_{ia} + h_{ij}E^j_a = 0 . \quad (2.6)$$

These equations are solved subject to the requirement that  $\Omega_{ij} = \dot{E}_{ia}E^j_a$  is symmetric. The coordinates are related by

$$\begin{aligned} z^i &= E^i_a(u)x^a , \\ v &= V + \frac{1}{2}\dot{E}_{ia}(u)E^i_b(u)x^ax^b , \end{aligned} \quad (2.7)$$

with  $u$  common to both sets. The zweibein is not unique and this property is shared by the Rosen coordinates which are specially adapted to describing the null congruence around  $\gamma$ .

The Van Vleck-Morette determinant is defined from the geodesic interval

$$\sigma(x, x') = \frac{1}{2} \int_0^1 d\tau g_{\mu\nu}(x)\dot{x}^\mu\dot{x}^\nu , \quad (2.8)$$

where  $x^\mu = x^\mu(\tau)$  is the geodesic joining  $x = x(0)$  and  $x' = x(1)$  and is given by

$$\Delta(x, x') = -\frac{1}{\sqrt{g(x)g(x')}} \det \frac{\partial^2 \sigma(x, x')}{\partial x^\mu \partial x'^\nu} . \quad (2.9)$$

For a plane wave, with  $g = g(u)$ , the VVM determinant is a function only of the null coordinate  $u$ , that is  $\Delta = \Delta(u, u')$ .

---

<sup>1</sup>Except that here we are following ref.[5] and using  $x^a$  and  $z^i$  for the transverse coordinates in Rosen and Brinkmann respectively, rather than  $Y^a$  and  $y^i$ , and have changed the sign convention for  $V, v$ .

<sup>2</sup>Note that  $i, j, \dots$  indices are raised and lowered using  $\delta_{ij}$  while  $a, b, \dots$  are raised and lowered with  $C_{ab}$ .



It is convenient when describing the mode functions on plane waves later in (2.20) to introduce the  $2 \times 2$  matrix  $\psi^{ab}(u)$  as the indefinite integral

$$\psi^{ab}(u) = \int^u du \left[ C(u)^{-1} \right]^{ab}, \quad (2.10)$$

together with  $\psi^{ab}(u, u') = \psi^{ab}(u) - \psi^{ab}(u')$ . This is related to the VVM determinant by

$$\Delta(u, u') = \frac{1}{\sqrt{g(u)g(u')}} \cdot \frac{(u - u')^2}{\det \psi(u, u')}. \quad (2.11)$$

The geodesic interval for a plane wave spacetime then takes the form [3]

$$\sigma(x, x') = (u - u')(V - V') + \frac{u - u'}{2} \psi(u, u')_{ab}^{-1} (x - x')^a (x - x')^b. \quad (2.12)$$

An equivalent way to construct and interpret the VVM determinant is by thinking of the behaviour of a spray of geodesics which emanate from the point  $(u', v = 0, z^i = 0)$  in Brinkmann coordinates. In the space-like directions the geodesics satisfy

$$\frac{dz^i}{du^2} + h_{ij}(u)z^j = 0. \quad (2.13)$$

If the initial conditions of the spray are chosen as  $z^i(u') = 0$  and  $dz^i(u')/du = \delta_{ij}$  then we write the solution as  $z^i(u) = A_{ij}(u, u')$ . The VVM matrix is then simply

$$\Delta_{ij}(u, u') = (u - u')[A^{-1}(u, u')]_{ji}, \quad (2.14)$$

whose determinant is  $\Delta(u, u')$ .

We will be especially interested later (see section 6) in the special class of symmetric plane waves, or Cahen-Wallach spaces. Here, the profile function  $h_{ij}(u)$  in the Brinkmann metric (2.4) is  $u$ -independent. It is convenient to choose transverse coordinates such that  $h_{ij} = \sigma_i^2 \delta_{ij}$  is diagonal. Then, in Rosen coordinates

$$C_{ab}(u) = \cos^2(\sigma_a u + c_a) \delta_{ab}. \quad (2.15)$$

Notice that  $\sigma_i$  can either be real or purely imaginary and  $c_a$  are constants.<sup>3</sup> The VVM

---

<sup>3</sup>If one wants to impose the null energy condition then at least one of the  $\sigma_i$  is real, say  $\sigma_1$ , and furthermore  $\sigma_1 \geq |\sigma_2|$ . However, since we are taking the background metric to be fixed and non-dynamical there is not really a physical reason to impose this condition. Later we shall look at an example with both  $\sigma_i$  imaginary since it leads to a particularly simple analytic structure. In fact the case with  $\sigma_1 = \sigma_2$  and both imaginary arises as the Penrose limit of the product geometry of three-dimensional de Sitter space with the real line, or circle. This is relevant to a version of the AdS/CFT correspondence [29].

determinant for a symmetric plane wave is

$$\Delta(u, u') = \prod_{i=1}^2 \frac{\sigma_i(u - u')}{\sin(\sigma_i(u - u'))} . \quad (2.16)$$

Symmetric plane waves are one class of homogeneous plane waves. Another is the class of singular homogeneous plane waves, where the profile function is  $h_{ij} = \frac{1}{4u^2}(1 - \alpha_i^2)\delta_{ij}$ . Like the symmetric plane waves, which have the translation symmetry  $u \rightarrow u + c$ , the singular homogeneous plane waves also have an enhanced symmetry, since the metric is invariant under the scaling  $u \rightarrow \lambda u, v \rightarrow \lambda^{-1}v$ . As a result, the VVM determinant  $\Delta(u, u')$  is a function of the single variable  $u'/u$ . Explicitly,

$$\Delta(u, u') = \prod_{i=1}^2 \frac{\alpha_i(u - u')(uu')^{\frac{\alpha_i-1}{2}}}{u^{\alpha_i} - u'^{\alpha_i}} . \quad (2.17)$$

This class of plane waves arises as the Penrose limit of certain spacetimes with singularities, notably black holes and some Robertson-Walker spacetimes, and will be considered in section 7.

## 2.2 QFT on a plane wave spacetime

To study QFT on a background spacetime, we would normally construct an appropriate basis of mode functions describing propagation from an initial Cauchy surface. Plane waves, however, do not admit Cauchy surfaces. Nevertheless, as described in ref.[26], we can still set up an initial value problem in a light-front formalism, choosing the null coordinate  $u$  to play the role of the time coordinate in the conventional case. While the surfaces  $u = \text{constant}$  are not genuine Cauchy surfaces the initial value problem is still well defined when suitable boundary conditions in the transverse directions are specified.

A special feature of plane waves spacetimes is that the solutions of the massive Klein-Gordon equation

$$(\square - m^2)\phi(x) = 0 , \quad (2.18)$$

are WKB exact [26]. We can write a basis for the solutions in Rosen coordinates as

$$\phi(x) = e^{-\frac{im^2u}{2\omega}}\Phi_p(x) , \quad (2.19)$$

in terms of the modes

$$\Phi_p(x) = g(u)^{-1/4} \exp \left[ i\omega V + ip_a x^a - \frac{i}{2\omega} \psi^{ab}(u) p_a p_b \right] , \quad (2.20)$$

where  $\psi^{ab}(u)$  is defined in (2.10). The symmetries of the metric allow the definition of a 3-momentum  $p = (\omega, p_a)$ , where  $\omega$  is a null component and the  $p_a$  are spacelike.<sup>4</sup>

The modes are classified as having positive or negative frequency with respect to evolution in the coordinate  $u$  according to whether  $\omega > 0$  or  $\omega < 0$ , respectively. On the null surfaces of constant  $u$ , there is a Klein-Gordon inner-product

$$(\Phi, \Phi') = -i \int dV d^2x \sqrt{g(u)} \Phi'^* \overleftrightarrow{\partial}_V \Phi , \quad (2.21)$$

with respect to which the modes satisfy the orthonormality property

$$(\Phi_p, \Phi_{p'}) = 2\omega(2\pi)^3 \delta(\omega - \omega') \delta^{(2)}(p_a - p'_a) . \quad (2.22)$$

At this point it is important to recognise, as shown by Gibbons [26], that for plane waves there is no particle creation via the usual curved spacetime Bogoliubov transformation. The reason is that since  $\partial_V$  is a Killing vector, a positive/negative frequency mode  $e^{\pm i\omega V}$  will remain a positive/negative frequency mode. As a consequence the vacuum state at some initial time remains empty of particles at later times. This plays an important role in the next section in simplifying the application of the Schwinger-Keldysh analysis. It also means that the type of particle creation arising through a non-trivial Bogoliubov relation between *in* and *out* vacua cannot be the explanation for the increase in amplitude of the photon field observed in some backgrounds.

The Green functions of (2.18) play an important role in the analysis that follows. As usual, we define the Wightman functions

$$G_+(x, x') = \langle 0 | \phi(x) \phi(x') | 0 \rangle , \quad G_-(x, x') = \langle 0 | \phi(x') \phi(x) | 0 \rangle , \quad (2.23)$$

with mode expansions:

$$G_{\pm} = \pm \frac{1}{(2\pi)^3} \int \frac{d\omega}{2\omega} \theta(\pm\omega) \int d^2p \Phi_p(x) \Phi_p(x')^\dagger e^{-\frac{im^2(u-u')}{2\omega}} . \quad (2.24)$$

---

<sup>4</sup>Notice that in general these modes have singularities at points where the metric is degenerate. For example, for a Cahen-Wallach space these occur when the cosine functions in (2.15) vanish. However, these are only coordinate singularities.

The ‘‘Feynman’’ Green function, adapting the definition to our choice of null coordinates, is then

$$iG_{\text{F}}(x, x') = \langle 0 | T_u \phi(x) \phi(x') | 0 \rangle = \theta(u - u') G_+(x, x') + \theta(u' - u) G_-(x, x') , \quad (2.25)$$

where  $T_u$  denotes  $u$ -ordering. A similar definition holds for the anti  $u$ -ordered Dyson function:

$$iG_{\text{D}}(x, x') = \langle 0 | \bar{T}_u \phi(x) \phi(x') | 0 \rangle = \theta(u' - u) G_+(x, x') = \theta(u - u') G_-(x, x') . \quad (2.26)$$

Retarded and advanced Green functions, with support in the forward and backward lightcones respectively, are also given in terms of the Wightman functions:

$$G_{\text{ret}}(x, x') = -\theta(u - u') G(x, x') , \quad G_{\text{adv}}(x, x') = \theta(u' - u) G(x, x') , \quad (2.27)$$

where the Pauli-Jordan, or Schwinger, function is given by the commutator,

$$iG(x, x') = \langle 0 | [\phi(x), \phi(x')] | 0 \rangle = G_+(x, x') - G_-(x, x') . \quad (2.28)$$

The Green functions can be written in a ‘‘proper-time’’ representation using the expression (2.24) in terms of the mode functions. Performing the Gaussian integral over the transverse momentum  $p^a$  using (2.10) and (2.12), and using the substitution  $T = \frac{u-u'}{2\omega}$  in the integration over  $\omega$ , we find

$$G_+(x, x') = \frac{i^{(1-\frac{d}{2})}}{(4\pi)^{\frac{d}{2}}} \sqrt{\det \Delta(x, x')} \int_0^\infty \frac{dT}{T^{\frac{d}{2}}} e^{\frac{i\sigma(x, x')}{2T}} e^{-im^2 T} , \quad (2.29)$$

for  $u - u' > 0$ . Note that, for future use, we have quoted the result for  $d - 2$  transverse dimensions. Similar results for  $G_+(x, x')$  for  $u - u' < 0$ , and for  $G_-(x, x')$ , follow from the identities  $G_-(x, x') = G_+(x', x) = G_+(x, x')^*$ .

The proper-time representations for all the other Green functions follow straightforwardly. For example,

$$iG_{\text{F}}(x, x') = \frac{i^{(1-\frac{d}{2})}}{(4\pi)^{\frac{d}{2}}} \sqrt{\det \Delta(x, x')} \int_0^\infty \frac{dT}{T^{\frac{d}{2}}} e^{\frac{i\sigma(x, x')}{2T}} e^{-im^2 T} , \quad (2.30)$$

for all  $u - u'$ .

### 3 Light-Front Evolution of Renormalized Quantum Fields

In this section, we set up and study the initial-value problem describing the evolution of a renormalized quantum field in a plane-wave background spacetime, incorporating the effect of vacuum polarization.

#### 3.1 The initial value problem

The techniques for studying real-time non-equilibrium phenomena in quantum field theory were established originally by Schwinger and Keldysh [14–17]. The essential idea is to develop an equation of motion, obtained from a suitably defined 1PI effective action, which describes the time evolution of the “*in-in*” vacuum expectation value  ${}_J\langle 0_{in}|A|0_{in}\rangle_J$  of the quantum field in the presence of a source, which can be used to engineer appropriate initial conditions. In our case, we will consider evolution in the light-cone variable  $u$  from an initial null surface, but the essential formalism is unchanged.

This should be contrasted with the more familiar 1PI effective action derived using the conventional Feynman rules, for which the corresponding equation of motion describes the “*in-out*” VEV  ${}_J\langle 0_{out}|A|0_{in}\rangle_J$ . The distinction is clearly important when the vacua do not coincide, *i.e.*  $|0_{out}\rangle \neq |0_{in}\rangle$ , and there is a non-trivial Bogoliubov transformation between the states and associated particle creation. As already emphasised [26], this is not the case for plane-wave backgrounds, so we expect our analysis to be independent of which formalism we choose. We now verify this explicitly, justifying *a posteriori* the treatment of the refractive index problem in curved spacetime in our earlier work.

The essential features of the Schwinger-Keldysh, or “*in-in*”, or “*closed-time-path*”, formalism are elegantly summarised in refs.[30–32] and we refer to these papers for further details. For simplicity, we describe the formalism first for the QFT of a single scalar field  $\phi$ . The key idea is to let the *in* vacuum evolve independently under two different sources  $J^\pm(x)$ , comparing in the far future, in the *out* region. This defines a generating functional

$$\begin{aligned} Z[J^+, J^-] &= \exp iW[J^+, J^-] \\ &= {}_{J^-}\langle 0_{in}|0_{in}\rangle_{J^+} \equiv \sum_{\psi} {}_{J^-}\langle 0_{in}|\psi_{out}\rangle\langle\psi_{out}|0_{in}\rangle_{J^+} . \end{aligned} \tag{3.1}$$

The “*in-in*” expectation value of the quantum field  $\phi(x)$  in the presence of a physical source  $J(x)$  is then given by the derivative with respect to either source, evaluated with the sources set equal to  $J$ ,

$${}_J\langle 0_{in}|\phi|0_{in}\rangle_J = \pm \frac{\delta W[J^+, J^-]}{\delta J^\pm} \Big|_{J^+=J^-=J}. \quad (3.2)$$

The generating functional has a path integral representation in terms of two field variables  $\phi^\pm(x)$  as follows:

$$Z[J^+, J^-] = \int \mathcal{D}\phi^+ \int \mathcal{D}\phi^- \exp i\left(S[\phi^+] - S[\phi^-] + J^+\phi^+ - J^-\phi^-\right), \quad (3.3)$$

where it is understood that the integrals are over field configurations which coincide on the *out* hypersurface corresponding to  $|\psi_{out}\rangle$ . Evaluating in the free theory gives the expression [30–32]

$$\begin{aligned} Z[J^+, J^-] = \exp & -\frac{i}{2} \int d^4x \sqrt{g} \int d^4x' \sqrt{g'} \left( J^+(x) G_F(x, x') J^+(x') \right. \\ & + i J^+(x) G_-(x, x') J^-(x') + i J^-(x) G_+(x, x') J^+(x') \\ & \left. + J^-(x) G_D(x, x') J^-(x') \right), \end{aligned} \quad (3.4)$$

so different derivatives of  $Z$  with respect to the two sources yield the full set  $G_F$ ,  $G_D$ ,  $G_+$  and  $G_-$  of Green functions.

Expressions (3.3) and (3.4) can then be used in perturbation theory as the basis of an extended diagrammatic expansion, with propagators  $G_{++} = -G_F$ ,  $G_{+-} = iG_-$ ,  $G_{-+} = iG_+$ ,  $G_{--} = -G_D$  linking vertices which are “all +” or “all -”, with opposite signs of the coupling. In turn, this allows the construction of a 1PI effective action  $\Gamma[\phi^+, \phi^-]$  by a Legendre transform in the usual way, written in terms of fields defined by  $\phi^\pm = \pm \frac{\delta W[J^+, J^-]}{\delta J^\pm}$ .

For our problem, we initially consider the equation of motion for a massless scalar field  $A$  interacting via an  $eA\phi^2$  interaction with a scalar field  $\phi$  of mass  $m$  with Green functions described in section 2. It is straightforward to see that the required equation for the *in-in* expectation value  $A(x) = {}_J\langle 0_{in}|A(x)|0_{in}\rangle_J$  is

$$\frac{\delta \Gamma}{\delta A^+(x)} \Big|_{A^+=A^-=A} = -J \quad (3.5)$$

(or similarly with  $A^+$  and  $A^-$  interchanged), where  $\Gamma[A^+, A^-]$  is the one-loop effective action with quadratic part

$$\begin{aligned} \Gamma[A^+, A^-] = & -\frac{1}{2} \int d^4x \sqrt{g} \left( A^+(x) \square A^+(x) - A^-(x) \square A^-(x) \right) \\ & - \frac{ie^2}{4} \int d^4x \sqrt{g} \int d^4x' \sqrt{g'} \left( A^+(x) G_{\text{F}}(x, x')^2 A^+(x') \right. \\ & + A^+(x) G_{-}(x, x')^2 A^-(x') + A^-(x) G_{+}(x, x')^2 A^+(x') \\ & \left. + A^- G_{\text{D}}(x, x')^2 A^-(x') \right) . \end{aligned} \quad (3.6)$$

This gives an equation of the form (2.1), with the vacuum polarization

$$\Pi_{\text{SK}}(x, x') = \frac{ie^2}{2} \left( G_{\text{F}}(x, x')^2 + G_{-}(x, x')^2 \right) . \quad (3.7)$$

From the definitions (2.23), (2.25) above, we now see that

$$\Pi_{\text{SK}}(x, x') = -\frac{ie^2}{2} \theta(u - u') \left( G_{+}(x, x')^2 - G_{-}(x, x')^2 \right) , \quad (3.8)$$

with support only for  $u' < u$ . Moreover, given that the commutator  $[\phi(x), \phi(x')]$  is a  $c$ -number, it follows readily that

$$\Pi_{\text{SK}}(x, x') = -\frac{ie^2}{4} \theta(u - u') \langle 0_{\text{in}} | [\phi(x)^2, \phi(x')^2] | 0_{\text{in}} \rangle . \quad (3.9)$$

Since the commutator vanishes for spacelike separated points, it follows that  $\Pi_{\text{SK}}(x, x')$  vanishes for  $x$  outside the forward light-cone of  $x'$ . This confirms that (2.1), with the vacuum polarization taken as  $\Pi_{\text{SK}}(x, x')$ , is a causal, albeit non-local, equation of motion for the *in-in* VEV  $A(x)$  of the field. In contrast, the usual *in-out* formalism with the Feynman vacuum polarization

$$\Pi_{\text{F}}(x, x') = \frac{ie^2}{2} G_{\text{F}}(x, x')^2 = -\frac{ie^2}{2} \left( \theta(u - u') G_{+}(x, x')^2 + \theta(u' - u) G_{-}(x, x')^2 \right) , \quad (3.10)$$

is not manifestly causal.

Now, for propagation in a plane-wave background, the only non-trivial behaviour is in the  $u$  direction and we can expand the solutions in terms of the basis (2.20) of on-shell modes. Accordingly, for a massless field  $A(x)$ , we take

$$A(x) = \mathcal{A}(u) \Phi_p(x) \quad (3.11)$$

and choose  $\omega > 0$ , so that it is a positive frequency solution. So for the simplest case where the transverse momentum  $p_a = 0$ , we just have (see (3.2))

$$A(x) = \mathcal{A}(u)\Phi_{(\omega,0)}(x) = \mathcal{A}(u)g(u)^{-1/4}e^{i\omega V} . \quad (3.12)$$

Notice that the amplitude factor  $\mathcal{A}(u)$  here is allowed to be complex and the physical solution for  $A(x)$  is the real part of (3.12).

A key result now is that if  $A(x)$  has positive frequency, it follows from the form of (2.24) that

$$\int dV' G_-(x, x')^2 A(x') = 0 , \quad (3.13)$$

for  $\omega > 0$ . This is a manifestation of  $\omega$ -conservation at the vertex, in itself a consequence of the  $\partial_V$  isometry of the plane-wave background. Hence, for solutions of the kind (3.11) we can replace  $\Pi_{\text{SK}}$  in (2.1) by the Feynman vacuum polarization  $\Pi_{\text{F}}$  if we wish, the difference vanishing by virtue of (3.13). This is the technical mechanism by which the isometry of the plane-wave background, which ensures the absence of particle creation and the identity of the *in* and *out* vacua, guarantees we recover the same final results for “photon” propagation and the refractive index whether we use the conventional Feynman or Schwinger-Keldysh formalisms.

If we now exploit the symmetries of the plane-wave background to define the “partial Fourier transform” of the vacuum polarization with respect to the modes (2.20), we can reduce the equation of motion to an effective one-dimensional problem. Defining

$$\begin{aligned} & (2\pi)^3 \delta(\omega - \omega') \delta^{(2)}(p_a - p'_a) \tilde{\Pi}_{\text{SK}}(u, u'; \omega, p_a) \\ &= \int d^3x \sqrt{g} \int d^3x' \sqrt{g'} \Phi_p^*(x) \Pi_{\text{SK}}(x, x') \Phi_{p'}(x') . \end{aligned} \quad (3.14)$$

we can rewrite (2.1) in the form

$$(-2i\omega\partial_u + M^2)\mathcal{A}(u) + \int_{u_0}^u du' \tilde{\Pi}(u, u'; \omega, p)\mathcal{A}(u') = 0 . \quad (3.15)$$

where for generality we have now introduced a mass  $M$  for the  $A$  field. For later use, we have assumed here that the coupling constant is “turned on” at some specified value  $u_0$ . This will clarify the later discussion of initial value conditions and the optical theorem; we can of course set  $u_0 \rightarrow -\infty$  at any point. The upper limit follows from the constraint  $u - u' > 0$  from (3.8).



We can further simplify the expression for  $\tilde{\Pi}(u, u'; \omega, p)$  by exploiting translation invariance in the *transverse* space to write it in terms of an integral over the relative coordinates,  $\hat{V} = V - V'$  and  $\hat{x}^a = x^a - x'^a$ . This gives simply:

$$\tilde{\Pi}_{\text{SK}}(u, u'; \omega, p) = \sqrt{g(u)g(u')} \int d^3 \hat{x} \Phi_{(\omega, p)}(x)^\dagger \Pi_{\text{SK}}(x, x') \Phi_{(\omega, p)}(x') . \quad (3.16)$$

We now come to the choice of initial conditions. The simplest choice, which we call “Type I”, is to assume the coupling is “switched on” at some initial value surface  $u = 0$  (so that  $u_0 = 0$ ) and specify the value of the field  $\mathcal{A}(0)$  on that surface. In this case, the equation of motion describing the evolution of the field  $\mathcal{A}(u)$  is simply

$$-2i\omega \dot{\mathcal{A}}(u) + M^2 \mathcal{A}(u) + \int_0^u du' \tilde{\Pi}_{\text{SK}}(u, u'; \omega, p) \mathcal{A}(u') = 0 . \quad (3.17)$$

Prior to switching on the coupling, the field simply evolves according to the tree-level equation as  $\mathcal{A}(u) = \mathcal{A}(0) \exp -\frac{iM^2 u}{2\omega}$ .

With this choice, the field on the initial value surface  $u = 0$  is a bare field, and as we follow the evolution for  $u > 0$  it will become dressed with a vacuum polarization cloud of virtual  $\phi$  pairs according to (3.17). For  $A\phi^2$  theory in  $d = 4$ , where the only UV divergence is absorbed by a mass renormalization, we can follow this real-time field renormalization explicitly. We expect an initial fall in  $\mathcal{A}(u)$  as the bare field becomes screened by the dressing.

As with transient phenomena in general in quantum field theory, this instantaneous “switching-on” of the coupling may be considered rather unphysical. However, we can simulate these initial conditions while allowing the coupling to be non-vanishing for all  $u$  ( $u_0 \rightarrow -\infty$ ) by introducing an appropriate source  $J(u)$  on the right-hand side of (2.1) chosen to cancel the contribution of the integral for  $-\infty < u' < 0$ , recovering (3.17). However, this requires  $J(u)$  to be non-vanishing also for  $u > 0$  and it is arguable whether the introduction of such a fine-tuned source for all  $u$  is really any more physical than the original model of switching on the coupling. As we will discover, studying the initial transient dressing even in flat space provides an important insight into the long-time behaviour of the field as it evolves in time-dependent curved spacetimes.

In the second part of this paper, we study examples of field theories with different short-distance behaviour, specifically  $A\phi^2$  in  $d = 6$ , which requires a UV divergent field renormalization but which is asymptotically free, and QED, which is IR free and where perturbation theory in the short-time, UV regime is afflicted by the Landau pole. In

these cases, we find a variety of problems with the Type I initial conditions. Since our primary aim is to study the universal long-time behaviour of the field, which we would expect to be independent of the preparation of the initial state, we also consider alternative initial conditions.

In “Type II” initial conditions, which have previously been used to study relaxation problems in non-equilibrium QFT (see, e.g. ref.[18]), we use the source to hold the field  $\mathcal{A}(u)$  fixed from  $u_0 \rightarrow -\infty$  to the initial surface  $u = 0$ . In this case, the equation of motion is:

$$\begin{aligned}
-2i\omega\dot{\mathcal{A}}(u) + M^2\mathcal{A}(u) + \int_0^u du' \tilde{\Pi}_{\text{SK}}(u, u'; \omega, p)\mathcal{A}(u') \\
+ \int_{-\infty}^0 du' \tilde{\Pi}_{\text{SK}}(u, u'; \omega, p)\mathcal{A}(0) = 0
\end{aligned} \tag{3.18}$$

In this scenario, the field at the initial value surface  $u = 0$  is already renormalized and partially dressed, and as  $u > 0$  we watch it relax from this state. This choice of initial conditions circumvents the problems with short-distance physics for theories such as QED, where the Type I conditions are not controllable in perturbation theory.

A further variant, “Type III”, is to constrain the field to evolve for  $u < 0$  with a phase  $\mathcal{A}(0) \exp -\frac{iM^2u}{2\omega}$ , where  $M^2$  is the renormalized mass (to be distinguished from the bare mass in the second term in (3.18)). The new equation of motion is the obvious generalisation of (3.18). In this case, the field at  $u = 0$  is already renormalized and fully dressed and, as we confirm in section 6, no further evolution occurs in flat spacetime. However, in curved spacetime, these initial conditions are particularly appropriate and allow us to study the effects of curvature on a fully-dressed quantum field, even in cases requiring a divergent UV field renormalization.

### 3.2 Vacuum polarization

We now sketch the evaluation of the vacuum polarization in a plane-wave background in the form we need here. Further details, including the equivalent calculation for QED, can be found in refs.[3, 4]. We consider initially the Feynman form,

$$\Pi_{\text{F}}(x, x') = -\frac{ie^2}{2}G_{\text{F}}(x, x')^2 . \tag{3.19}$$

First, consider briefly the equivalent calculation in flat spacetime. Here,  $\sigma(x, x') = \frac{1}{2}(x - x')^2$  and  $\Delta(x, x') = 1$ , and because of translational invariance the self-energy only

depends on the relative position. We can therefore Fourier transform with respect to the four relative coordinates  $\hat{x}^\mu = x^\mu - x'^\mu$ . Writing the two proper-time variables as  $T_1$  and  $T_2$ , we then change variables from  $(T_1, T_2)$  to  $(T, \xi)$ , where  $T = T_1 + T_2$  and  $\xi = T_1/T$ ,

$$\int_0^\infty \frac{dT_1 dT_2}{(T_1 T_2)^2} = \int_0^\infty \frac{dT}{T^3} \int_0^1 \frac{d\xi}{[\xi(1-\xi)]^2} \quad (3.20)$$

and find:

$$\tilde{\Pi}(p^2) = \int d^4 \hat{x} e^{-ip \cdot \hat{x}} \Pi(\hat{x}) = \frac{1}{2} \frac{e^2}{(4\pi)^2} \int_0^1 d\xi \int_0^\infty \frac{dT}{T} e^{-i(m^2 + p^2 \xi(1-\xi))T}. \quad (3.21)$$

This displays a UV logarithmic divergence as the proper time  $T \rightarrow 0$ . This is a conventional UV divergence that is cancelled by a mass renormalization for the  $A$  field. We can evaluate the integral by Wick rotating the proper-time  $T \rightarrow -iT$  and by introducing an explicit cut-off  $\Lambda^{-2}$  on the  $T$  integral, where  $\Lambda$  is a momentum scale:

$$\begin{aligned} \tilde{\Pi}(p^2) &= \frac{1}{2} \frac{e^2}{(4\pi)^2} \int_0^1 d\xi \int_{\Lambda^{-2}}^\infty \frac{dT}{T} e^{-(m^2 + p^2 \xi(1-\xi))T} \\ &= \frac{1}{2} \frac{e^2}{(4\pi)^2} \int_0^1 d\xi \log \left( \frac{m^2 + p^2 \xi(1-\xi)}{\Lambda^2 e^{-\gamma E}} \right). \end{aligned} \quad (3.22)$$

This is the standard result for the one-loop contribution in momentum space.

Now consider the calculation of the vacuum polarization in curved spacetime from (3.16), initially using the Feynman form  $\Pi_F(x, x')$ . The Green functions are given in (2.30). The integrals over  $\hat{x}^a$  are Gaussian, while the integral over  $\hat{V}$  generates a delta function:

$$\begin{aligned} \int d\hat{V} \exp \left[ i \left( \frac{u-u'}{2T\xi(1-\xi)} - \omega \right) \hat{V} \right] &= 4\pi T \xi(1-\xi) \delta(u - u' - 2\omega \xi(1-\xi)T), \\ \int d^2 \hat{x} \exp \left[ \frac{i}{4T\xi(1-\xi)} (u - u') \psi(u, u')_{ab}^{-1} \hat{x}^a \hat{x}^b \right] \exp[-ip_a \hat{x}^a] \\ &= 4i\pi T \xi(1-\xi) \frac{\sqrt{\det \psi(u, u')}}{(u - u')} \exp \left[ -i \frac{T \xi(1-\xi)}{(u - u')} p^a \psi_{ab} p^b \right]. \end{aligned} \quad (3.23)$$

Since  $u - u' = 2\omega \xi(1-\xi)T$ , the conditions  $\omega > 0$  and  $T \geq 0$  mean that  $u \geq u'$ . This is the calculational mechanism already encountered in (3.13) which ensures that, when acting on a positive frequency solution, the Feynman self-energy is only non-vanishing when  $u > u'$  and therefore gives the same result as the retarded, Schwinger-Keldysh, self-energy.

Imposing the delta function constraint, cancelling the  $p^a$ -dependent terms in (3.23) against the identical terms in the mode functions, and collecting terms, we find:

$$\tilde{\Pi}_F(u, u'; \omega, p) = -\frac{1}{2} \frac{e^2}{(4\pi)^2} \theta(u - u') \frac{\sqrt{\Delta(u, u')}}{u - u'} \int_0^1 d\xi e^{-\frac{im^2(u-u')}{2\omega\xi(1-\xi)}}. \quad (3.24)$$

The usual UV divergence now appears as the singularity in the limit  $u \rightarrow u'$  and can be renormalised in the standard way. Crucially, there are further “geometric” singularities when  $u$  and  $u'$  are conjugate points on the null geodesic describing the classical “photon” trajectory. At these points, the VVM determinant diverges. As explored in detail in refs.[3], it is these singularities which give rise to the novel analytic structure of the refractive index in curved spacetime which modifies the conventional form of the Kramers-Kronig dispersion relation while maintaining consistency with causality. The correct prescription for dealing with these singularities follows from the Feynman prescription in real space; namely  $u - u' \rightarrow u - u' - i0^+$ .

Alternatively, we can derive the Schwinger-Keldysh vacuum polarization function  $\tilde{\Pi}_{\text{SK}}(u, u'; \omega, p)$  directly from (3.16) with  $\Pi_{\text{SK}}(x, x') \rightarrow -ie^2\theta(u - u')G_+(x, x')^2$ , immediately exploiting (3.13). Writing the Green functions directly in terms of the modes according to (2.24), we have:

$$\begin{aligned} \tilde{\Pi}_{\text{SK}}(u, u'; \omega, p) = & -\frac{ie^2}{2} \theta(u - u') \sqrt{g(u)g(u')} \int d^3\hat{x} \int \frac{d^3p_1}{(2\pi)^3 2\omega_1} \int \frac{d^3p_2}{(2\pi)^3 2\omega_2} \\ & \times e^{-im^2(u-u')\left(\frac{1}{2\omega_1} + \frac{1}{2\omega_2}\right)} \Phi_{(p)}(x)^\dagger \Phi_{p_1}(x) \Phi_{p_1}(x')^\dagger \Phi_{p_2}(x) \Phi_{p_2}(x')^\dagger \Phi_{(p)}(x'), \end{aligned} \quad (3.25)$$

where  $d^3p_i = d\omega_i dp_i^1 dp_i^2$  and the integrals over  $\omega_i$  are restricted to  $\omega_i \geq 0$ . The integrals over the relative transverse positions  $\hat{x}$  impose momentum conservation

$$p^a = p_1^a + p_2^a, \quad \omega = \omega_1 + \omega_2. \quad (3.26)$$

It is convenient to solve the second constraint by taking  $\omega_1 = \omega\xi$  and  $\omega_2 = (1 - \xi)\omega$  with  $0 \leq \xi \leq 1$ . This leaves a Gaussian integral over  $p_1^a$ :

$$\begin{aligned} \tilde{\Pi}_{\text{SK}}(u, u'; \omega, p) = & -\frac{ie^2}{2} \theta(u - u') [g(u)g(u')]^{-1/4} \int_0^1 d\xi \frac{1}{4\omega\xi(1-\xi)} e^{-\frac{im^2(u-u')}{2\omega\xi(1-\xi)}} \\ & \times \int \frac{d^2p_1}{(2\pi)^3} \exp\left[-\frac{i}{2\omega\xi(1-\xi)} (p_1 - \xi p)^a \psi_{ab}(u, u') (p_1 - \xi p)^b\right] \\ = & -\frac{1}{2} \frac{e^2}{(4\pi)^2} \theta(u - u') \frac{\sqrt{\Delta(u, u')}}{u - u'} \int_0^1 d\xi e^{-\frac{im^2(u-u')}{2\omega\xi(1-\xi)}}, \end{aligned} \quad (3.27)$$

where we have again used (2.11) to write the result in terms of the VVM determinant. Naturally, this reproduces precisely the expression (3.24).

### 3.3 Field evolution and the dynamical renormalization group

The solution to the initial value problem, for Type I initial conditions, is given by solving the equation of motion (3.17) for the  $u$ -dependent amplitude factor  $\mathcal{A}(u)$  defined in (3.11). We write the solution as a perturbative expansion in  $e^2$  as:<sup>5</sup>

$$\mathcal{A}(u) = \mathcal{A}(u_0) e^{-\frac{iM^2(u-u_0)}{2\omega}} (1 + i\mathcal{Q}^{(1)}(u) + \dots) . \quad (3.28)$$

Implementing the constraint that  $\Pi_{\text{SK}}(x, x')$  has support only for  $u > u'$ , we find:

$$\mathcal{Q}^{(1)}(u) = -\frac{1}{2\omega} \int_{u_0}^u du'' \int_{u_0}^{u''} du' \tilde{\Pi}_{\text{SK}}(u'', u'; \omega, p) e^{\frac{iM^2(u''-u')}{2\omega}} , \quad (3.29)$$

so from (3.27),

$$\mathcal{Q}^{(1)}(u) = \frac{e^2}{(4\pi)^2} \frac{1}{4\omega} \int_{u_0}^u du'' \int_{u_0}^{u''} du' \frac{\sqrt{\Delta(u'', u')}}{u'' - u'} \int_0^1 d\xi e^{i\frac{u''-u'}{2\omega} (M^2 - \frac{m^2}{\xi(1-\xi)})} . \quad (3.30)$$

Re  $\mathcal{Q}^{(1)}(u)$  is of course UV divergent and, for the  $d = 4$   $A\phi^2$  theory, this divergence is absorbed as usual in a mass renormalization of  $M^2$ , as shown explicitly in section 5.

The imaginary part,  $\text{Im } \mathcal{Q}^{(1)}(u)$ , controls the amplification or attenuation of the amplitude and plays a vital role in our analysis from now on. Using the symmetry property  $\Delta(x, x') = \Delta(x', x)$ , we can show that this is given by an expression almost identical to (3.30), but with the integration range extended:

$$2i \text{Im } \mathcal{Q}^{(1)}(u) = \frac{e^2}{(4\pi)^2} \frac{1}{4\omega} \int_{u_0}^u du'' \int_{u_0}^u du' \frac{\sqrt{\Delta(u'', u')}}{u'' - u'} \int_0^1 d\xi e^{i\frac{u''-u'}{2\omega} (M^2 - \frac{m^2}{\xi(1-\xi)})} . \quad (3.31)$$

This expression, with the integration limits shown, is key to clarifying issues related to positivity and the optical theorem in the next section. Note also that  $\text{Im } \mathcal{Q}^{(1)}(u)$  is

---

<sup>5</sup>For Type II or III initial conditions, with initial value surface  $u = 0$ , the solution for  $u > 0$  is written as

$$\mathcal{A}(u) = \mathcal{A}(0) e^{-\frac{iM^2 u}{2\omega}} (1 + i\mathcal{Q}^{(1)}(u) - i\mathcal{Q}^{(1)}(0) + \dots) .$$

Note that at this order, the equations of motion for Type III and Type I initial conditions are identical for  $u > 0$ .

free of UV divergences since the  $u'$  integral avoids the singularity at  $u' = u''$  by virtue of the Feynman prescription  $u'' - u' \rightarrow u'' - u' - i0^+$ .

Now, for backgrounds which are translation invariant in  $u$  (the symmetric, or Cahen-Wallach, plane waves), the VVM determinant will be a function only of the separation of the two points, i.e.  $\Delta = \Delta(x - x')$ . It follows that for large  $u$ ,  $\mathcal{Q}^{(1)}(u) \sim u$ . When  $u$  is large, therefore, the  $\mathcal{O}(e^2)$  correction will itself be large and perturbation theory should break down. In fact, such large *secular* terms are a common occurrence in perturbation theory and in this translation-invariant case, the problem is overcome by a resummation which exponentiates the dependence on  $\mathcal{Q}^{(1)}(u)$  in (3.28).

More generally, this kind of resummation is performed by what is known as the *dynamical renormalization group* (see [18] and references therein). This is a way of absorbing the secular terms into a renormalization of the amplitude  $\mathcal{A}(u)$  at an arbitrary time  $u^*$ . The quickest way to arrive at the re-summed formula is to write in perturbation theory

$$\mathcal{A}(u) = \mathcal{A}(u^*) e^{-\frac{iM^2(u-u^*)}{2\omega}} (1 + i[\mathcal{Q}^{(1)}(u) - \mathcal{Q}^{(1)}(u^*)] + \dots) . \quad (3.32)$$

Since the right-hand side cannot depend on the arbitrary scale  $u^*$  we have, to  $\mathcal{O}(e^2)$ ,

$$0 = \frac{d}{du^*} \mathcal{A}(u^*) + i \frac{M^2}{2\omega} \mathcal{A}(u^*) - i \frac{d\mathcal{Q}^{(1)}(u^*)}{du^*} \mathcal{A}(u^*) . \quad (3.33)$$

Solving this, using the initial condition  $\mathcal{Q}^{(1)}(u_0) = 0$ , and finally setting  $u^* \rightarrow u$  gives

$$\mathcal{A}(u) = \mathcal{A}(u_0) e^{-\frac{iM^2(u-u_0)}{2\omega}} e^{i\mathcal{Q}^{(1)}(u)} . \quad (3.34)$$

The effect of the resummation is to exponentiate the first order perturbative correction. The importance of the dynamical renormalization group is that we can apply it even in the non-translationally invariant cases.

Notice now that a positive imaginary part of  $\mathcal{Q}^{(1)}(u)$  signals an exponential decay of the amplitude, which is the standard expectation. For translation-invariant backgrounds, where  $\text{Im } \mathcal{Q}^{(1)}(u)$  is proportional to  $u$  in the long-time limit, this allows us to identify a constant *decay rate*. However, this interpretation does not extend to a general non-symmetric plane-wave background where the usual concept of a decay rate is not well-defined.

### 3.4 Refractive index and analyticity

At this point, we make contact with our previous work [3, 4] on photon propagation and the refractive index for curved spacetime.

In the massless ( $M = 0$ ) case, after applying the dynamical renormalization group resummation, we have found the solution for the field  $A(x)$  in the form

$$A(x) = \mathcal{A}(u_0)\Phi_p(x)e^{i\mathcal{Q}^{(1)}(u)} , \quad (3.35)$$

where

$$\frac{d}{du}\mathcal{Q}^{(1)}(u) = -\frac{1}{2\omega} \int_{u_0}^u du' \tilde{\Pi}_{\text{SK}}(u, u' : \omega, p) . \quad (3.36)$$

Note again that whereas previously we used the Feynman, *in-out*, formalism, all our previous results for the refractive index are identical with those found using the Schwinger-Keldysh, *in-in*, formalism. Comparing with refs.[3, 4], we identify the refractive index associated with the solution (3.35) as

$$n(u; \omega) = 1 + \frac{1}{\omega} \frac{d}{du}\mathcal{Q}^{(1)}(u) \quad (3.37)$$

and so

$$n(u; \omega) = 1 - \frac{1}{2\omega^2} \int_{u_0}^u du' \tilde{\Pi}_{\text{SK}}(u, u'; \omega, p) . \quad (3.38)$$

To complete the identification of notation, substitute the explicit expression (3.30) for  $\mathcal{Q}^{(1)}(u)$  and introduce the variable  $t = u - u'$ . We then have

$$n(u; \omega) = 1 + \frac{e^2}{(4\pi)^2} \frac{1}{4\omega^2} \int_0^1 d\xi \int_0^{u-u_0} \frac{dt}{t} e^{-\frac{im^2 t}{2\omega\xi(1-\xi)}} \sqrt{\Delta(u, u-t)} . \quad (3.39)$$

The upper limit of the  $t$  integral goes to  $\infty$ , as in our previous discussions of the refractive index, when we take the switch-on time  $u_0 \rightarrow -\infty$ . Of course, this expression still requires renormalization. This will be considered in this formalism in section 7, after the detailed analysis of translation invariant spacetimes in sections 5 and 6 using Laplace transform methods. In ref.[3], we also introduced a variable  $z = \frac{m^2}{2\omega\xi(1-\xi)}$  and wrote (3.39) in the form:

$$n(u; \omega) = 1 + \frac{e^2}{(4\pi)^2} \frac{1}{4\omega^2} \int_0^1 d\xi \mathcal{F}(u; z) , \quad (3.40)$$

with

$$\mathcal{F}(u; z) = \int_0^\infty \frac{dt}{t} e^{-izt} \sqrt{\Delta(u, u-t)} . \quad (3.41)$$

Apart from the obvious differences because here we are considering a pure scalar theory rather than QED, these expressions match the forms presented in [3, 4], in particular section 6 of [3].

From this point, ref.[3] discusses in detail how the singularities in the  $t$ -plane, which arise from the VVM determinant when  $u$  and  $u-t$  are conjugate points along the null geodesic describing the classical photon trajectory, integrate up to give a novel analytic structure in the complex  $\omega$ -plane for the refractive index. In particular, the presence of new cuts related to the background geometry violate hermitian analyticity, which is a standard property of S-matrix theory. The resulting modification of standard theorems of flat-space quantum field theory, especially the Kramers-Kronig dispersion relation, allow the apparent paradoxes associated with low-frequency super-luminal phase velocities – that is,  $\text{Re } n(u; 0) < 1$  – to be resolved while causality is maintained. In what follows, our emphasis is different as we try to reconcile the amplification of the field implied by a negative imaginary part of the refractive index with unitarity.

### 3.5 Dressing and undressing a quantum field

One of the most remarkable features to emerge from our analysis of the refractive index for QED was the discovery of cases where  $\text{Im } n(u; \omega)$  is negative, corresponding to an amplification of the field as it propagates through the background curved spacetime. To begin to develop some intuition into this phenomenon, we consider first the weak curvature limit. Here, we can expand the VVM determinant to linear order in the curvature

$$\Delta(u, u') = 1 + \frac{1}{6} R_{uu}(u)(u-u')^2 - \frac{1}{12} \dot{R}_{uu}(u)(u-u')^3 + \dots \quad (3.42)$$

where the Ricci tensor  $R_{uu} = R^i{}_{uiu}$ . Substituting this expansion into the integral (3.36), and after UV regularization, we determine the correction to the refractive index:

$$n(u; \omega) = 1 - \frac{e^2}{(4\pi)^2} \frac{1}{360m^4} R_{uu}(u) - \frac{e^2}{(4\pi)^2} \frac{i\omega}{840m^6} \dot{R}_{uu}(u) + \dots . \quad (3.43)$$

The analogues of this expansion for scalar and spinor QED appear in appendix A and (1.1) for the latter. In this approximation, the ratio of the amplitude for two points



$u_1, u_2$  on the null trajectory  $\gamma$ , in the long-time limit, is

$$\mathcal{A}(u_1) = \mathcal{A}(u_2) \exp \left[ \frac{e^2}{(4\pi)^2} \frac{\omega^2}{840m^6} (R_{uu}(u_1) - R_{uu}(u_2)) \right]. \quad (3.44)$$

If the Ricci curvature component  $R_{uu}(u)$  decreases along  $\gamma$ , then from the Jacobi equation (see [4]) we see that the rate of acceleration of the nearby geodesics is positive, i.e. the tidal forces are increasing in the direction of stretching the virtual cloud. In this case, the amplitude decreases because more virtual  $\phi$  pairs are being produced:  $A$  is becoming more dressed. On the contrary, if  $R_{uu}(u)$  increases along  $\gamma$ , i.e. the tidal forces are increasing in the direction of squeezing, then the amplitude increases because virtual pairs are recombining:  $A$  is being “undressed” and is returning to its bare state [5].<sup>6</sup> These effects are illustrated heuristically in Fig. 1 with the role of the photon being played by  $A$  and the  $e^+e^-$  pairs by  $\phi$  pairs.

We now come to the second, non-perturbative, mechanism which can produce an imaginary part for the refractive index. If  $R_{uu}(u)$  is constant, in which case the metric (2.4) describes a symmetric plane wave, or Cahen-Wallach space [19], then to linear order in the curvature the amplitude is constant. In fact,  $\text{Im } n(\omega) = 0$  to all orders in the curvature expansion. However, in the case where at least one of the eigenvalues of the constant  $h_{ij}$  is negative, there is a positive contribution to  $\text{Im } n(\omega)$ , so a decaying amplitude, which is non-perturbative in the curvature. The simplest case to consider is  $h_{ij} = -\sigma^2 \delta_{ij}$ , which is discussed in detail in section 6. In this case, the VVM determinant is

$$\Delta(u, u') = \left[ \frac{\sigma(u - u')}{\sinh \sigma(u - u')} \right]^2. \quad (3.45)$$

we then have

$$n(\omega) = 1 + \frac{e^2}{(4\pi)^2} \frac{1}{4\omega^2} \int_0^\infty \frac{dt}{\sinh(\sigma t)} \int_0^1 d\xi e^{-\frac{im^2 t}{2\omega\xi(1-\xi)}}. \quad (3.46)$$

The imaginary part is then given by (3.46) by extending the contour to run from  $-\infty$  to  $+\infty$  just under the real axis.  $\text{Im } n(\omega)$  can then be computed by deforming the integration contour so that it picks up the residues of all the poles along the negative imaginary axis at  $t = \frac{n\pi}{\sigma}$ ,  $n = 1, 2, \dots$ . This gives

$$\text{Im } n(\omega) = \frac{e^2}{(4\pi)^2} \frac{\pi}{\omega^2} \int_0^1 d\xi \left[ 1 + e^{\frac{\pi m^2}{2\omega\sigma\xi(1-\xi)}} \right]^{-1}, \quad (3.47)$$

---

<sup>6</sup>A related physical picture for particle creation in a background gravitational field, based on quantum mechanical tunnelling, has recently been presented in ref.[33]. This shares our basic intuition of relating these curved-spacetime phenomena to geodesic deviation through the Jacobi equation, though here we are considering one-loop quantum field theoretic effects due to vacuum polarization.

which is non-perturbative in the curvature. In this case the result is independent of  $u$  and so it implies a constant rate of production of  $\phi$  pairs. This process would be kinematically disallowed in flat space, but there is no such threshold constraint in curved spacetime. This kind of below-threshold decay is a well-known property of curved space arising from the lack of time-translation invariance. In particular the situation in de Sitter space has been known about for a long time [36–39].

This result essentially confirms the proposal of ref.[28] that interacting quantum fields in a plane wave background with negative eigenvalues of  $h_{ij}$  will decay. We have shown that the process is perfectly consistent with unitarity and if one starts from an initial value surface then only a finite number of  $\phi^2$  pairs will be produced per unit volume. In the next section we turn to the issue of fate of the optical theorem in curved space.

## 4 Optical Theorem in Curved Spacetime

The observation that the imaginary part of the refractive index can be negative, at least for trajectories and spacetimes where the metric in the Penrose plane-wave limit is  $u$ -dependent, brings us to the critical issue – how can we reconcile the increase in the amplitude associated with  $\text{Im } n(u; \omega) < 0$  with unitarity and the optical theorem?

The optical theorem is familiar from the discussion of scattering amplitude in flat space: in the context of the present model, it states that the imaginary part of the one-loop vacuum polarisation diagram yields the rate for the tree-level process  $A \rightarrow \phi\phi$  and is therefore non-vanishing only above threshold. In curved spacetime we need a reformulation of the theorem that avoids the use of asymptotic particle states. The initial-value problem provides a suitable formalism. For clarity, we consider Type I initial conditions where the interaction is switched on at  $u = u_0$ . We then calculate the total probability for the tree-level process  $A \rightarrow \phi\phi$  to occur between times  $u_0$  and  $u$  and compare with the solution of the initial value problem for  $A(x)$ . This gives a generalised version of the optical theorem that holds in curved spacetime and directly relates the dissipation of the  $A$  field to the creation of  $\phi$  pairs.

The resolution of the apparent paradox that  $\text{Im } n(u; \omega)$  can be negative lies in the fact that we have only shown that the amplitude can increase over a local region. In order to verify unitarity, and relate  $\text{Im } \tilde{\Pi}$  to the (positive) probability of production of  $\phi$  pairs, we have to integrate over the whole region from the “switch-on” surface  $u_0$  to  $u$  (see eq.(4.2) below). It turns out that while the amplitude  $\mathcal{A}(u)$  can increase locally,

compared with its value at the initial value surface it must always decrease. The initial transient dressing of the  $A$  field plays an important rôle since it is only a field that is already dressed that can increase its amplitude by “undressing”; a bare field, however, cannot be undressed any further.

To derive the optical theorem, note first that

$$\int_{u_0}^u du'' \operatorname{Im} n(u''; \omega) = \frac{1}{\omega} \operatorname{Im} \mathcal{Q}^{(1)}(u) = -\frac{1}{2\omega^2} \int_{u_0}^u du'' \int_{u_0}^{u''} du' \operatorname{Im} \tilde{\Pi}_{\text{SK}}(u'', u'; \omega, p) . \quad (4.1)$$

where  $\operatorname{Im} \mathcal{Q}^{(1)}(u)$  is given in eq.(3.31). We also leave  $M = 0$ , so it is appropriate to use the refractive index nomenclature as in section 3.4. Otherwise,  $\tilde{\Pi}_{\text{SK}}(u, u'; \omega, p)$  in (4.6),(4.8) is accompanied by a simple  $M$ -dependent phase, as in (3.34).

Now consider the the transition probability for the tree-level process  $A \rightarrow \phi\phi$ :

$$P_{A \rightarrow \phi\phi}(u) = \frac{e^2}{\mathcal{N}} \int \frac{d^3 p_1}{(2\pi)^3 2\omega_1} \frac{d^3 p_2}{(2\pi)^3 2\omega_2} \left| \int_{u_0}^u d^4 x \sqrt{g} A^{(0)}(x)^\dagger \phi_{p_1}(x) \phi_{p_2}(x) \right|^2 . \quad (4.2)$$

Here,  $\phi_p(x)$  are the massive on-shell modes defined in (2.19) and the final-state phase space integrals are over the three-dimensional  $p = (\omega, p_a)$ . The normalization factor  $\mathcal{N} = (A^{(0)}, A^{(0)}) = 2\omega\delta^{(3)}(0)$  cancels against an overall integration on  $(V, x^a)$ . All the frequencies,  $\omega, \omega_1$  and  $\omega_2$  in (4.2) are positive since they refer to physical particles.

The evaluation of (4.2) follows closely the calculation of  $\tilde{\Pi}_{\text{SK}}(u, u'; \omega, p)$  directly from the mode functions in eqs.(3.25)–(3.27). For convenience, recall here the definition of  $\Pi_{\text{SK}}(x, x')$ :

$$\Pi_{\text{SK}}(x, x') = -\frac{ie^2}{2} \theta(u - u') \left( G_+(x, x')^2 - G_-(x, x')^2 \right) , \quad (4.3)$$

the expression for the Wightman functions in terms of the modes  $\phi_p(x)$ :

$$G_\pm(x, x') = \pm \int \frac{d^3 p}{(2\pi)^3 2\omega} \theta(\pm\omega) \phi_p(x) \phi_p(x')^\dagger . \quad (4.4)$$

and the observation (3.13) that  $\int dV' G_-(x, x')^2 A^{(0)}(x') = 0$  for positive frequency  $\omega$ . It then follows that

$$P_{A \rightarrow \phi\phi}(u) = \frac{e^2}{\mathcal{N}} \int_{u_0}^u du'' \sqrt{g''} \int_{u_0}^u du' \sqrt{g'} \int d^3 x'' \int d^3 x' \Phi_p(x'')^\dagger G_+(x'', x')^2 \Phi_p(x) . \quad (4.5)$$

Separating out an overall volume factor using translation invariance in the transverse space, as in (3.16), and using the properties  $G_+(x, x')^* = G_-(x, x')$  and  $G_+(x', x) = G_-(x, x')$ , we find:

$$P_{A \rightarrow \phi\phi}(u) = -\frac{2}{\omega} \int_{u_0}^u du'' \int_{u_0}^{u''} du' \operatorname{Im} \tilde{\Pi}_{\text{SK}}(u'', u'; \omega, p), \quad (4.6)$$

where note again that we could equally have written  $\tilde{\Pi}_{\text{F}}$  above, and so

$$P_{A \rightarrow \phi\phi}(u) = 4\omega \int_{u_0}^u du'' \operatorname{Im} n(u''; \omega). \quad (4.7)$$

This is the statement of the optical theorem in curved spacetime. Unitarity is respected and the integral over the whole trajectory of  $\operatorname{Im} n(u; \omega)$  is positive. This shows how unitarity prevents a local amplification of the amplitude from becoming unbounded.<sup>7</sup>

We can also write a local version, defining  $\Gamma(u) = \partial_u P_{A \rightarrow \phi\phi}(u)$  as the “instantaneous rate” of pair production. Then,

$$\Gamma(u) = 4\omega \operatorname{Im} n(u; \omega) = -\frac{2}{\omega} \int_{u_0}^u du' \operatorname{Im} \tilde{\Pi}_{\text{SK}}(u, u'; \omega, p). \quad (4.8)$$

Unlike the integrated form, there is no positivity constraint on (4.8) in general. This explains why there is no conflict with unitarity in the examples where we have found  $\operatorname{Im} n(u; \omega) < 0$ . However, in cases where we have translation invariance along the photon trajectory, as in flat spacetime,  $n(\omega)$  becomes  $u$ -independent in the large  $u$  limit beyond the transient region (equivalently  $u_0 \rightarrow -\infty$ ; see (3.39)) and  $P_{A \rightarrow \phi\phi}(u)$  is then proportional to  $u$ , so unitarity implies  $\operatorname{Im} n(\omega) > 0$  and  $\Gamma > 0$  can be properly interpreted as the rate of  $A \rightarrow \phi\phi$ .

To summarise, we have shown how the effect of gravitational tidal forces on vacuum polarization can alter the dressing of a photon as it propagates through space. In

---

<sup>7</sup> To emphasise the importance of integrating over the entire region from the “switch-on” surface  $u_0$  in these expressions, consider the change  $\Delta P(u_2|u_1)$  in the total probability of pair production between two null surfaces  $u_1$  and  $u_2$ . From (4.6) this is:

$$\Delta P(u_2|u_1) = -\frac{2}{\omega} \int_{u_1}^{u_2} du'' \int_{u_0}^{u''} du' \operatorname{Im} \tilde{\Pi}_{\text{SK}}(u'', u'; \omega, p).$$

Contrast this with the integral  $I(u_2|u_1)$  defined as  $\Delta P(u_2|u_1)$  but with the lower limit of the  $u'$  integral set to  $u_1$ . This is a positive quantity, since by the above construction it can be written as a  $|\dots|^2$  as in (4.2), but it does *not* represent the probability of pair production between  $u_1$  and  $u_2$ . In fact, while  $P(u_1)$ ,  $P(u_2)$  and  $I(u_2|u_1)$  are all positive quantities, because of the extra region of integration from the switch-on surface  $u_0$  to  $u_1$ ,  $\Delta P(u_2|u_1)$  itself need not be positive.

particular, we have seen how the imaginary part  $\text{Im } n(u; \omega)$  of the position-dependent refractive index can be negative as well as positive, corresponding to “undressing” of the photon rather than the conventional dressing. Two mechanisms were identified. The first, of order  $\omega \partial_u \mathfrak{R}/m^4$ , admits an intuitive interpretation in terms of curvature variations along the  $A$  field (“photon”) trajectory altering the balance of the bare field with its virtual  $e^+e^-$  cloud, with increasing stretching (squeezing) giving rise to more dressing (undressing). The second, which is non-perturbative in  $\omega^2 \mathfrak{R}/m^4$ , can occur even when the curvature is constant and is related to the existence of conjugate points on the photon’s null geodesic.

Nevertheless, unitarity is still respected and the optical theorem still holds in curved spacetime. In its integrated form (4.6), (4.7), it relates the total probability for  $e^+e^-$  pair production to the integral of  $\text{Im } n(u; \omega)$  along the photon trajectory, which is manifestly positive. Except in the special case of translation invariance along the null geodesic, the corresponding local form (4.8) has no positivity constraint and the usual interpretation of  $\text{Im } n(u; \omega)$  as the rate of pair production can break down. However, it does describe the variation of the amplitude and its interpretation in terms of dressing and undressing of the photon field. In a sense, photon propagation in curved spacetime resembles the initial transient phase in flat spacetime, with the characteristic features of an oscillating amplitude and below-threshold decay.

## 5 Real-time Field Renormalization

In the second part of this paper, we illustrate these general principles with a range of examples featuring different quantum field theories, initial conditions and plane-wave backgrounds.

Most of the discussion will focus on spacetimes with  $u$ -translation invariance. In this case, a particularly powerful method of analysing the equation of motion for  $\mathcal{A}(u)$  is provided by the Laplace transform, which automatically re-sums chains of one-loop vacuum polarization diagrams and provides a convenient formalism in which to exploit their analytic structure.

After introducing the Laplace transform method, the remainder of this section specialises to flat spacetime. As well as providing a relatively simple example to develop our techniques, it turns out that by studying real-time field renormalization in the transient region in flat spacetime, we develop a lot of insight into the evolution of a renormalized quantum field in a curved spacetime background.

## 5.1 Laplace Transform and $u$ -translation invariance

To introduce the Laplace transform method [18], consider first the  $A\phi^2$  theory in  $d = 4$ . To simplify notation for these  $u$ -translation invariant cases, we define the kernel function in the equation of motion as  $\Sigma(u, u') = \tilde{\Pi}(u, u'; \omega, p)$  and note that  $\Sigma(u, u') = \Sigma(t)$ , where as in section 3.4 we let  $t = u - u'$ .

The equation of motion, with Type I boundary conditions and  $u_0 = 0$ , is then (see (3.17)):

$$-2i\omega\dot{\mathcal{A}}(u) + M^2\mathcal{A}(u) + \int_0^u dt \Sigma(t)\mathcal{A}(u-t) = 0 . \quad (5.1)$$

Since the final term is a convolution, this can be solved by introducing the Laplace transform,

$$\tilde{\mathcal{A}}(s) = \int_0^\infty du e^{-su}\mathcal{A}(u) , \quad \tilde{\Sigma}(s) = \int_0^\infty dt e^{-st}\Sigma(t) . \quad (5.2)$$

The transform of (5.1) is simply

$$-2i\omega(s\tilde{\mathcal{A}}(s) - \mathcal{A}(0)) + M^2\tilde{\mathcal{A}}(s) + \tilde{\Sigma}(s)\tilde{\mathcal{A}}(s) = 0 \quad (5.3)$$

and so

$$\tilde{\mathcal{A}}(s) = \frac{2i\omega\mathcal{A}(0)}{2i\omega s - M^2 - \tilde{\Sigma}(s)} . \quad (5.4)$$

The inverse transform is then implemented by the usual Bromwich integral

$$\mathcal{A}(u) = \int_{c-i\infty}^{c+i\infty} \frac{ds}{2\pi i} \frac{2i\omega\mathcal{A}(0)e^{su}}{2i\omega s - M^2 - \tilde{\Sigma}(s)} , \quad (5.5)$$

where the contour lies to the right of any singularities in the complex  $s$  plane.

Now consider the renormalization of the theory. The analytic structure for the inverse transform depends on properties of the vacuum polarization kernel  $\tilde{\Sigma}(s)$  and is model-dependent. Suppose first (this will be the below threshold case in flat space) that there is an isolated pole at  $s = s_0$  given from (5.4) as the solution of

$$2i\omega s_0 - M_B^2 - \tilde{\Sigma}_B(s_0) = 0 , \quad (5.6)$$

where we have explicitly indicated the bare quantities in (5.5) with a subscript. We renormalize by identifying the mass counterterm,  $M_B^2 = M^2 + \delta M^2$ , in such a way that  $M$  is the physical mass defined as the position of the single particle pole, i.e.

$$2i\omega s_0 = M^2 . \quad (5.7)$$

It follows from (5.6) that the counterterm is

$$\delta M^2 = -\tilde{\Sigma}_B\left(\frac{M^2}{2i\omega}\right), \quad (5.8)$$

which is real if we are below threshold. The expression  $\mathcal{A}(u)$  in (5.5) then takes the same form with the mass interpreted as the renormalized mass  $M^2$  and the kernel replaced by the subtracted form

$$\tilde{\Sigma}(s) = \tilde{\Sigma}_B(s) - \tilde{\Sigma}_B\left(\frac{M^2}{2i\omega}\right). \quad (5.9)$$

Field renormalization will be considered in section 5.3.

## 5.2 $A\phi^2$ in $d = 4$ : transient evolution in flat spacetime

In a  $u$ -translation invariant spacetime, the Fourier transform of the kernel  $\Sigma(t)$  is simply the usual vacuum polarization with momentum  $p = (\omega, -is - \frac{1}{2}C_{ab}p^ap^b, p^a)$ , which implies  $p^2 = -2i\omega s$ . So in flat spacetime, we can immediately read off the expression for the bare  $\tilde{\Sigma}(s)$  from (3.22):

$$\tilde{\Sigma}_B(s) = \Pi_B(-2i\omega s) = \frac{1}{2} \frac{e^2}{(4\pi)^2} \int_0^1 d\xi \log\left(\frac{m^2 - 2i\omega\xi(1-\xi)s}{\Lambda^2 e^{-\gamma_E}}\right). \quad (5.10)$$

Implementing the mass renormalization subtraction (5.9), we therefore have

$$\tilde{\Sigma}(s) = \frac{1}{2} \frac{e^2}{(4\pi)^2} \int_0^1 d\xi \log\left(\frac{m^2 - 2i\omega s\xi(1-\xi)}{m^2 - M^2\xi(1-\xi)}\right). \quad (5.11)$$

The analytic structure of the Laplace transform is illustrated in the left part of Fig. 2.  $\tilde{\Sigma}(s)$  itself has a branch cut at  $s = -\frac{2im^2}{\omega}$ , equivalent to  $p^2 = -4m^2$ , which is the threshold for the production of pairs of  $\phi$  particles. It is convenient in the following discussion using the spectral density to introduce the variable  $\nu^2 = -p^2 = 2i\omega s$ . Notice that with this definition, the  $\nu$  plane is a double cover of the  $s$  plane. Consequently, whereas in the  $s$ -plane there is only a single 2-particle cut beginning at the branch-point  $s = -\frac{2im^2}{\omega}$ , in  $\nu$  plane there are two threshold branch points at  $\nu = \pm 2m$  and we take the cuts to lie along  $-\infty \leq \nu \leq -2m$  and  $2m \leq \nu \leq \infty$ .

The spectral density, which plays a key role in our analysis, is then given as usual by the imaginary part of the vacuum polarization kernel,

$$\rho(\nu) = -\frac{1}{\pi} \text{Im} \tilde{\Sigma}\left(\frac{\nu^2}{2i\omega}\right), \quad (5.12)$$

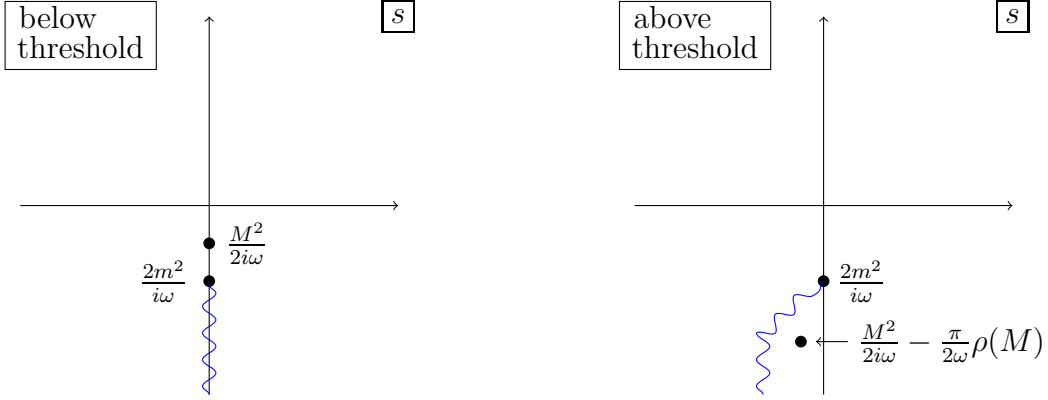


**Figure 2.** The analytic structure of the Laplace transform in the below threshold (left) and above threshold (right) situations. The diagrams show the particle pole at  $s = \frac{M^2}{2i\omega}$  and the 2-particle threshold branch point and associated cut at  $s = \frac{2m^2}{i\omega}$ . In the case above threshold we have deformed the cut to expose the simple pole on the un-physical sheet.

defined implicitly with  $\nu \rightarrow \nu + i0^+$ , i.e. as the limit from just above the cut. For  $A\phi^2$  theory in  $d = 4$ , it is related to  $\tilde{\Sigma}$  by the once-subtracted dispersion relation,

$$\tilde{\Sigma}\left(\frac{\nu^2}{2i\omega}\right) = \tilde{\Sigma}(0) - \nu \int_{-\infty}^{\infty} \frac{d\nu'}{\nu'} \frac{\rho(\nu')}{\nu' - \nu - i0^+} \quad (5.13)$$

From the one-loop expression (5.11), we find the imaginary part:

$$\text{Im} \tilde{\Sigma}\left(\frac{\nu^2}{2i\omega}\right) = -\frac{1}{2} \frac{e^2}{(4\pi)^2} \theta(\nu - 2m) \pi \int_{\xi_-}^{\xi_+} d\xi, \quad (5.14)$$

where  $\xi_{\pm}$  are the roots of  $\xi^2 - \xi + \frac{m^2}{\nu^2} = 0$ . The spectral function for  $A\phi^2$  theory in  $d = 4$  is therefore:

$$\rho(\nu) = \frac{1}{2} \frac{e^2}{(4\pi)^2} \theta(\nu - 2m) \sqrt{1 - \frac{4m^2}{\nu^2}}, \quad (5.15)$$

valid for  $\nu > 0$ . The  $\nu$  dependence of this expression explains the need for the subtraction in (5.13) to ensure convergence of the integral for large  $\nu$ . For negative  $\nu$ , we have  $\rho(-\nu) = -\rho(\nu)$ . Notice that the imaginary part of  $\tilde{\Sigma}(s)$  and the spectral density are UV finite quantities.

Below threshold  $M < 2m$ , the contribution from the pole and cut are disentangled and the result is simply a sum of the two contributions,

$$\mathcal{A}(u) = \mathcal{A}_{\text{pole}}(u) + \mathcal{A}_{\text{cut}}(u). \quad (5.16)$$



The single particle pole contributes

$$\mathcal{A}_{\text{pole}}(u) = \frac{\mathcal{A}(0)e^{s_0 u}}{1 - \frac{1}{2i\omega}\tilde{\Sigma}'(s_0)} = \frac{\mathcal{A}(0)e^{-\frac{iM^2 u}{2\omega}}}{1 + \frac{e^2}{(4\pi)^2} \frac{1}{2M^2} f\left(\frac{4m^2}{M^2}\right)}, \quad (5.17)$$

where, using (5.11) and evaluating the  $\xi$  integral, we have

$$f(z) = \frac{z}{\sqrt{z-1}} \arctan \frac{1}{\sqrt{z-1}} - 1, \quad (5.18)$$

with  $z = \frac{4m^2}{M^2}$ . So the contribution from the pole is simply the classical solution with a quantum corrected amplitude. The contribution from the cut is:

$$\mathcal{A}_{\text{cut}}(u) = -2\mathcal{A}(0) \int_{2m}^{\infty} d\nu \frac{\nu \rho(\nu) e^{-\frac{i\nu^2 u}{2\omega}}}{\left[\nu^2 - M^2 - \text{Re} \tilde{\Sigma}\left(\frac{\nu^2}{2i\omega}\right)\right]^2 + \pi^2 \rho(\nu)^2}, \quad (5.19)$$

We can immediately check consistency by evaluating the sum rule<sup>8</sup>

$$\left[1 + \frac{e^2}{(4\pi)^2} \frac{1}{2M^2} f\left(\frac{4m^2}{M^2}\right)\right]^{-1} - 2 \int_{2m}^{\infty} d\nu \frac{\nu \rho(\nu)}{\left[\nu^2 - M^2 - \text{Re} \tilde{\Sigma}\left(\frac{\nu^2}{2i\omega s}\right)\right]^2 + \pi^2 \rho(\nu)^2} = 1. \quad (5.20)$$

It is also important to notice that the solution that we have found using the Laplace transform remains perturbative throughout the evolution. In other words, in the inverse transform (5.5) we can consistently expand in powers of the coupling:

$$\mathcal{A}(u) = \mathcal{A}(0) \int_{c-i\infty}^{c+i\infty} \frac{ds}{2\pi i} e^{su} \left[ \frac{1}{s - \frac{M^2}{2i\omega}} + \frac{1}{\left(s - \frac{M^2}{2i\omega}\right)^2} \frac{\tilde{\Sigma}(s)}{2i\omega} + \dots \right]. \quad (5.21)$$

The pole at  $s = \frac{M^2}{2i\omega}$  yields the terms

$$\mathcal{A}(0) e^{-\frac{iM^2 u}{2\omega}} \left[ 1 + \frac{1}{2i\omega} \tilde{\Sigma}'\left(\frac{M^2}{2i\omega}\right) + \dots \right], \quad (5.22)$$

which are precisely the terms of order  $\mathcal{O}(e^2)$  in the expansion of (5.17). At this order, the cut contribution is

$$\mathcal{A}_{\text{cut}}(u) = \mathcal{A}(0) \frac{e^2}{(4\pi)^2} \int_{2m}^{\infty} d\nu \frac{\nu}{(\nu^2 - M^2)^2} \sqrt{1 - \frac{4m^2}{\nu^2}} e^{-\frac{i\nu^2 u}{2\omega}}. \quad (5.23)$$

---

<sup>8</sup>This follows from the fact that at  $u = 0$  we can pull the contribution from the pole and the cut off to a large circle at infinity. In this limit,  $2i\omega s - M^2 - \tilde{\Sigma}(s) \rightarrow 2i\omega s$  and so the contribution is a simple pole at infinity with residue  $\mathcal{A}(0)$ .

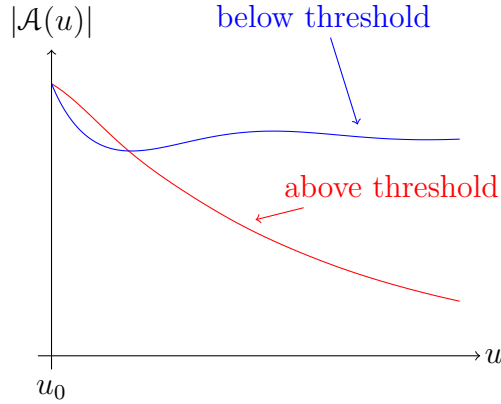


**Figure 3.** The amplitude of the field as a function of  $u$  for the below and above threshold cases for a representative choice of parameters. The case above threshold illustrates exponential decay while the case below threshold oscillates transiently before going asymptotically to a constant which gives the finite wave-function renormalization .

Evaluating this integral and comparing with  $f(\frac{4m^2}{M^2})$ , we readily verify the sum rule (5.20) explicitly at  $\mathcal{O}(e^2)$ .

Since the spectral density is positive, for positive  $\nu$ , the contribution to  $\mathcal{A}(u)$  from the cut is positive. Although it cannot be evaluated analytically, we can calculate its large  $u$  behaviour, which is dominated by the form of the integrand near the branch point  $\nu = m$ . This gives the long-time behaviour,

$$\mathcal{A}_{\text{cut}}(u) \sim \left(\frac{M^2 u}{2\omega}\right)^{-3/2} e^{-i\frac{2m^2 u}{\omega}}, \quad (5.24)$$

up to  $u$ -independent prefactors.<sup>9</sup>

The combined result for  $\mathcal{A}(u)$  is plotted numerically in Fig. 3. For large  $u$ , the cut contribution to the amplitude itself (factoring out the overall  $e^{-i\frac{M^2 u}{2\omega}}$  phase), oscillates with a scale  $u_O = \frac{2\omega}{4m^2 - M^2}$  while decaying as a power law on the scale  $u_D = \frac{2\omega}{M^2}$ , and ultimately  $\mathcal{A}(u)$  converges to the constant  $\mathcal{A}_{\text{pole}}(u)$ . Note that the scale of the oscillations increases as  $M^2$  approaches (from below) the threshold  $4m^2$ . We recognise the ratio

$$Z = \left| \frac{\mathcal{A}(\infty)}{\mathcal{A}(0)} \right| = \left[ 1 - \frac{\partial \Pi(p)}{\partial p^2} \Big|_{p^2 = -M^2} \right]^{-1} = \frac{1}{1 + \frac{e^2}{(4\pi)^2} \frac{1}{2M^2} f\left(\frac{4m^2}{M^2}\right)}, \quad (5.25)$$

---

<sup>9</sup>In the large  $u$  limit, we use the fact that  $\int_{2m}^{\infty} d\nu \nu e^{-\frac{i\nu^2 u}{2\omega}} \sqrt{\nu - 2m}$  is given approximately by  $\frac{\sqrt{\pi}}{2} u^{-3/2} \exp\left(-\frac{2im^2 u}{\omega} - \frac{3i\pi}{2}\right)$ .

as the wave-function renormalization factor evaluated in the equilibrium theory. In particular, due to the positivity of the spectral density the contribution from the cut is positive and therefore the sum rule (5.20) implies  $Z < 1$ . So intuitively what is happening is that we are seeing the dressing of the field  $A$  in real time by the creation of  $\phi$  pairs even though we are below the threshold for decay. The fact that such a decay cannot happen energetically is by-passed here because we are looking over a finite region of time and consequently the energy has an associated uncertainty which allows the below-threshold process to occur. It is important that this effect does not involve a constant rate but is just a transient effect.

We now discuss what happens above threshold, when  $M > 2m$ . In this case the position of the single particle pole (5.6)  $s_0$  moves off the imaginary axis. To  $\mathcal{O}(e^2)$

$$s_0 = \frac{M^2}{2i\omega} + \frac{1}{2\omega} \text{Im} \tilde{\Sigma} \left( \frac{M^2}{2i\omega} \right) + \dots . \quad (5.26)$$

Notice that the mass counterterm is now specified more precisely as

$$\delta M^2 = -\text{Re} \tilde{\Sigma} \left( \frac{M^2}{2i\omega} \right) , \quad (5.27)$$

Since the 2-particle cut arises from a square-root branch point, the function  $\tilde{\Sigma}(s)$  is defined on a 2-sheeted cover of the  $s$ -plane with the Bromwich contour on what we call the upper sheet. A closer analysis reveals that with the 2-particle cut lying along the negative imaginary axis in the  $s$ -plane, the single particle pole lies on the lower sheet. Hence, the Bromwich integral only receives a contribution from the cut. However, in order to determine the large  $u$  behaviour we can deform the cut to the left of the pole as illustrated in the right-hand side of Fig. 2 and then the pole *does* contribute

$$\mathcal{A}_{\text{pole}}(u) = \mathcal{A}(0) e^{\frac{M^2 u}{2i\omega} - \frac{\pi}{2\omega} \rho(M) u} \left[ 1 + \frac{1}{2i\omega} \tilde{\Sigma}' \left( \frac{M^2}{2i\omega} \right) + \dots \right] , \quad (5.28)$$

to order  $\mathcal{O}(e^2)$ . So above threshold, for large  $u$  the  $A$  decays into  $\phi$  pairs with a characteristic life-time

$$\Gamma = \frac{\pi}{2\omega} \rho(M) = \frac{e^2}{(4\pi)^2} \frac{\pi}{4\omega} \sqrt{1 - \frac{4m^2}{M^2}} . \quad (5.29)$$

The behaviour of the field is illustrated in Fig. 3. Again note that as  $M^2$  approaches threshold (from above), the lifetime becomes large.

### 5.3 $A\phi^2$ in $d = 6$ : field renormalization and initial conditions

We now consider the initial value problem for a theory,  $A\phi^2$  in  $d = 6$ ,<sup>10</sup> which requires a UV divergent field (wave-function) renormalization. The theory is asymptotically free and short distance physics remains perturbative. Nevertheless, we would expect difficulties with applying the Type I initial conditions due to the UV divergence when the interaction is switched on instantaneously at the initial value surface  $u = u_0 = 0$ . Indeed, this is what happens, and we illustrate these difficulties before moving on to a solution of the initial value problem for Type II and Type III initial conditions, where  $u_0 \rightarrow -\infty$ .

Incorporating a field renormalization to  $\mathcal{O}(e^2)$  in the equation of motion (3.17), we have

$$-2i\omega Z\dot{\mathcal{A}}(u) + M_B^2 Z\mathcal{A}(u) + \int_0^u du' \tilde{\Pi}_B(u, u'; \omega, p)\mathcal{A}(u') = 0 . \quad (5.30)$$

The solution for  $\tilde{\mathcal{A}}(s)$  is then

$$\tilde{\mathcal{A}}(s) = \frac{2i\omega Z\mathcal{A}(0)}{(2i\omega s - M_B^2)Z - \tilde{\Sigma}_B(s)} . \quad (5.31)$$

The Laplace transform kernel  $\tilde{\Sigma}_B(s)$  is again obtained from the flat space  $\Pi_B(p^2)$  by the substitution  $p^2 \rightarrow -2i\omega s$ . In dimensional regularization, this gives

$$\tilde{\Sigma}_B(s) = -\frac{e^2}{(4\pi)^3} \int_0^1 d\xi [m^2 - 2i\omega s\xi(1-\xi)] \left( \frac{1}{d-6} + \frac{1}{2} \log \left[ \frac{m^2 - 2i\omega s\xi(1-\xi)}{4\pi\mu^2 e^{-\gamma}} \right] \right) , \quad (5.32)$$

for the bare kernel. Physical mass renormalization is as before,

$$\tilde{\Sigma}_r(s) = \tilde{\Sigma}_B(s) - \tilde{\Sigma}_B\left(\frac{M^2}{2i\omega}\right) , \quad (5.33)$$

where  $M$  is the renormalized mass, and the field renormalization corresponds to the further subtraction

$$\tilde{\Sigma}(s) = \tilde{\Sigma}_r(s) - (Z-1)(2i\omega s - M^2) , \quad (5.34)$$

---

<sup>10</sup>The extra dimension for  $d = 6$  are taken to be a trivial extension of the transverse space, with the 6-dimensional plane wave metric being simply  $ds^2 = 2dudV + C_{ab}(u)dx^a dx^b$  with  $a, b = 1, \dots, 4$ .

where in  $\overline{\text{MS}}$ ,  $Z = 1 + \frac{1}{6} \frac{e^2}{(4\pi)^3} \left( \frac{1}{d-6} + \log 4\pi - \gamma \right)$ . Note that this introduces a scheme dependence into  $\tilde{\Sigma}(s)$ , though of course physical results must be independent of this choice. We therefore find the following expression for  $\tilde{\mathcal{A}}(s)$ :

$$\tilde{\mathcal{A}}(s) = \frac{2i\omega Z \mathcal{A}(0)}{2i\omega s - M^2 - \tilde{\Sigma}(s)}, \quad (5.35)$$

where the renormalized kernel in  $\overline{\text{MS}}$  is:

$$\begin{aligned} \tilde{\Sigma}(s) = & -\frac{1}{2} \frac{e^2}{(4\pi)^3} \int_0^1 d\xi \left( [m^2 - 2i\omega s \xi(1-\xi)] \log [m^2 - 2i\omega s \xi(1-\xi)] \mu^{-2} \right. \\ & \left. - [m^2 - M^2 \xi(1-\xi)] \log [m^2 - M^2 \xi(1-\xi)] \mu^{-2} \right). \end{aligned} \quad (5.36)$$

The physical mass renormalization condition we are using ensures that the renormalized kernel satisfies the condition  $\tilde{\Sigma}(\frac{M^2}{2i\omega}) = 0$ . In the following section on curved spacetime, we will find it convenient to use a RG scheme where the freedom to add a further finite counterterm in  $Z$  is used to impose the additional condition  $\tilde{\Sigma}'(\frac{M^2}{2i\omega}) = 0$ . This is achieved by the definition<sup>11</sup>

$$\tilde{\Sigma}(s) = \tilde{\Sigma}_B(s) - \tilde{\Sigma}_B\left(\frac{M^2}{2i\omega}\right) - \left(s - \frac{M^2}{2i\omega}\right) \tilde{\Sigma}'_B\left(\frac{M^2}{2i\omega}\right). \quad (5.37)$$

The spectral function, which is independent of renormalization issues, is identified as before, and a short calculation gives:

$$\begin{aligned} \rho(\nu) &= -\frac{1}{\pi} \text{Im} \tilde{\Sigma}\left(\frac{\nu^2}{2i\omega}\right) \\ &= \frac{1}{12} \frac{e^2}{(4\pi)^3} \theta(\nu - 2m) \nu^2 \left(1 - \frac{4m^2}{\nu^2}\right)^{3/2}. \end{aligned} \quad (5.38)$$

This time, because of the extra  $\nu^2$  factor in (5.38) compared to (5.15), the relation to the kernel is via a twice-subtracted dispersion relation,

$$\tilde{\Sigma}\left(\frac{\nu^2}{2i\omega}\right) = \tilde{\Sigma}(0) + \nu^2 \tilde{\Sigma}'(0) - \nu^3 \int_{-\infty}^{\infty} \frac{d\nu'}{\nu'^3} \frac{\rho(\nu')}{\nu' - \nu - i0^+}. \quad (5.39)$$

This may again be checked explicitly by performing the integrals over  $\nu$  and  $\xi$  in (5.39) and (5.36).<sup>12</sup>

<sup>11</sup>We assume here that the subtractions are real, which will be the case below threshold where  $M^2 < 4m^2$ . In general, the subtractions are specified as the real parts of  $\tilde{\Sigma}_B(\frac{M^2}{2i\omega})$  and  $\tilde{\Sigma}'_B(\frac{M^2}{2i\omega})$ .

<sup>12</sup>The integral over the spectral function on the rhs of (5.39) is explicitly

$$\frac{1}{6} \frac{e^2}{(4\pi)^3} \left[ (z-1)^{3/2} \arctan \frac{1}{\sqrt{z-1}} + \frac{4}{3} - z \right],$$

for  $z > 1$ , where here  $z = \frac{4m^2}{\nu^2}$ .

The first indication of problems with Type I initial conditions is the remaining presence of the  $Z$  factor in the numerator of (5.35). Essentially, this is indicating that in a theory requiring field renormalization, and in the absence of a physical short-distance cut-off, the initial value at  $u_0 = 0$  must be divergent if the long-time evolution is to remain finite. The analytic structure is the same as for the  $A\phi^2$  theory in  $d = 4$ , and the inverse Laplace transform again separates, below threshold, into distinct  $\mathcal{A}_{\text{pole}}(u)$  and  $\mathcal{A}_{\text{cut}}(u)$  contributions. For Type I initial conditions, the analysis of the pole contribution is very similar to the 4-dim theory. The new problem arises with the cut contribution where, substituting the spectral function, we find to  $\mathcal{O}(e^2)$ :

$$\mathcal{A}_{\text{cut}}(u) = \frac{1}{6} \mathcal{A}(0) \frac{e^2}{(4\pi)^3} \int_{2m}^{\infty} d\nu \frac{\nu^3}{(\nu^2 - M^2)^2} \left(1 - \frac{4m^2}{\nu^2}\right)^{3/2} e^{-\frac{i\nu^2 u}{2\omega}}. \quad (5.40)$$

Contrast this with the corresponding expression for  $A\phi^2$  in  $d = 4$ , eq.(5.23). Here, the  $\nu$  integral is log divergent for large  $\nu^2$ , due to the extra  $\nu^2$  power dependence in  $\rho(\nu)$ . In turn, this can be traced back to the behaviour of the kernel for large  $s$ , where from (5.36) we see that  $\tilde{\Sigma}(s) \sim s \log s$  rather than  $\tilde{\Sigma}(s) \sim \log s$  in the  $d = 4$  theory.

To evade these problems, which are intimately related to the divergent short distance behaviour, we choose instead to analyse the theory using Type II or Type III initial conditions. This shifts the divergent physics off to the switch-on surface at  $u_0 \rightarrow -\infty$ , so that we start the initial value problem from  $u = 0$  with a renormalized field, already at least partially dressed.

The Laplace transform of the equation of motion (3.18) for Type II initial conditions is:

$$-2i\omega Z(s\tilde{\mathcal{A}}(s) - \mathcal{A}(0)) + M_B^2 Z\tilde{\mathcal{A}}(s) + \tilde{\Sigma}_B(s)\tilde{\mathcal{A}}(s) - \mathcal{A}(0)\frac{1}{s}(\tilde{\Sigma}_B(s) - \tilde{\Sigma}_B(0)) = 0, \quad (5.41)$$

Solving this, and writing in terms of renormalized quantities, we have

$$\tilde{\mathcal{A}}(s) = \frac{\mathcal{A}(0)}{s} \left[ 1 + \frac{\tilde{\Sigma}(0) + M^2}{2i\omega s - M^2 - \tilde{\Sigma}(s)} \right]. \quad (5.42)$$

It is straightforward to check directly in this expression how the subtractions (5.33), (5.34) implement the usual mass and field renormalizations. In particular, note how all factors of  $Z$  are absorbed by the subtraction (5.34).

Once again, this has a pole at  $s = s_0$  (see (5.6)) and a cut with branch point at  $2i\omega s = 4m^2$  from (5.36). Note that, for  $M^2 \neq 0$ , there is no pole at  $s = 0$  despite the

1/s factor in (5.42). The inverse Laplace transform is evaluated as usual, and we find

$$\mathcal{A}(u) = \mathcal{A}_{\text{pole}}(u) + \mathcal{A}_{\text{cut}}(u) , \quad (5.43)$$

where now

$$\mathcal{A}_{\text{pole}}(u) = \mathcal{A}(0)e^{-\frac{iM^2u}{2\omega}} \frac{1 + \frac{\tilde{\Sigma}(0)}{M^2}}{1 - \frac{1}{2i\omega}\tilde{\Sigma}'(\frac{M^2}{2i\omega})} , \quad (5.44)$$

and

$$\mathcal{A}_{\text{cut}}(u) = 2\mathcal{A}(0) \left(1 + \frac{\tilde{\Sigma}(0)}{M^2}\right) M^2 \int_{2m}^{\infty} \frac{d\nu}{\nu} \frac{\rho(\nu)e^{-i\frac{\nu^2u}{2\omega}}}{[\nu^2 - M^2 - \text{Re}\tilde{\Sigma}(\frac{M^2}{2i\omega})]^2 + \pi^2\rho(\nu)^2} , \quad (5.45)$$

Note the differences from the Type I case – the extra  $\left(1 + \frac{\tilde{\Sigma}(0)}{M^2}\right)$  factor, which affects the asymptotic ratio  $\mathcal{A}(u)/\mathcal{A}(0)$ , and the extra  $M^2/\nu^2$  factor in the cut contribution, which plays the role of a subtraction in a normal dispersion relation in providing the necessary convergence factor for the integral over  $\nu$ .

It is instructive to evaluate these expressions at  $\mathcal{O}(e^2)$ . For the pole contribution, we have:

$$\begin{aligned} \mathcal{A}_{\text{pole}}(u) &= \mathcal{A}(0)e^{-\frac{iM^2u}{2\omega}} \left[ 1 + \frac{\tilde{\Sigma}(0)}{M^2} + \frac{1}{2i\omega}\tilde{\Sigma}'\left(\frac{M^2}{2i\omega}\right) \right] \\ &= \mathcal{A}(0)e^{-\frac{iM^2u}{2\omega}} \left[ 1 + \frac{1}{12} \frac{e^2}{(4\pi)^3} h\left(\frac{4m^2}{M^2}\right) \right] , \end{aligned} \quad (5.46)$$

where

$$h(z) = 3z\sqrt{z-1} \arctan \frac{1}{\sqrt{z-1}} - 3z + 1 . \quad (5.47)$$

Since  $h(z) < 0$  for all  $z > 1$  (i.e. below threshold,  $M^2 < 4m^2$ ), the effect of the pole contribution is to give a  $u$ -independent reduction in the amplitude. Note that the renormalization scheme ambiguity cancels in the combination  $\tilde{\Sigma}(0) + \frac{M^2}{2i\omega}\tilde{\Sigma}'(\frac{M^2}{2i\omega})$ , as is easily checked from (5.34); in particular, this ensures the disappearance of any  $\mu$ -dependence in  $h(z)$ .

At  $\mathcal{O}(e^2)$ , substituting the explicit form (5.38) of the spectral function, we find the cut contribution is

$$\mathcal{A}_{\text{cut}}(u) = \mathcal{A}(0) \frac{1}{6} \frac{e^2}{(4\pi)^3} M^2 \int_{2m}^{\infty} d\nu \frac{\nu}{(\nu^2 - M^2)^2} \left(1 - \frac{4m^2}{\nu^2}\right)^{3/2} e^{-\frac{i\nu^2u}{2\omega}} . \quad (5.48)$$

For  $u = 0$ , the integral over  $\nu$  can be performed analytically and, together with (5.44), confirms the sum rule  $\mathcal{A}_{\text{pole}}(0) + \mathcal{A}_{\text{cut}}(0) = \mathcal{A}(0)$  required for consistency.

The physical picture emerging from (5.46) and (5.48) closely resembles that already described for the  $A\phi^2$  theory in  $d = 4$ . Evaluating the cut contribution for large  $u$ , we find

$$\mathcal{A}_{\text{cut}}(u) \sim \left(\frac{M^2 u}{2\omega}\right)^{-5/2} e^{-\frac{i2m^2 u}{\omega}}, \quad (5.49)$$

similar to (5.24) but with a faster power law decay. The overall behaviour is similar to Fig. 3 in the below threshold case. Once again, factoring out the overall phase  $e^{-\frac{iM^2}{2\omega}}$ , the amplitude oscillates on a scale  $u_O = \frac{2\omega}{4m^2 - M^2}$ , while the power law decay is on a scale  $u_D = \frac{2\omega}{M^2}$ . Although the field at the initial value surface is renormalized, rather than bare as with Type I initial conditions, once the source holding the amplitude fixed at  $\mathcal{A}(0)$  for all  $u < 0$  is removed, the field relaxes in real time, tending asymptotically to the constant value given by  $\mathcal{A}_{\text{pole}}(u)$ . This further, finite, dressing of the field, as well as the transient behaviour for small  $u$  is of course consistent with the general unitarity constraints encoded in the optical theorem.

It is also instructive to analyse this theory with the Type III initial conditions introduced in section 3.1. The Laplace transform of the equation of motion in this case is (compare (5.41)):

$$\begin{aligned} -2i\omega Z \left( s\tilde{\mathcal{A}}(s) - \mathcal{A}(0) \right) + M_B^2 Z \tilde{\mathcal{A}}(s) + \tilde{\Sigma}_B(s) \tilde{\mathcal{A}}(s) \\ - \frac{\mathcal{A}(0)}{s - \frac{M^2}{2i\omega}} \left( \tilde{\Sigma}_B(s) - \tilde{\Sigma}_B\left(\frac{M^2}{2i\omega}\right) \right) = 0, \end{aligned} \quad (5.50)$$

where the inclusion of the phase with the renormalized mass makes a crucial modification to the final term. The solution is

$$\tilde{\mathcal{A}}(s) = \frac{\mathcal{A}(0)}{s - \frac{M^2}{2i\omega}} \left[ 1 + \frac{\tilde{\Sigma}\left(\frac{M^2}{2i\omega}\right)}{2i\omega s - M^2 - \tilde{\Sigma}(s)} \right]. \quad (5.51)$$

Again, we see how all the renormalization counterterms are absorbed into the subtractions in the renormalized kernel.

However, for flat spacetime – though *not* in curved spacetime as we shall shortly see – there is a further simplification. Here, it follows immediately from the mass and field renormalization conditions (5.33) and (5.34) that  $\tilde{\Sigma}\left(\frac{M^2}{2i\omega}\right) = 0$ . So then, we simply have

$$\tilde{\mathcal{A}}(s) = \frac{\mathcal{A}(0)}{s - \frac{M^2}{2i\omega}} \quad (5.52)$$



and only the simple pole remains. The inverse Laplace transform gives

$$\mathcal{A}(u) = \mathcal{A}(0)e^{-\frac{iM^2u}{2\omega}} . \quad (5.53)$$

The physical explanation is simple. Since for these Type III conditions, the field at the initial value surface has been prepared in a fully dressed, renormalized state, it simply continues with that evolution for  $u > 0$ . This is, however, special to flat spacetime. As we see in the next section, the subsequent evolution in curved spacetime can be highly non-trivial.

#### 5.4 Quantum electrodynamics

Our final example is quantum electrodynamics which, as well as requiring a UV divergent field renormalization, is not asymptotically free. As we shall see, this introduces further problems with Type I initial conditions. We quote results for QED with both scalar and spinor ‘‘electrons’’, with non-zero mass  $m$ .

The source-free equation of motion for QED in curved spacetime takes the form

$$\frac{1}{\sqrt{g}}\partial_\nu(\sqrt{g}g^{\mu\lambda}g^{\nu\sigma}F_{\lambda\sigma}) + \int d^4x' \sqrt{g(x')} \Pi^{\mu\nu}(x, x')A_\nu(x') = 0 . \quad (5.54)$$

In a plane-wave background, the solutions of the classical Maxwell equations are

$$\Phi_{p,\mu}^{(i)}(x) = \delta_{\mu a} E^i_a(u) \Phi_p(x) . \quad (5.55)$$

Here,  $E_{ia}(u)$  is the zweibein for the transverse metric  $C_{ab}(u)$  defined in (2.5). The index,  $i = 1, 2$  (which are associated to the transverse Brinkmann coordinates) labels the two physical polarization states. To solve the initial-value problem, we then make a similar ansatz to the scalar  $A\phi^2$  theory (compare (3.11)):

$$A_\mu^{(i)}(x) = \mathcal{A}_{ij}(u) \Phi_{p,\mu}^{(j)} . \quad (5.56)$$

Specialising to flat spacetime for the remainder of this section, where the polarization dependence is trivial and  $\mathcal{A}_{ij}(u) = \mathcal{A}(u)\delta_{ij}$ , the full equation of motion reduces to the following equation for a single complex amplitude  $\mathcal{A}(u)$ :

$$-2i\omega\dot{\mathcal{A}}(u) + \int_{u_0}^u du' \Sigma(u, u')\mathcal{A}(u') = 0 , \quad (5.57)$$

subject to the various initial conditions considered above. The Laplace transform of the kernel  $\tilde{\Sigma}(s)$  is determined from the usual momentum-space vacuum polarization tensor  $\Pi(p^2)$  as in (5.10) with the substitution  $p^2 \rightarrow -2i\omega s$ :

$$\tilde{\Sigma}(s) = \Pi(-2i\omega s) , \quad (5.58)$$

where for scalar QED, in dimensional regularisation,

$$\Pi_B(p^2) = -p^2 \left[ \frac{\alpha}{6\pi} \frac{1}{(d-4)} + \frac{\alpha}{4\pi} \int_0^1 d\xi (1-2\xi)^2 \log \left( \frac{m^2 + \xi(1-\xi)p^2}{4\pi\mu^2 e^{-\gamma_E}} \right) \right] . \quad (5.59)$$

Note again that we are free to use the usual Feynman vacuum polarization here since it gives the same result in (5.57) as the Schwinger-Keldysh form.

Gauge invariance ensures there is no mass renormalization and the field renormalization in  $\overline{\text{MS}}$  is implemented by the subtraction

$$\begin{aligned} \tilde{\Sigma}(s) &= \tilde{\Sigma}_B(s) - (Z-1)2i\omega s \\ &= 2i\omega s \frac{\alpha}{4\pi} \int_0^1 d\xi (1-2\xi)^2 \log \left( \frac{m^2 - 2i\omega s \xi(1-\xi)}{\mu^2} \right) . \end{aligned} \quad (5.60)$$

Note that  $\tilde{\Sigma}(0) = 0$ . The spectral function is readily evaluated as before and we find<sup>13</sup>

$$\rho(\nu) = -\frac{1}{\pi} \text{Im} \tilde{\Sigma} \left( \frac{\nu^2}{2i\omega} \right) = \frac{\alpha}{12\pi} \theta(\nu - 2m) \nu^2 \left( 1 - \frac{4m^2}{\nu^2} \right)^{3/2} . \quad (5.61)$$

With Type I initial conditions, the solution to the initial value problem (compare (5.35)) is given by the inverse Laplace transform

$$\tilde{\mathcal{A}}(s) = \frac{2i\omega Z \mathcal{A}(0)}{2i\omega s - \tilde{\Sigma}(s)} . \quad (5.62)$$

Once again, the analytic structure of the solution consists of a single particle pole, this time at  $s = 0$ , and the 2-particle threshold cut starting at  $2i\omega s = -4m^2$ . In addition,

---

<sup>13</sup> The equivalent results for spinor QED are

$$\tilde{\Sigma}(s) = 2i\omega s \frac{2\alpha}{\pi} \int_0^1 d\xi \xi(1-\xi) \log \left( \frac{m^2 - 2i\omega s \xi(1-\xi)}{\mu^2} \right)$$

and

$$\rho(\nu) = \frac{\alpha}{3\pi} \theta(\nu - 2m) \nu^2 \left( 1 + \frac{2m^2}{\nu^2} \right) \left( 1 - \frac{4m^2}{\nu^2} \right)^{1/2} .$$

though, there is the infamous Landau pole  $s = s_L$  determined by the solution of the equation,

$$1 - \frac{\alpha}{4\pi} \int_0^1 d\xi (1 - 2\xi)^2 \log \left( \frac{m^2 - 2i\omega s_L \xi(1 - \xi)}{\mu^2} \right) = 0 . \quad (5.63)$$

Notice that this pole is at a non-perturbatively large Euclidean value of the momentum  $p^2 \sim e^{12\pi/\alpha}$ .

The contribution from the simple pole at  $s = 0$  is just a constant

$$\mathcal{A}_{\text{pole}}(u) = \frac{Z\mathcal{A}(0)}{1 - \frac{1}{2i\omega} \tilde{\Sigma}'(0)} . \quad (5.64)$$

Again, the explicit presence of  $Z$  the fundamental problem of Type I conditions in a theory requiring a UV divergent field renormalization, although once again we see that to  $\mathcal{O}(e^2)$ , the right-hand side of (5.64) is scheme independent.

The cut contribution, at  $\mathcal{O}(\alpha)$  is

$$\mathcal{A}_{\text{cut}}(u) = 2\mathcal{A}(0) \int_{2m}^{\infty} \frac{d\nu}{\nu^3} \rho(\nu) e^{-\frac{i\nu^2 u}{2\omega}} . \quad (5.65)$$

With the spectral function (5.61),  $\rho(\nu) \sim \nu^2$  for large  $\nu$  and the cut contribution is logarithmically divergent. The power counting responsible for this is of course linked to the presence of UV divergences.

Finally, the contribution from the Landau pole is the rapidly oscillating function

$$\mathcal{A}_{\text{LP}}(u) = \frac{e^{s_L u}}{\alpha} , \quad (5.66)$$

since  $s_L$  is purely imaginary. This contribution is non-perturbatively large and contaminates the solution for  $\mathcal{A}(u)$  at large  $u$ . This reflects the fact that not only does QED require a UV divergent field renormalization but it is not asymptotically free, so the short-distance physics is non-perturbative.

These problems are specific to Type I initial conditions and arise because the interaction is being turned on at the initial value surface,  $u_0 = 0$ .<sup>14</sup> Instead, we can analyse the theory with initial conditions with  $u_0 \rightarrow -\infty$ . Since gauge invariance

---

<sup>14</sup> Another way to see how problems arise, not specific to flat spacetime, is to recall from (3.36) that

$$\mathcal{Q}^{(1)}(u) = -\frac{1}{2\omega} \int_{u_0}^u du'' \int_{u_0}^{u''} du' \Sigma(u'', u') .$$

ensures the photon in QED is massless, in this theory there is no distinction between Type II and Type III initial conditions. From (5.42), we immediately have the solution

$$\tilde{\mathcal{A}}(s) = \frac{\mathcal{A}(0)}{s} \left( 1 + \frac{\tilde{\Sigma}(0)}{2i\omega s - \tilde{\Sigma}(s)} \right). \quad (5.67)$$

However, in flat spacetime (though *not* in curved spacetime)  $\tilde{\Sigma}(0) = 0$  and so the solution of the initial-value problem is trivial:  $\tilde{\mathcal{A}}(s)$  only has the simple pole at  $s = 0$  and  $\mathcal{A}(u) = \mathcal{A}(0)$  for all  $u$ . Even the Landau pole is absent. The photon field is set up at the initial value surface  $u = 0$  already in a renormalized, fully-dressed state. No further dressing can take place in flat spacetime, so the evolution for  $u > 0$  is trivial. However, this initial condition will be particularly appropriate in the following section when we analyse QFTs in curved spacetime, since it allows us to distinguish clearly the effects of curvature on dressing from the short-distance transient phenomena present even in flat spacetime.

## 6 Field Propagation in Symmetric Plane Waves

We now return to curved spacetime and in this section consider field evolution in a special class of plane-wave spacetimes where the metric is  $u$ -translation invariant. These are the symmetric plane waves, or Cahen-Wallach spaces.

The  $u$ -translation symmetry means that the initial value problem can be analysed using all the formalism of the Laplace transform method discussed in the previous section. We also note the relation with the general formalism for the refractive index and optical theorem described in sections 3 and 4 and our previous work [3, 4].

### 6.1 The initial value problem and renormalization in curved spacetime

Since we are interested here in the effects of curvature on the evolution of the field and not on transient phenomena, we consider initial conditions with  $u_0 \rightarrow -\infty$ , in particular Type III.

---

In QED, the imaginary part involves the integral

$$\int_{u_0}^u du'' \int_{u_0}^u du' \frac{1}{(u'' - u' - i0^+)^2}.$$

which is divergent. In contrast, for the scalar  $A\phi^2$  theory in  $d = 4$ , the same integral has one less power in the denominator and is convergent.

The Laplace transform analysis of the equation of motion goes through exactly as before and so, for massive scalar  $A\phi^2$  theory, we find

$$\tilde{\mathcal{A}}(s) = \frac{\mathcal{A}(0)}{s - \frac{M^2}{2i\omega}} \left[ 1 + \frac{\tilde{\Sigma}\left(\frac{M^2}{2i\omega}\right)}{2i\omega s - M^2 - \tilde{\Sigma}(s)} \right] \quad (6.1)$$

written entirely in terms of the renormalized quantities. The subtractions which implement mass and field renormalization are the same as in the flat spacetime theory since the UV divergences are curvature independent. However, this has important implications for the final results for  $\mathcal{A}(u)$ . Implementing the physical mass renormalization and the scheme choice (5.37) for the field renormalization (adapted for curved spacetime) the required subtraction in the kernel is

$$\tilde{\Sigma}(s) = \tilde{\Sigma}_B(s) - \text{Re} \tilde{\Sigma}_B^{\text{flat}}\left(\frac{M^2}{2i\omega}\right) - \left(s - \frac{M^2}{2i\omega}\right) \text{Re} \tilde{\Sigma}_B^{\text{flat}'}\left(\frac{M^2}{2i\omega}\right). \quad (6.2)$$

While this ensures the renormalization conditions  $\tilde{\Sigma}^{\text{flat}}\left(\frac{M^2}{2i\omega}\right) = 0$  and  $\tilde{\Sigma}^{\text{flat}'}\left(\frac{M^2}{2i\omega}\right) = 0$  in flat spacetime, crucially this is no longer true in curved spacetime and as a result the expression (6.1) for  $\tilde{\mathcal{A}}(s)$  for Type III initial conditions becomes non-trivial.

The simple pole in the inverse Laplace transform

$$\mathcal{A}(u) = \mathcal{A}(0) \int_{c-i\infty}^{c+i\infty} \frac{ds}{2\pi i} e^{su} \frac{1}{s - \frac{M^2}{2i\omega}} \left[ 1 + \frac{\tilde{\Sigma}\left(\frac{M^2}{2i\omega}\right)}{2i\omega s - M^2 - \tilde{\Sigma}(s)} \right] \quad (6.3)$$

is shifted to  $s_0$ , where now

$$2i\omega s_0 = M^2 + \tilde{\Sigma}\left(\frac{M^2}{2i\omega}\right). \quad (6.4)$$

Evaluating the pole contribution, we therefore find

$$\mathcal{A}_{\text{pole}}(u) = \mathcal{A}(0) e^{-\frac{iM^2 u}{2\omega}} e^{-\frac{i}{2\omega} \tilde{\Sigma}\left(\frac{M^2}{2i\omega}\right) u} \left[ 1 - \frac{1}{2i\omega} \tilde{\Sigma}'\left(\frac{M^2}{2i\omega}\right) + \dots \right], \quad (6.5)$$

to  $\mathcal{O}(e^2)$  in the pre-factor. As before, the cut contribution goes to zero for large  $u$ , so (6.5) gives the asymptotic solution for the amplitude  $\mathcal{A}(u)$ . This should be compared with (5.28) for  $\mathcal{A}(u)$  in flat spacetime above threshold. Clearly, (6.5) opens up the possibility of particle decay in curved spacetime even below threshold. Also note the similarity with (3.34), which shows that the Laplace transform method has automatically performed the DRG resummation of secular terms into the exponent.

In what follows, we use the leading order approximation

$$\mathcal{A}(u) = \mathcal{A}(0) e^{-\frac{iM^2 u}{2\omega}} e^{-\frac{i}{2\omega} \tilde{\Sigma}\left(\frac{M^2}{2i\omega}\right) u}, \quad (6.6)$$

to study the evolution of the field amplitude in a variety of symmetric plane-wave spacetimes. The identifications with the general formalism in sections 3.3 and 3.4 are evident.

The kernel  $\tilde{\Sigma}(s)$  for  $A\phi^2$  in  $d = 4$  is immediately read off from (3.24). The bare kernel is

$$\tilde{\Sigma}_B(s) = -\frac{1}{2} \frac{e^2}{(4\pi)^2} \int_0^1 d\xi \int_0^\infty \frac{dt}{t} \sqrt{\Delta(t)} e^{-\frac{im^2 t}{2\omega\xi(1-\xi)}} e^{-st}, \quad (6.7)$$

where we simply write  $\Delta(t)$  for the VVM determinant  $\Delta(u, u-t)$ , which is  $u$ -independent. The integral over  $t$  is defined by the Feynman prescription  $t \rightarrow t - i0^+$ , which ensures that the contour may normally be evaluated by rotating into the Euclidean region,  $t \rightarrow -it + 0^+$ . The integral is divergent at  $t = 0$ , corresponding to the usual UV divergence. Although this can be removed by a mass renormalization alone, we choose to use the scheme (6.2) and introduce a (finite) field renormalization as well. The renormalized kernel is then

$$\begin{aligned} \tilde{\Sigma}(s) = -\frac{1}{2} \frac{e^2}{(4\pi)^2} \int_0^1 d\xi \left[ \int_0^\infty \frac{dt}{t} e^{\frac{i}{2\omega} \left(M^2 - \frac{m^2}{\xi(1-\xi)}\right)t} \sqrt{\Delta(t)} e^{-\left(s - \frac{M^2}{2i\omega}\right)t} \right. \\ \left. - \text{Re} \int_0^\infty \frac{dt}{t} e^{\frac{i}{2\omega} \left(M^2 - \frac{m^2}{\xi(1-\xi)}\right)t} \left(1 - \left(s - \frac{M^2}{2i\omega}\right)t\right) \right]. \end{aligned} \quad (6.8)$$

This expression clearly simplifies at  $s = \frac{M^2}{2i\omega}$ , so the crucial exponent in (6.6) is given by

$$\text{Re} \tilde{\Sigma}\left(\frac{M^2}{2i\omega}\right) = -\frac{1}{2} \frac{e^2}{(4\pi)^2} \text{Re} \int_0^1 d\xi \int_0^\infty \frac{dt}{t} e^{\frac{i}{2\omega} \left(M^2 - \frac{m^2}{\xi(1-\xi)}\right)t} \left[\sqrt{\Delta(t)} - 1\right] \quad (6.9)$$

and

$$\text{Im} \tilde{\Sigma}\left(\frac{M^2}{2i\omega}\right) = \frac{i}{4} \frac{e^2}{(4\pi)^2} \int_0^1 d\xi \int_{-\infty}^\infty \frac{dt}{t} e^{\frac{i}{2\omega} \left(M^2 - \frac{m^2}{\xi(1-\xi)}\right)t} \sqrt{\Delta(t)}. \quad (6.10)$$

Note that there is no subtraction in the imaginary part. To derive (6.10), we need the property  $\Delta^*(-t) = \Delta(t)$  of the VVM determinant. The location of the integration contour is important. According to the Feynman prescription, it lies just *below* the real  $t$ -axis, in particular evading the pole at  $t = 0$ .

The real part of the kernel  $\tilde{\Sigma}\left(\frac{M^2}{2i\omega}\right)$  modifies the phase of  $\mathcal{A}(u)$ , while the imaginary part determines the amplitude. Note that both are explicitly  $\omega$ -dependent in curved spacetime, in contrast to the flat space case. In our previous papers, we have studied

this frequency-dependence extensively for QED with massless photons, where it determines the refractive index as described in section 3. All this analysis, including the all-important analyticity properties, goes through in the same way here for the massive  $A\phi^2$  theory with only straightforward modifications. In particular, section 7 of ref.[3] gives explicit calculations for QED in symmetric plane waves which complement the discussion that follows and can usefully be read in parallel.

Here, we wish to concentrate on the imaginary part of  $\tilde{\Sigma}(\frac{M^2}{2i\omega})$ , which determines the evolution of the amplitude  $|\mathcal{A}(u)|$  itself, and in particular to investigate the effect of curvature on the decay thresholds. For these  $u$ -translation invariant spacetimes, the amplitude  $|\mathcal{A}(u)|$  can only decrease for large enough  $u$  (beyond the transient region), in line with the general constraints of the optical theorem. This is consistent with positivity of the spectral density  $\rho(M; \omega) = -\frac{1}{\pi} \text{Im} \tilde{\Sigma}(\frac{M^2}{2i\omega})$ . We have,

$$|\mathcal{A}(u)| = |\mathcal{A}(0)| e^{-\frac{\pi}{2\omega} \rho(M)u} , \quad (6.11)$$

with the decreasing amplitude corresponding to real  $A \rightarrow \phi\phi$  decay with the well-defined rate  $\frac{\pi}{2\omega} \rho(M; \omega)$ . Moreover, the discussion in section 3 and 4 shows that this decay rate can only be non-perturbative in the curvature. However, we will find that for certain classes of plane-wave background, this decay can take place below the usual flat-space threshold.

## 6.2 Particle decay in symmetric plane-wave spacetimes

We now study the rate of  $A \rightarrow \phi\phi$  decay in symmetric plane-wave backgrounds according to the formula (6.11) with the spectral function  $\rho(M; \omega)$  given by

$$\rho(\nu; \omega) = -\frac{i}{4\pi} \frac{e^2}{(4\pi)^2} \int_0^1 d\xi \int_{-\infty}^{\infty} \frac{dt}{t} e^{-i\hat{z}t} \sqrt{\Delta(t)} . \quad (6.12)$$

Here, we have introduced the notation  $\hat{z} = \frac{1}{2\omega} (\frac{m^2}{\xi(1-\xi)} - \nu^2)$ , generalising that in section 3.4.

As a preliminary check, we recover the result already obtained in the flat space limit, where the VVM determinant  $\Delta(t) = 1$ . For  $\hat{z} > 0$ , the contour can be closed in the lower-half complex  $t$ -plane. Since there are no singularities there, the integral vanishes and we simply find  $\rho(M) = 0$ , corresponding to the below threshold case where there is no decay. For  $\hat{z} < 0$ , the contour is closed in the upper-half plane and picks up the pole at  $t = 0$ , giving

$$\rho(M) = \frac{1}{2} \frac{e^2}{(4\pi)^2} \int_{\xi_-}^{\xi_+} d\xi , \quad (6.13)$$

where  $\xi_{\pm}$  are the upper and lower solutions of the quadratic  $\xi(1 - \xi) - m^2/M^2 = 0$ , and we recover (5.29) in the above threshold case.

We now consider the three classes of symmetric plane wave in turn:

(i) *Conformally flat symmetric plane wave:*

The VVM determinant for a conformally flat symmetric plane wave, for which  $\sigma_1 = \sigma_2 = \sigma$  (with  $\sigma$  real), is

$$\Delta(u, u') = \left[ \frac{\sigma(u - u')}{\sin \sigma(u - u')} \right]^2, \quad (6.14)$$

where  $u - u' = t$ . Inserting into (6.7) and rotating the contour  $t \rightarrow -it$ , we have

$$\tilde{\Sigma}(s) = -\frac{\sigma}{2} \frac{e^2}{(4\pi)^2} \int_0^1 d\xi \int_0^\infty dt \frac{e^{-\hat{z}t}}{\sinh(\sigma t)}, \quad (6.15)$$

using  $\nu^2 = 2i\omega s$  in the definition of  $\hat{z}$ .

Using the renormalization prescription (6.2), we can evaluate the renormalized kernel exactly and find<sup>15</sup>

$$\begin{aligned} \tilde{\Sigma}(s) = \frac{1}{2} \frac{e^2}{(4\pi)^2} \int_0^1 d\xi \left[ \psi \left( \frac{1}{2} - \frac{is}{2\sigma} + \frac{m^2}{4\sigma\omega\xi(1-\xi)} \right) \right. \\ \left. - \text{Re} \log \left( \frac{m^2}{4\sigma\omega\xi(1-\xi)} - \frac{M^2}{4\sigma\omega} \right) + \text{Re} \frac{2i\omega s - M^2}{M^2 - \frac{m^2}{\xi(1-\xi)}} \right]. \end{aligned} \quad (6.16)$$

The final term is just the optional finite field renormalization factor in (6.2). We can now see explicitly how the analytic structure of the kernel is changed in curved spacetime. Since the di-gamma function  $\psi(x)$  has simple poles at  $x = 0, -1, -2, \dots$  with residue -1, it follows that  $\tilde{\Sigma}(s)$  now has an infinite series of branch points at

$$s = -\frac{2im^2}{\omega} - i(2p - 1)\sigma, \quad p = 1, 2, \dots \quad (6.17)$$

---

<sup>15</sup>In the notation of section 3 and ref.[3], (6.16) involves

$$\mathcal{F}(\hat{z}) = \psi \left( \frac{1}{2} + \frac{\hat{z}}{2\sigma} \right) - \text{Re} \log \frac{\hat{z}}{2\sigma},$$

where  $\hat{z} = \frac{1}{2\omega} \left( \frac{m^2}{\xi(1-\xi)} - M^2 \right)$ . This should be compared directly with eq.(7.6) of ref.[3]. This reference also illustrates the  $\omega$ -dependence of the QED analogues of (6.16) for conformally flat, Ricci flat and general plane-wave spacetimes.



Consequently, the 2-particle branch cut of the flat space case has become an infinite sequence of branch cuts with branch points down the negative imaginary axis.

It is useful to understand how this arises by considering a less direct method of evaluation. If we expand the denominator in (6.15) in powers of  $e^{-\sigma t}$  and then perform the  $t$  integral, using a small  $t$  cut-off  $\delta$ , we find

$$\tilde{\Sigma}_B(s) = -\frac{1}{2} \frac{e^2}{(4\pi)^2} \int_0^1 d\xi \sum_{p=1}^{\infty} \frac{2\sigma e^{-(\hat{z}+(2p-1)\sigma)\delta}}{\hat{z} + (2p-1)\sigma} \quad (6.18)$$

and (6.16) can be recovered from the summation after renormalization. In this method, we see clearly the origin of the poles, which become the branch points (6.17) after the  $\xi$  integration.

The analytic structure of  $\tilde{\Sigma}(\frac{M^2}{2i\omega})$  therefore comprises a sequence of branch cuts with branch points at

$$M^2 = 4m^2 \left( 1 + (2p-1) \frac{\omega\sigma}{2m^2} \right) \quad p = 1, 2, \dots \quad (6.19)$$

These new curvature-dependent branch points therefore depend on the parameter  $\omega\sqrt{\mathfrak{R}}/m^2$  which, as we have frequently encountered, is a characteristic scale for non-perturbative phenomena for fields propagating in curved spacetime. As we take the flat space limit, the branch points all converge on the single threshold branch point at  $M^2 = 4m^2$ .

The spectral density is found from the imaginary part of  $\tilde{\Sigma}(s)$  by integrating around the simple poles of the digamma function. This gives

$$\rho(\nu; \omega) = \frac{e^2}{(4\pi)^2} \sum_{n=0}^{n_0} \left| \frac{d\xi}{dn} \right|, \quad (6.20)$$

where  $\xi(n)$  is the root of the equation

$$n = -\frac{1}{2} + \frac{\nu^2}{4\omega\sigma} - \frac{m^2}{4\omega\sigma\xi(1-\xi)}, \quad (6.21)$$

with  $0 \leq \xi(n) \leq \frac{1}{2}$ , and  $n_0$  is the smallest integer

$$n_0 \in \mathbb{Z}, \quad n_0 \geq -\frac{1}{2} + \frac{\nu^2 - 4m^2}{4\omega\sigma}. \quad (6.22)$$

One can check that in the flat space limit  $\sigma \rightarrow 0$ , the sum over  $n$  becomes a continuum and recovers the result (5.15).

The long-distance behaviour of the initial value problem then follows from (6.11). The solution for  $|\mathcal{A}(u)|$  dissipates with a decay rate  $\Gamma = \frac{\pi}{\omega}\rho(M)$  which is non-vanishing above a threshold

$$M^2 > 4m^2 + 2\omega\sigma . \quad (6.23)$$

There is then a series of further curvature-dependent thresholds at

$$M^2 > 4m^2 + 2\omega\sigma(2n + 1) , \quad n \in \mathbb{Z} > 0 , \quad (6.24)$$

at which the decay rate  $\Gamma$  jumps discontinuously. Note that the threshold is raised relative to the flat space value and that in this case there is no below-threshold decay. We can therefore conclude that in the conformally-flat plane wave backgrounds, the curvature is suppressing the  $A \rightarrow \phi\phi$  decays.

(ii) *Ricci flat symmetric plane wave:*

If we take  $\sigma_1 = \sigma$  and  $\sigma_2 = i\sigma$ , the plane-wave is Ricci flat and the VVM determinant is

$$\Delta(u, u') = \frac{(\sigma(u - u'))^2}{\sin \sigma(u - u') \sinh \sigma(u - u')} . \quad (6.25)$$

In this case the integrand in (6.5) has branch points on the imaginary  $t$ -axis as well as the real axis.

In this case, the integral does not have a simple explicit solution as in (6.16). However, we can readily find the analytic structure of  $\tilde{\Sigma}(s)$  using the method above by expanding the integrand in a double sum coming from the  $\sin \sigma t$  and  $\sinh \sigma t$  and then perform the  $t$  integral:

$$\tilde{\Sigma}_B(s) = -\frac{1}{2} \frac{e^2}{(4\pi)^2} \int_0^1 d\xi \sum_{p,q=1}^{\infty} c_{pq} \frac{\sigma e^{-(\hat{z} + (2p - 2iq - 1)\sigma)\hat{\delta}}}{\hat{z} + (2p - 2iq - 1)\sigma} , \quad (6.26)$$

for some coefficients  $c_{pq}$ . It follows that in this case,  $\tilde{\Sigma}(s)$  has branch points at

$$s = -\frac{im^2}{2\omega} - i(2p - 2iq - 1)\sigma , \quad p, q = 1, 2, \dots . \quad (6.27)$$

The spectral density can be written in the form (see (6.10))

$$\rho(\nu; \omega) = -\frac{1}{\pi} \text{Im} \tilde{\Sigma} \left( \frac{M^2}{2i\omega} \right) = \frac{\sigma}{4} \frac{e^2}{(4\pi)^2} \int_0^1 d\xi \int_{-\infty}^{\infty} dt e^{-i\hat{z}t} \frac{1}{\sqrt{\sin \sigma t \sinh \sigma t}} . \quad (6.28)$$

The branch points on the imaginary  $t$ -axis give rise to a non-vanishing spectral density  $\rho(\nu; \omega)$  even below the threshold  $\nu = 2m$ . To see this, we evaluate the  $t$ -integral by deforming the contour so that it wraps around the negative imaginary axis. The imaginary part of  $\tilde{\Sigma}(\frac{M^2}{2i\omega})$  in the limit  $4m^2 - \nu^2 \gg \sigma\omega$  is dominated by the contribution around the first branch point at  $t = -i\frac{\pi}{\sigma}$ :

$$\begin{aligned} \rho(\nu; \omega) &\simeq \frac{e^2}{(4\pi)^2} \frac{\sqrt{2\sigma}}{4\pi} \int_0^1 d\xi \int_{\frac{\pi}{\sigma}}^{\infty} dt \frac{e^{-(\hat{z} + \frac{\sigma}{2})t}}{\sqrt{t - \frac{\pi}{\sigma}}} \\ &= \frac{e^2}{(4\pi)^2} \frac{1}{2\sqrt{2\pi}} \int_0^1 d\xi e^{-(\hat{z} + \frac{\sigma}{2})\frac{\pi}{\sigma}}. \end{aligned} \quad (6.29)$$

In the same limit the  $\xi$  integral is then dominated by the saddle-point at  $\xi = \frac{1}{2}$ :

$$\int_0^1 d\xi e^{-\frac{\pi m^2}{2\sigma\omega\xi(1-\xi)}} \simeq \sqrt{\frac{\sigma\omega}{8m^2}} e^{-\frac{2\pi m^2}{\sigma\omega}}. \quad (6.30)$$

Consequently, in this limit we have

$$\rho(\nu; \omega) \simeq \frac{e^2}{(4\pi)^2} \frac{1}{4\pi} \sqrt{\frac{\pi\omega\sigma}{4m^2}} e^{-\frac{\pi(4m^2 - \nu^2)}{2\sigma\omega} - \frac{\pi}{2}}. \quad (6.31)$$

As a consequence, the large  $u$  behaviour of the solution  $\mathcal{A}(u)$  of the initial-value problem dissipates with a characteristic decay rate

$$\Gamma = \frac{\pi}{2\omega} \rho(M; \omega) \simeq \frac{1}{8} \frac{e^2}{(4\pi)^2} \sqrt{\frac{\pi\sigma}{4m^2\omega}} e^{-\frac{\pi(4m^2 - M^2)}{2\sigma\omega} - \frac{\pi}{2}}, \quad (6.32)$$

valid when  $4m^2 - M^2 \gg \sigma\omega$ .

So for a Ricci-flat plane-wave background, the curvature induces below-threshold decays of  $A \rightarrow \phi\phi$ , with a decay rate which is non-perturbative in the curvature.

(iii) *Null energy violating symmetric plane wave:*

In this example we take  $\sigma_1 = \sigma_2 = i\sigma$  so that the VVM determinant is

$$\Delta(u, u') = \left[ \frac{\sigma(u - u')}{\sinh \sigma(u - u')} \right]^2. \quad (6.33)$$

This background violates the null-energy condition so would not be considered a valid solution of Einstein's equations. However, we are free to consider it as an example of a fixed background. It also admits a valuable check of our use of the Penrose limit to study field propagation in curved spacetimes. This is explained in the appendix B.

In this case, the integrand has simple poles on the imaginary  $t$  axis at  $t = -i\frac{n\pi}{\sigma}$ ,  $\pi \in \mathbb{Z}$ . In the below threshold regime,  $z > 0$ , the contribution is from the poles at  $t = -i\frac{n\pi}{\sigma}$ ,  $n \in \mathbb{Z} > 0$ , while in the above threshold region,  $z < 0$ , the contribution is from the poles at  $t = i\frac{n\pi}{\sigma}$ ,  $n \in \mathbb{Z} \geq 0$ . In both cases we can sum up the contribution into a common analytic function valid for either  $z < 0$  or  $z > 0$  yielding an expression for the spectral density which is valid for all  $\nu$ :

$$\rho(\nu; \omega) = \frac{1}{2} \frac{e^2}{(4\pi)^2} \int_0^1 d\xi \frac{1}{1 + e^{\frac{\pi}{2\omega\sigma} \left( \frac{m^2}{\xi(1-\xi)} - \nu^2 \right)}}. \quad (6.34)$$

It is straightforward to check that the flat-space limit is correctly recovered since as  $\sigma \rightarrow 0$  the integral only receives support from the region  $\xi_0 \leq \xi \leq 1 - \xi_0$ , where  $\xi_0$  is the smallest root of the equation  $\xi(1 - \xi) - m^2/\nu^2 = 0$ .

This expression for the spectral density  $\rho(M; \omega)$  shows that the decay  $A \rightarrow \phi\phi$  can take place even below threshold, with a rate once again non-perturbatively small in the curvature.

### 6.3 Quantum Electrodynamics

Now consider quantum electrodynamics in a symmetric plane wave background. The bare kernel for scalar QED<sup>16</sup> was evaluated in ref.[3], and it follows directly that the renormalized, Laplace transform kernel is:

$$\tilde{\Sigma}_{ij}(s) = \frac{\alpha}{\pi} \omega \int_0^1 d\xi \xi(1 - \xi) \int_0^\infty \frac{dt}{t^2} i e^{-\frac{im^2t}{2\omega\xi(1-\xi)}} \left[ \Delta_{ij}(t) \sqrt{\Delta(t)} e^{-st} - 1 - st \right]. \quad (6.35)$$

using the renormalization condition (6.2). This ensures  $\tilde{\Sigma}(0) = \tilde{\Sigma}'(0) = 0$  in flat spacetime, though not in curved spacetime, where

$$\text{Re } \tilde{\Sigma}_{ij}(0) = \frac{\alpha}{\pi} \omega \int_0^1 d\xi \xi(1 - \xi) \int_0^\infty \frac{dt}{t^2} i e^{-\frac{im^2t}{2\omega\xi(1-\xi)}} \left[ \Delta_{ij}(t) \sqrt{\Delta(t)} - \delta_{ij} \right] \quad (6.36)$$

and

$$\text{Im } \tilde{\Sigma}_{ij}(0) = \frac{1}{2} \frac{\alpha}{\pi} \omega \int_0^1 d\xi \xi(1 - \xi) \int_{-\infty}^\infty \frac{dt}{t^2} e^{-\frac{im^2t}{2\omega\xi(1-\xi)}} \Delta_{ij}(t) \sqrt{\Delta(t)}, \quad (6.37)$$

---

<sup>16</sup>The equivalent expression for spinor QED is given in eq.(5.28) of ref.[4]. Note that in refs.[3, 4] there is an overall sign error in the refractive index for scalar QED, arising from omitting the relative minus sign between the scalar and spinor loop in the vacuum polarization (corrected in arXiv versions). In particular, as we have proved here, for the symmetric plane wave examples,  $\text{Im } n(\omega)$  is always positive, whether for scalar or spinor QED.

With Type III initial conditions (equivalent to Type II for massless photons), the field  $\mathcal{A}(u)$  is given by the inverse Laplace transform as

$$\mathcal{A}(u) = \mathcal{A}(0) \int_{c-i\infty}^{c+i\infty} \frac{ds}{2\pi i} \frac{e^{su}}{s} \left( 1 + \frac{\tilde{\Sigma}(0)}{2i\omega s - \tilde{\Sigma}(s)} \right), \quad (6.38)$$

where we have suppressed the matrix indices. This is regular at  $s = 0$ , the curvature shifting the simple pole to

$$s_0 = \frac{1}{2i\omega} \tilde{\Sigma}(0). \quad (6.39)$$

The contribution from the pole is therefore

$$\mathcal{A}_{\text{pole}}(u) = \mathcal{A}(0) e^{\frac{u}{2i\omega} \tilde{\Sigma}(0)} \left[ 1 - \frac{1}{2i\omega} \tilde{\Sigma}'(0) \right]. \quad (6.40)$$

The contribution from the Landau pole is now, however, highly suppressed:

$$\mathcal{A}_{\text{LP}}(u) \sim e^{-\frac{4\pi}{\alpha} e^{i|s_L|u}}, \quad (6.41)$$

so this choice of initial conditions gives a formulation of the initial-value problem that circumvents the problems that arise from the Landau pole and leads to a consistent perturbative expansion. Once again, for large  $u$  the contribution from the cut goes to zero, so asymptotically (6.40) gives the full result for  $\mathcal{A}(u)$ .

Recalling the series of formulae in section 3.4, we see by comparison with the exponent in (6.40) that the refractive index is given to leading order by

$$n_{ij}(\omega) = \delta_{ij} - \frac{1}{2\omega^2} \tilde{\Sigma}_{ij}(0). \quad (6.42)$$

That is,

$$n_{ij}(\omega) = \delta_{ij} - \frac{\alpha}{\pi} \frac{1}{2\omega} \int_0^1 d\xi \xi(1-\xi) \mathcal{F}_{ij}(z), \quad (6.43)$$

where

$$\mathcal{F}_{ij}(z) = \int_0^\infty \frac{dt}{t^2} i e^{-izt} [\Delta_{ij}(t) \sqrt{\Delta(t)} - \delta_{ij}]. \quad (6.44)$$

This reproduces the result found originally in ref.[3]. In that paper, the analytic properties of  $n(\omega)$  are explored and an extensive discussion is given (see especially section 7 of ref.[3]) of the frequency dependence of the refractive index in symmetric plane wave backgrounds, showing how conventional dispersion relations are violated in curved spacetime while causality is maintained. Just as for the scalar  $A\phi^2$  theory described in the last section, we find examples of backgrounds, notably the Ricci flat plane waves, where  $\text{Im } n(\omega) = \frac{\pi}{2\omega^2} \rho(0)$  is non-vanishing, showing that the curvature induces the (necessarily below threshold) decay of the photon into electron-positron pairs.

## 7 Homogeneous Plane Waves and Singularities

Finally, we consider the initial value problem in a class of backgrounds without  $u$ -translation symmetry. In this case,  $\text{Im } n(u; \omega)$  can be negative and it is interesting to see explicitly how this is reconciled with the optical theorem. In particular, we shall consider singular homogeneous plane waves, which we have already studied in detail in ref.[4]. These arise as Penrose limits in the near singularity region of black holes and in cosmological FRW spacetimes with an initial singularity.

The profile function for a singular homogeneous plane wave (see section 2) is  $h_{ij}(u) = \frac{1-\alpha_i^2}{4} \frac{1}{u^2} \delta_{ij}$  for some constants  $\alpha_i$ . The  $\alpha_i$  characterise the nature of the singularity and display a remarkable universality [4, 12] due to their relation with the Szekeres-Iyers classification of power-law singularities [34, 35]. As an example, the near-singularity Penrose limit of a null geodesic with non-vanishing angular momentum in the Schwarzschild metric has this form with  $\alpha_1 = \frac{1}{5}$  and  $\alpha_2 = \frac{7}{5}$ . This implies  $h_{ij} = \frac{6}{25} \frac{1}{u^2} \text{diag}(1, -1)$ . Note that, like the original spacetime, the Penrose limit is Ricci flat. In general the parameters  $\alpha_i$  are real and  $\geq 0$ , or imaginary.

The VVM matrix can easily be extracted from the equation for the geodesics in (2.13):

$$\frac{dz^i}{du^2} + \frac{1 - \alpha_i^2}{4u^2} z^i = 0 . \quad (7.1)$$

Since the equation is homogeneous, the solution for the geodesic spray  $z^i(u) = A_{ij}(u, u')$ , defined above (2.14), is

$$A_{ij}(u, u') = \alpha_i^{-1} (uu')^{(1-\alpha_i)/2} (u^{\alpha_i} - u'^{\alpha_i}) \delta_{ij} , \quad (7.2)$$

which gives the VVM matrix as

$$\Delta_{ij}(u, u') = \frac{\alpha_i (u - u') (uu')^{\frac{\alpha_i-1}{2}}}{u^{\alpha_i} - u'^{\alpha_i}} \delta_{ij} . \quad (7.3)$$

As noted in section 2, the singular homogeneous plane waves have an enhanced scaling symmetry, as a result of which the VVM matrix is a function only of the ratio  $r = u'/u$ . In particular, the VVM determinant is simply

$$\Delta(u, u') = \frac{\alpha_1 \alpha_2 (1 - r)^2 r^{-p}}{(1 - r^{\alpha_1})(1 - r^{\alpha_2})} , \quad (7.4)$$

where  $p = 1 - \frac{(\alpha_1 + \alpha_2)}{2}$ . Note  $p < 1$  for  $\alpha_i > 0$ . The leading behaviour for large and small  $r$  follows immediately:

$$\Delta(r) \sim \sqrt{\alpha_1 \alpha_2} r^p \quad (r \rightarrow \infty), \quad \Delta(r) \sim \sqrt{\alpha_1 \alpha_2} r^{-p} \quad (r \rightarrow 0), \quad (7.5)$$

while  $\Delta(r) = 1$  in the limit  $r \rightarrow 1$ .

We shall focus here on the imaginary part of the refractive index. Recall from sections 3.3, 3.4 that this is related to the field amplitude through the formula  $\mathcal{A}(u) = \mathcal{A}(u_0)(1 + i\mathcal{Q}^{(1)}(u))$  (before applying the DRG), where

$$\text{Im } \mathcal{Q}^{(1)}(u) = \omega \int_{u_0}^u du'' \text{Im } n(u''; \omega). \quad (7.6)$$

We consider both scalar  $A\phi^2$  theory and QED which, as we see, exhibit distinct and interesting physical effects.

*A $\phi^2$  theory:*

For the purely scalar  $A\phi^2$  theory in  $d = 4$ ,

$$\text{Im } n(u; \omega) = \frac{e^2}{(4\pi)^2} \frac{1}{4\omega^2} \int_0^1 d\xi \text{Im } \mathcal{F}(u; z), \quad (7.7)$$

where

$$\text{Im } \mathcal{F}(u; z) = \text{Im} \int_0^{u-u_0} \frac{dt}{t} e^{-izt} \sqrt{\Delta(u, u-t)}. \quad (7.8)$$

As usual,  $z = \frac{1}{2\omega} \left( \frac{m^2}{\xi(1-\xi)} - M^2 \right)$  and we restrict to the below-threshold case where  $z$  is real and positive. Note that here we have kept  $u_0$  explicit, as in (3.36). In general, the refractive index  $n(u; u_0; \omega)$  is now a function of both  $u$  and the initial value  $u_0$ , though to simplify notation we suppress the  $u_0$  dependence and just continue to write  $n(u; \omega)$  as before.

The analysis of cosmological FRW spacetimes requires us to start from an initial value surface  $u = u_0$  with  $u_0$  finite and positive, rather than letting  $u_0 \rightarrow -\infty$  as we can do in the black hole case. This raises some important subtleties, especially with regard to renormalization, which we consider first.

It follows from the description of renormalization in the context of the Laplace transform method in section 5 that the vacuum polarization  $\tilde{\Pi}(u, u'; \omega, p)$ , incorporating the subtraction corresponding to mass renormalization, is:

$$\tilde{\Pi}(u, u'; \omega, p) = \tilde{\Pi}_B(u, u'; \omega, p) + \delta M^2 \delta(u, u'). \quad (7.9)$$

From the definition  $\delta M^2 = -\text{Re} \tilde{\Sigma}_B^{\text{flat}}\left(\frac{M^2}{2i\omega}\right)$ , together with the explicit expression (6.7) for  $\tilde{\Sigma}_B(s)$ , we therefore have

$$\tilde{\Pi}(u, u'; \omega, p) = -\frac{1}{2} \frac{e^2}{(4\pi)^2} \int_0^1 d\xi \left[ \frac{\sqrt{\Delta(u, u')}}{u - u'} e^{-iz(u-u')} - \text{Re} \int_0^\infty \frac{dt}{t} e^{-izt} \delta(u, u') \right]. \quad (7.10)$$

The refractive index itself is

$$n(u; \omega) = 1 - \frac{1}{2\omega^2} \int_{u_0}^u du' \tilde{\Pi}(u, u'; \omega, p) \quad (7.11)$$

and so, changing variable to  $t = u - u'$  in the first term, we find

$$n(u; \omega) = 1 + \frac{e^2}{(4\pi)^2} \frac{1}{4\omega^2} \int_0^1 d\xi \left[ \int_0^{u-u_0} \frac{dt}{t} e^{-izt} \sqrt{\Delta(u, u-t)} - \text{Re} \int_0^\infty \frac{dt}{t} e^{-izt} \right]. \quad (7.12)$$

The UV divergence at  $t = 0$  cancels between the two terms in (7.12). The subtraction, by definition, is real and so the expression (7.7) for  $\text{Im} n(u; \omega)$  is unaffected by renormalization. The crucial point, though, is that the upper limits on the  $t$ -integrals of the bare and subtraction terms in (7.13) are *not* the same for finite  $u_0$ . In the flat spacetime limit and with  $u_0 \rightarrow -\infty$ , we confirm as expected that  $n(u; \omega) = 1$ . However, even in flat spacetime, this difference in limits implies that  $n(u; \omega)$  has a non-trivial,  $u$ -dependent behaviour when we start from an initial value surface at finite  $u_0$ . In turn, this implies a non-vanishing  $\mathcal{Q}^{(1)}(u)$  and  $u$ -dependent evolution of the amplitude  $\mathcal{A}(u)$ .

Of course, this is precisely the transient behaviour we have already studied using the Laplace transform method in section 5. It is interesting, however, to see this behaviour reproduced by the general expression (7.12) in the case of flat spacetime, and in fact very similar results follow in the FRW cosmology considered below.

We can evaluate the integral explicitly to give<sup>17</sup>

$$\text{Im} n(u; \omega) = \frac{e^2}{(4\pi)^2} \frac{1}{4\omega^2} \int_0^1 d\xi \left[ \frac{\pi}{2} - \text{Si}(\hat{u} - \hat{u}_0) \right], \quad (7.13)$$

---

<sup>17</sup> Note that the integrals require care near the pole at  $t = 0$ . The correct prescription matches that explained following (6.7), with the  $t$  contour lying below the axis and picking up a contribution from the pole. For example,

$$\text{Im} \int_0^{u-u_0} \frac{dt}{t} e^{-izt} = \frac{\pi}{2} - \int_0^{u-u_0} \frac{dt}{t} \sin(zt).$$



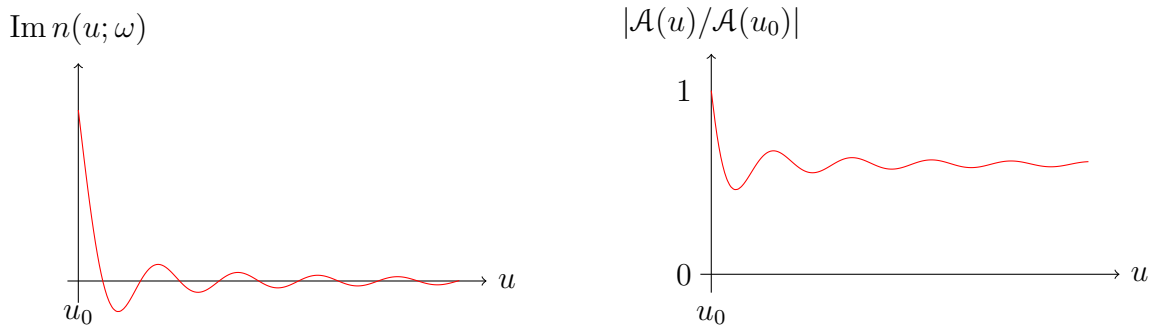


**Figure 4.** The left-hand diagram shows  $\text{Im } n(u; \omega)$  as a function of  $u$  in flat spacetime. Note that  $\text{Im } n(u; \omega)$  is non-zero at the initial value surface  $u_0$  and can take negative values. The right-hand diagram shows the evolution of the field amplitude  $|\mathcal{A}(u)|$  showing the characteristic transient behaviour as the bare field becomes dressed in real time.

introducing the notation  $\hat{u} = zu$ . Si is the sine integral. Similarly,

$$\begin{aligned} \text{Im } \mathcal{Q}(u) &= \frac{1}{2} \frac{e^2}{(4\pi)^2} \int_0^1 d\xi \frac{1}{\frac{m^2}{\xi(1-\xi)} - M^2} \\ &\times \left[ (\hat{u} - \hat{u}_0) \left( \frac{\pi}{2} - \text{Si}(\hat{u} - \hat{u}_0) \right) - \cos(\hat{u} - \hat{u}_0) + 1 \right]. \end{aligned} \quad (7.14)$$

Plots of  $\text{Im } n(u; \omega)$  and the amplitude  $|\mathcal{A}(u)| = |\mathcal{A}(u_0)|(1 - \text{Im } \mathcal{Q}^{(1)}(u))$  are shown in Fig. 4. These display all the features previously described in section 5 – an oscillatory transient behaviour where  $|\mathcal{A}(u)|$  falls as the bare field becomes dressed, before settling to a fixed value in the asymptotic large- $u$  region where  $\text{Im } n(u; \omega) \rightarrow 0$ . Note that  $\text{Im } n(u; \omega)$  is locally negative in the transient phase, corresponding to the oscillatory behaviour of  $|\mathcal{A}(u)|$ , while its integral  $\text{Im } \mathcal{Q}^{(1)}(u)$  remains positive, in accordance with the optical theorem.

#### *Quantum Electrodynamics:*

The analysis for QED follows the same lines, but there are important differences, both technical and in the resulting physics. In scalar QED, there are two contributions to the vacuum polarization, corresponding to the Feynman diagrams in Fig. 5.

For the Schwinger-Keldysh (retarded) vacuum polarization, we have previously

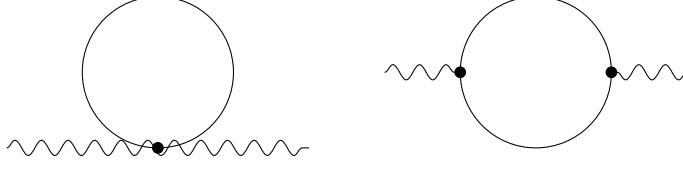


**Figure 5.** The two Feynman diagrams contributing to the vacuum polarization in scalar QED.

shown [3] that

$$\begin{aligned} \tilde{\Pi}_{ij}(u, u'; \omega, p) = & -\frac{\alpha}{\pi} \omega \int_0^1 d\xi \xi(1-\xi) \left[ i \frac{e^{-iz(u-u')}}{(u-u')^2} \theta(u-u') \Delta_{ij}(u, u') \sqrt{\Delta(u, u')} \right. \\ & \left. + i\delta_{ij} \int_0^\infty \frac{dt}{t^2} e^{-izt} \delta(u, u') \right], \end{aligned} \quad (7.15)$$

where the term proportional to  $\delta(u, u')$  comes from the first Feynman diagram in Fig. 5, and as usual  $z = \frac{m^2}{2\omega\xi(1-\xi)}$ . The two transverse polarizations are labelled by the Brinkmann coordinates  $i, j = 1, 2$  and  $\tilde{\Pi}_{ij}$  can be taken as diagonal with no loss of generality.

Given the relation (3.38) of the refractive index to the vacuum polarization,

$$n_{ij}(u; \omega) = \delta_{ij} - \frac{1}{2\omega^2} \int_{u_0}^u du' \tilde{\Pi}_{\text{SK},ij}(u, u'; \omega, p), \quad (7.16)$$

we therefore have

$$n_{ij}(u; \omega) = \delta_{ij} - \frac{\alpha}{\pi} \frac{1}{2\omega} \int_0^1 d\xi \xi(1-\xi) \mathcal{F}_{ij}(u; z), \quad (7.17)$$

with

$$\mathcal{F}_{ij}(u; z) = \int_0^{u-u_0} \frac{dt}{t^2} i e^{-izt} \Delta_{ij}(u, u-t) \sqrt{\Delta(u, u-t)} - \delta_{ij} \int_0^\infty \frac{dt}{t^2} i e^{-izt}. \quad (7.18)$$

Notice that the limits on the  $t$ -integrals in the two terms are different in general. Only when we take  $u_0 \rightarrow -\infty$  (as in our previous papers) do they both become the same, as the dependence on the initial value surface disappears.

It is clear that the second contribution acts very much like the mass counterterm subtraction for  $A\phi^2$  theory in (7.12), but with important differences. Although it

removes the potential singularity at  $t = 0$ , it is not a counterterm and is *not* simply the real part as in (7.12). It is essential in QED to maintain gauge invariance, and it is gauge invariance which keeps the photon massless, with no mass renormalization. Also note the  $t^{-2}$  power in the integrals, which arises through power counting and is ultimately related to the need for field (wave-function) renormalization in QED. These differences make a subtle, but vitally important, difference in the behaviour of the field amplitude in QED, even in flat spacetime.

Consider first QED in flat spacetime. Combining the two terms in (7.18), we have  $\mathcal{F}_{ij}(u; z) = \mathcal{F}(u; z)\delta_{ij}$  where

$$\mathcal{F}(u; z) = \int_{u-u_0}^{\infty} \frac{dt}{t^2} i e^{-izt} = -\frac{1}{(u-u_0)} \int_1^{\infty} \frac{d\hat{t}}{\hat{t}^2} i e^{-iz(u-u_0)\hat{t}}, \quad (7.19)$$

with the change of variable  $t = (u-u_0)\hat{t}$ . Notice the occurrence of the vital factor  $1/(u-u_0)$ , which appears because of the different power-counting in QED compared to  $A\phi^2$  in  $d=4$ . For the imaginary part (note that both vacuum polarization diagrams are contributing),

$$\text{Im } \mathcal{F}(u; z) = -\frac{1}{(u-u_0)} \int_1^{\infty} \frac{d\hat{t}}{\hat{t}^2} \cos(z(u-u_0)\hat{t}). \quad (7.20)$$

The integral can be done analytically and we find the following expression for the refractive index

$$\text{Im } n(u; \omega) = \frac{\alpha}{\pi} \frac{m^2}{4\omega^2} \int_0^1 d\xi \left[ \text{Si}(\hat{u} - \hat{u}_0) - \frac{\pi}{2} + \frac{1}{\hat{u} - \hat{u}_0} \cos(\hat{u} - \hat{u}_0) \right], \quad (7.21)$$

where  $\hat{u} = zu$ .

This is plotted in Fig. 6. Again we see the characteristic oscillations which occur when the initial value surface is taken at finite  $u_0$ . The key point, however, is that for QED,  $\text{Im } n(u; \omega)$  diverges as  $1/(u-u_0)$  for  $u$  close to the initial value surface. For small  $(u-u_0)$ ,  $\text{Im } n(u; \omega)$  is positive, so this is consistent with the observation in section 6 of a divergent initial dressing in a theory like QED which requires wave function renormalization.

We can see this more explicitly by comparing the amplitude  $\mathcal{A}(u)$  at some small value of  $u$  with its value  $\mathcal{A}(u_1)$  for some reference value  $u_1$  sufficiently removed from the initial value surface. Evaluating  $\text{Im } Q(u)$  from

$$\text{Im } Q(u_1) - \text{Im } Q(u) = \omega \int_u^{u_1} du'' \text{Im } n(u''; \omega), \quad (7.22)$$

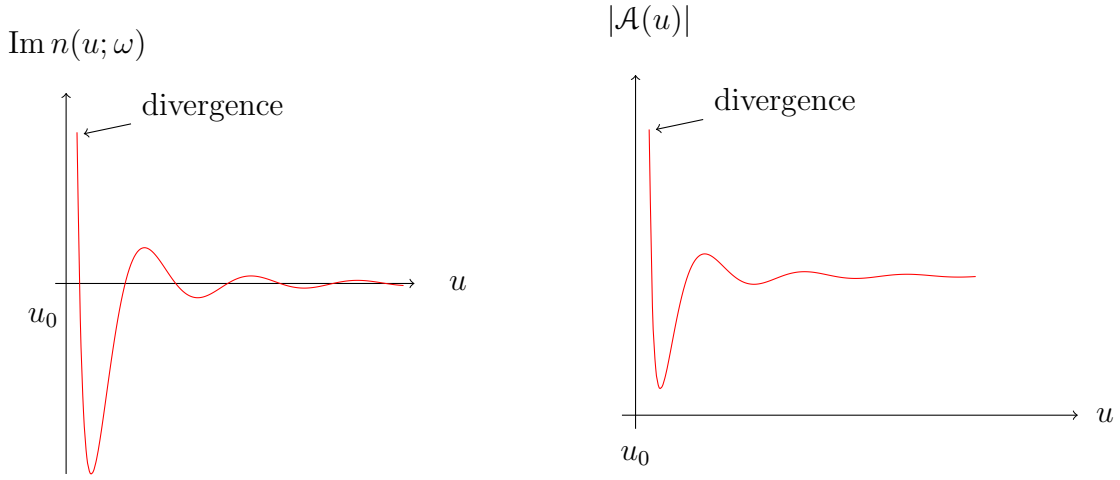


**Figure 6.** This shows (left)  $\text{Im } n(u; \omega)$  for QED in flat spacetime as a function of  $u$ . Note that for  $u \sim u_0$ ,  $\text{Im } n(u; \omega)$  is positive and divergent. The right-hand diagram shows the equivalent behaviour for the amplitude  $|\mathcal{A}(u)|$ , showing the expected divergence on the initial value surface.

with  $\text{Im } n(u; \omega)$  as in (7.21), we find

$$\frac{|\mathcal{A}(u)|}{|\mathcal{A}(u_1)|} = 1 - (\text{Im } Q(u) - \text{Im } Q(u_1)) , \quad (7.23)$$

with

$$\begin{aligned} \text{Im } Q(u) - \text{Im } Q(u_1) &= \frac{\alpha}{2\pi} \int_0^1 d\xi \xi(1-\xi) \left( \left[ (\hat{u} - \hat{u}_0) \text{Si}(\hat{u} - \hat{u}_0) + \text{Ci}(\hat{u} - \hat{u}_0) \right. \right. \\ &\quad \left. \left. + \cos(\hat{u} - \hat{u}_0) - \frac{\pi}{2}(\hat{u} - \hat{u}_0) \right] - \left[ \hat{u} \rightarrow \hat{u}_1 \right] \right) . \end{aligned} \quad (7.24)$$

This is shown in Fig. 6. For small  $(u - u_0)$ , the dominant term arises from the Ci function, which diverges logarithmically, and we find

$$\frac{|\mathcal{A}(u)|}{|\mathcal{A}(u_1)|} = 1 - \frac{\alpha}{12\pi} \log(u - u_0) . \quad (7.25)$$

We can exponentiate this using the dynamical renormalization group and conclude that for small  $(u - u_0)$ ,

$$\frac{|\mathcal{A}(u)|}{|\mathcal{A}(u_1)|} \sim (u - u_0)^{-\frac{\alpha}{12\pi}} . \quad (7.26)$$

The physical picture, as inferred in section 6, is that in order to obtain a finite evolution of the photon field in QED, we have to start from a divergent value on the initial value

surface itself. This is the expected behaviour for a theory requiring field (wave-function) renormalization. Nevertheless, we can still study the evolution of the field amplitude in QED, either by simply taking  $u_0 \rightarrow -\infty$  as in our previous work, or by comparing the ratio of  $|\mathcal{A}(u)|$  to its value at a fixed reference point away from the initial value surface where the interaction is assumed to be switched on. Of course, this is the essential idea behind the Type II or III initial value conditions introduced in section 6.

## 7.1 Cosmological FRW spacetimes

As a first example, consider a spatially-flat FRW spacetime. As shown in ref.[4], the Penrose limit for null geodesics with no angular momentum in the transverse space is a conformally-flat, singular homogeneous plane wave with profile function<sup>18</sup>

$$h_{ij} = \frac{\gamma}{(\gamma + 1)^2} \frac{1}{u^2} \delta_{ij} . \quad (7.27)$$

Spatially flat FRW spacetimes are special in that the Penrose limit is a singular homogeneous plane wave for all  $u$ , not simply in the near-singularity limit  $u \simeq 0$ .

We are considering an initial value problem where the interaction is turned on at some finite value  $u_0 > 0$ , since clearly we have to start away from the initial singularity. We then study the development of the field amplitude along the null geodesic as the universe evolves.

*$A\phi^2$  theory:*

Specialising first to  $A\phi^2$  theory with  $M = 0$ , and making the convenient change of variable from  $t = u - u'$  to  $\hat{t} = 1 - \frac{u'}{u} = 1 - r$ , we find from (7.8),

$$\text{Im } \mathcal{F}(u; z) = \text{Im} \int_{0-i\epsilon}^{1-\frac{u_0}{u}} \frac{d\hat{t}}{\hat{t}} e^{-iz\hat{t}} F(\hat{t}) , \quad (7.28)$$

where  $z = \frac{m^2}{2\omega\xi(1-\xi)}$  and

$$F(\hat{t}) = \frac{\tilde{\alpha}\hat{t}(1-\hat{t})^{\frac{\tilde{\alpha}-1}{2}}}{1 - (1-\hat{t})^{\tilde{\alpha}}} . \quad (7.29)$$

---

<sup>18</sup>The coefficient  $\gamma$  is related to the usual  $w$  parameter in the FRW equation of state  $p = w\rho$  by  $\gamma = \frac{2}{3(1+w)}$ , so that  $\gamma = \frac{2}{3}, \frac{1}{2}$  or  $\infty$  for a matter, radiation or cosmological constant dominated universe respectively. The FRW scale factor is  $a(t) \sim t^\gamma$ . The interesting example of the Milne universe considered in ref.[4] with  $\gamma = 1$  corresponds to  $w = -\frac{1}{3}$ , at the boundary between a decelerating and accelerating universe. The  $\tilde{\alpha} \equiv \alpha_1 = \alpha_2$  (to avoid confusion with the fine structure constant) parameter in the profile function is  $\tilde{\alpha} = \left| \frac{1-\gamma}{1+\gamma} \right|$ . The null coordinate  $u$  in the Penrose limit is related to  $t$  in the FRW metric by  $u \sim t^{\gamma+1}$ . The flat space limit is  $\gamma = 0$ , corresponding to  $\tilde{\alpha} = 1$ .

The integral requires careful treatment of the pole at  $\hat{t} = 0$  (see footnote 17) and follows the prescription described following (6.7). There, in flat spacetime, the  $t$ -integral ran from  $-\infty$  to  $\infty$  with the contour running below the real axis – this ensured that below threshold ( $z > 0$ ) the contour could be closed in the lower half-plane so that  $\text{Im } n(u; \omega)$  vanished. Here, the same  $i\epsilon$  prescription in (7.28) picks up a contribution  $\frac{1}{2}\pi i \text{Res}(\hat{t} = 0)$  from the pole at  $t = 0$ , and since  $F(0) = 1$ , we find

$$\text{Im } \mathcal{F}(u; z) = \frac{\pi}{2} - \int_0^{1-\frac{u_0}{u}} \frac{d\hat{t}}{\hat{t}} \sin(zu\hat{t})F(\hat{t}) . \quad (7.30)$$

The refractive index is then

$$\text{Im } n(u; \omega) = \frac{e^2}{(4\pi)^2} \frac{1}{4\omega^2} \int_0^1 d\xi \left[ \frac{\pi}{2} - \int_0^{1-\frac{u_0}{u}} \frac{d\hat{t}}{\hat{t}} \sin(zu\hat{t})F(\hat{t}) \right] . \quad (7.31)$$

The integrals over  $\hat{t}$  and  $\xi$  can now be performed numerically for various values of the FRW parameter  $\tilde{\alpha}$ . In fact, the function  $F(\hat{t})$  is very flat over most of the range  $t = 0$  to 1. The refractive index therefore has the same qualitative behaviour as shown in Fig. 4. In particular,  $\text{Im } n(u; \omega)$  falls from an initially positive value and oscillates as  $u$  increases away from  $u_0$ , and is locally negative. In those regions,  $\mathcal{Q}^{(1)}(u)$  decreases and in turn the amplitude  $|\mathcal{A}(u)|$  increases. In Fig. 7, we subtract the transient flat-spacetime result and plot the curvature-induced contribution to  $\text{Im } n(u; \omega)$ , viz.

$$\text{Im } n(u; \omega) \Big|_{\text{curved}} = -\frac{e^2}{(4\pi)^2} \frac{1}{4\omega^2} \int_0^1 d\xi \int_0^{1-\frac{u_0}{u}} \frac{d\hat{t}}{\hat{t}} \sin(zu\hat{t}) [F(\hat{t}) - 1] . \quad (7.32)$$

This shows clearly how the time-varying gravitational tidal forces induce both a local dressing and undressing of the renormalized quantum field. The amplitude  $\mathcal{A}(u)$  decreases or increases as the screening due to the cloud of virtual  $\phi$  pairs is enhanced or reduced.

### *Quantum Electrodynamics:*

The situation is very similar for QED and the behaviour of  $\text{Im } n(u; \omega)$  and  $|\mathcal{A}(u)|$  in the FRW background is qualitatively the same as in flat spacetime, including the divergence for  $u \sim u_0$ . Both polarizations have the same refractive index, since the homogeneous plane wave in the Penrose limit is conformally flat.

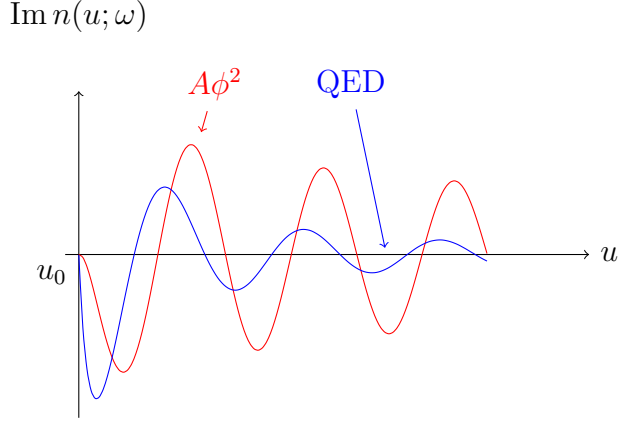


**Figure 7.** The curvature contribution to  $\text{Im } n(u; \omega)$  plotted as a function of  $u - u_0$ , for  $A\phi^2$  and QED, for a fixed choice of  $u_0$  in a FRW spacetime with  $\tilde{\alpha} = \frac{1}{3}$ . Note that  $\text{Im } n(u; \omega)$  can be locally negative, corresponding to a curvature-induced “undressing” of the quantum field.

If we split  $\text{Im } n(u; \omega)$  into the flat spacetime result already found and the curvature-dependent contribution, we find

$$\text{Im } n(u; \omega)|_{\text{curved}} = -\frac{\alpha}{\pi} \frac{1}{2\omega} \int_0^1 d\xi \xi(1-\xi) \frac{1}{u} \int_0^{1-\frac{u}{u_0}} \frac{d\hat{t}}{\hat{t}^2} \cos(zu\hat{t}) [F(\hat{t}) - 1], \quad (7.33)$$

where

$$F(\hat{t}) = \Delta_{ii}(r) \sqrt{\Delta(r)} = \frac{\tilde{\alpha}^2 \hat{t}^2 (1-\hat{t})^{\tilde{\alpha}-1}}{[1 - (1-\hat{t})^{\tilde{\alpha}}]^2}, \quad (7.34)$$

recalling  $\hat{t} = 1 - r$ . Notice that the subtraction  $-1$  in the integrand in (7.33) is the flat spacetime contribution, not the contribution of the extra vacuum polarization diagram for scalar QED. The  $\hat{t}$  integration is well-defined here, since the properties  $F(0) = 1$ ,  $F'(0) = 0$  ensure the absence of a singularity at  $\hat{t} = 0$ . This result for  $\text{Im } n(u; \omega)$  is plotted in Fig. 7. The results are very similar to the scalar  $A\phi^2$  theory, with an enhancement for  $u \sim u_0$  for QED reflecting the usual power counting  $\hat{t}^{-2}$  factor in (7.33).

## 7.2 Black holes and the near-singularity limit

A particularly interesting question is what happens to a dressed photon as it approaches a spacetime singularity. This can be addressed in a similar way, using the singular

homogeneous plane wave as the Penrose limit of a Schwarzschild black hole in the near-singularity limit. For this case, we have  $\alpha_1 = \frac{1}{5}$  and  $\alpha_2 = \frac{7}{5}$  and the geodesic spray defined above (2.14) is described by

$$\begin{aligned} A_{11}(u, u') &= 5(uu')^{2/5} \left( u^{1/5} - u'^{1/5} \right), \\ A_{22}(u, u') &= \frac{5}{7}(uu')^{-1/5} \left( u^{7/5} - u'^{7/5} \right). \end{aligned} \quad (7.35)$$

In the direction  $z^1$ , the geodesics focus on the point  $u = 0$  which is the singularity. For the other direction  $z^2$ , the geodesics diverge as the singularity is approached. If we define the usual Schwarzschild coordinates  $(t, r, \theta, \phi)$  then by symmetry we can take the geodesics in the plane  $\phi = 0$ . The transverse space-like coordinates  $z^i$  are related to these coordinates via  $z^1 = r \sin \theta$  and  $z^2 = r dr/du$ . Here,  $z^1$  is orthogonal to the plane of the orbit while  $z^2$  lies in the plane of the orbit [4].

*A $\phi^2$  theory:*

This time, therefore, we take the initial value surface  $u_0 < 0$  and study  $\text{Im } n(u; \omega)$  as  $u$  approaches zero. In this case, the appropriate integration variable is  $\hat{t} = r - 1 = -\frac{t}{u}$ , and we have

$$\text{Im } \mathcal{F}(u; z) = \text{Im} \int_{0-i\epsilon}^{\frac{u_0}{u}-1} \frac{d\hat{t}}{\hat{t}} e^{-iz|u|\hat{t}} F(\hat{t}), \quad (7.36)$$

where

$$F(\hat{t}) = \sqrt{\frac{\alpha_1 \alpha_2 \hat{t}^2 (1 + \hat{t})^{-p}}{((1 + \hat{t})^{\alpha_1} - 1)((1 + \hat{t})^{\alpha_2} - 1)}}. \quad (7.37)$$

The VVM determinant function  $F(\hat{t})$  satisfies  $F(0) = 1$ ,  $F'(0) = 0$  and  $F(\hat{t}) \simeq \sqrt{\alpha_1 \alpha_2} \hat{t}^{p/2}$  at large  $\hat{t}$ . Note that  $p$  for the background geometry is defined in (7.4).

We are interested in the near-singularity behaviour of the refractive index, so now let  $u_0 \rightarrow -\infty$ . The integral over  $\hat{t}$  can be expressed as in (7.30), but here, since the upper limit of integration becomes infinity, it is possible to rotate the contour in the complex  $\hat{t}$  plane to run down the negative imaginary axis. Then, with  $\tau = i\hat{t}$ , we have the computationally more convenient form,

$$\text{Im } \mathcal{F}(u; z) = \int_0^\infty \frac{d\tau}{\tau} e^{-z|u|\tau} G(\tau), \quad (7.38)$$

where  $G(\tau) = \text{Im } F(-i\tau)$ . Note that the lower limit is safe from singularities since  $G(0) = 0$ . At large  $\tau$ ,  $G(\tau) = -\sqrt{\alpha_1 \alpha_2} \sin \frac{\pi p}{4} \tau^{p/2} \left( 1 + \mathcal{O}(\tau^{-\min(\alpha_1, \alpha_2)}) \right)$  and, crucially, is negative provided  $p > 0$ . For Schwarzschild,  $p = \frac{1}{5}$ .



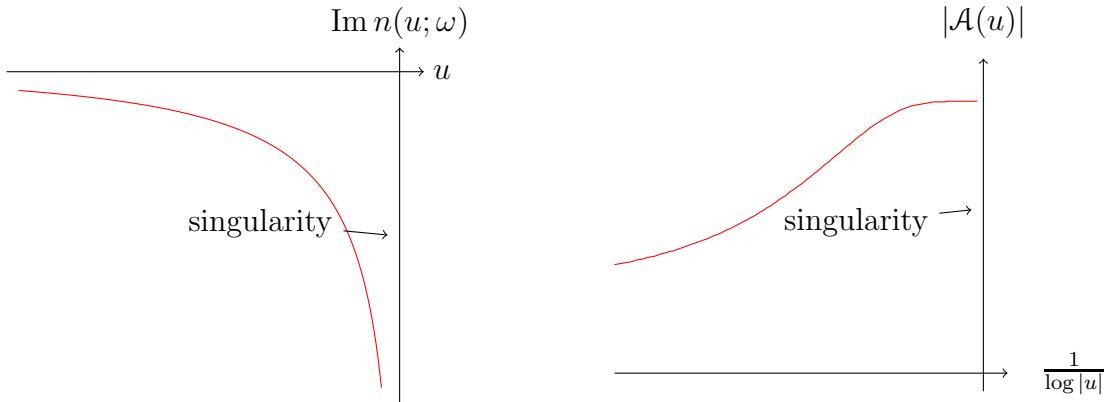


**Figure 8.** Plot of the imaginary part of the refractive index  $\text{Im } n(u; \omega)$  in  $A\phi^2$  theory in a Schwarzschild background as  $u$  approaches the singularity at  $u = 0$  from  $u < 0$ . The right-hand diagram shows the corresponding result for the amplitude  $|\mathcal{A}(u)|$  (plotted on an inverse log scale) showing the bounded behaviour following from  $Q(u) \rightarrow -\text{constant}$  as  $u \rightarrow 0$ .

The resulting form for  $\text{Im } n(u; \omega)$  is shown in Fig. 8. Note immediately that  $\text{Im } n(u; \omega) < 0$  and diverges for small  $u$ . A key point then is whether the amplitude remains bounded, *i.e.* whether  $\text{Im } \mathcal{Q}^{(1)}(u)$ , given here by

$$\text{Im } \mathcal{Q}^{(1)}(u) = \omega \int_{-\infty}^u du'' \text{Im } n(u''; \omega) , \quad (7.39)$$

remains finite as  $u \rightarrow 0$ . This is shown in the second plot in Fig. 8, confirming that  $\text{Im } \mathcal{Q}^{(1)}(u) \rightarrow -\text{constant}$  as  $u \rightarrow 0$ , ensuring that  $|\mathcal{A}(u)|$  is bounded.

To see this explicitly, we can rescale the integral (7.38) to get

$$\text{Im } \mathcal{F}(u; z) = \int_0^\infty \frac{d\tau}{\tau} e^{-\tau} G\left(\frac{\tau}{z|u|}\right) , \quad (7.40)$$

then pick out the leading small  $|u|$  behaviour from the leading term in the expression for  $G(\tau)$  for large  $\tau$ . This gives

$$\text{Im } \mathcal{F}(u; z) \simeq -\sqrt{\alpha_1 \alpha_2} \sin\left(\frac{\pi p}{4}\right) \Gamma\left(\frac{p}{2}\right) \frac{1}{(z|u|)^{\frac{p}{2}}} . \quad (7.41)$$

In practice, since  $\alpha_1 = \frac{1}{5}$  for the Schwarzschild black hole, the approach to the asymptotic limit is slow. However, this limit is sufficient to show that  $\text{Im } \mathcal{Q}^{(1)}(u)$  is bounded and tends to a constant as  $|u| \rightarrow 0$  provided  $0 < \frac{p}{2} < 1$ , which is ensured by  $0 < \alpha_i < 1$ .

The physical interpretation is as follows. With the initial value surface set at  $u_0 \rightarrow -\infty$ , the incoming photon is already fully dressed as it approaches the small  $u$ ,

near-singularity region. Here,  $\text{Im } n(u; \omega)$  is negative, corresponding to an increasing amplitude  $|\mathcal{A}(u)|$ . The photon is becoming “undressed”, i.e. the gravitational tidal forces are stripping away its cloud of virtual  $\phi$  pairs. This reduces the level of screening and the renormalized field amplitude increases as it reverts towards its bare state. Since this process cannot continue indefinitely, the increase in  $|\mathcal{A}(u)|$  must be bounded, as we find. Once again, all this is consistent with the interpretation in sections 4 and 5 of the curved-spacetime generalisation of the optical theorem.

*Quantum Electrodynamics:*

Finally, we consider QED itself and look at the evolution of a dressed photon as it approaches a Schwarzschild singularity at  $u = 0$ . Here, once again taking  $u_0 \rightarrow -\infty$ ,

$$\text{Im } n_{ij}(u; \omega) = -\frac{\alpha}{\pi} \frac{1}{2\omega} \int_0^1 d\xi \xi(1-\xi) \text{Im } \mathcal{F}_{ij}(u; z), \quad (7.42)$$

with

$$\mathcal{F}_{ij}(u; z) = \int_0^\infty \frac{dt}{t^2} e^{-izt} \left[ \Delta_{ij}(u, u-t) \sqrt{\Delta(u, u-t)} - \delta_{ij} \right] \quad (7.43)$$

and with no loss-of-generality we can take  $\mathcal{F}_{ij}(u; z) = \mathcal{F}_i(u; z) \delta_{ij}$ .

We use the same rescaling  $\hat{t} = r - 1 = -t/u$  as above, so that

$$\mathcal{F}_i(u; z) = \frac{1}{|u|} \int_0^\infty \frac{d\hat{t}}{\hat{t}^2} e^{-iz|u|\hat{t}} (F_i(\hat{t}) - 1), \quad (7.44)$$

where for the first polarization,

$$F_1(\hat{t}) = \sqrt{\frac{\alpha_1^3 \alpha_2 \hat{t}^4 (1 + \hat{t})^{-q_1}}{((1 + \hat{t})^{\alpha_1} - 1)^3 ((1 + \hat{t})^{\alpha_2} - 1)}}, \quad (7.45)$$

with  $q_1 = 2 - \frac{(3\alpha_1 + \alpha_2)}{2}$ . The equivalent result holds for the second polarization. It is straightforward to check that at small  $\hat{t}$ ,  $F_i(0) = 1$ ,  $F'_i(0) = 0$  while at large  $\hat{t}$ ,  $F_1(\hat{t}) \rightarrow \sqrt{\alpha_1^3 \alpha_2} \hat{t}^{q_1/2}$  and  $F_2(\hat{t}) \rightarrow \sqrt{\alpha_1 \alpha_2^3} \hat{t}^{q_2/2}$ .

These properties of  $F_i(\hat{t})$  ensure that the  $\hat{t}$  integral in (7.44) is non-singular at  $\hat{t} = 0$ , and since the upper limit in this case is infinity (because we have taken  $u_0 \rightarrow -\infty$ ) we can again rotate the contour just as in the  $A\phi^2$  example and find

$$\mathcal{F}_i(u; z) = -\frac{1}{|u|} \int_0^\infty \frac{d\tau}{\tau^2} e^{-z|u|\tau} (F_i(-i\tau) - 1), \quad (7.46)$$

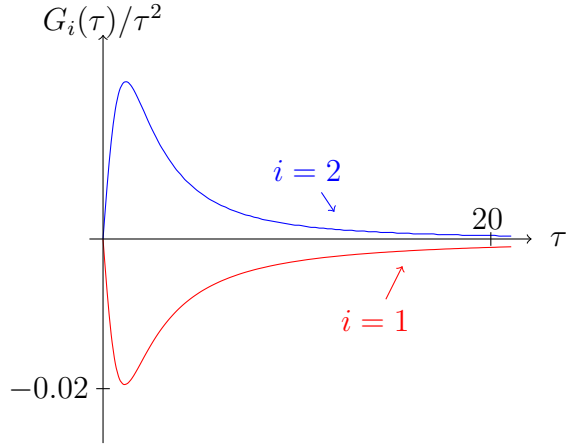


**Figure 9.** Plot of the functions  $G_i(\tau)/\tau^2$  derived from the VVM matrix which determine the asymptotic behaviour of the refractive index in QED for the two polarizations.

and so

$$\text{Im } \mathcal{F}_i(u; z) = -\frac{1}{|u|} \int_0^\infty \frac{d\tau}{\tau^2} e^{-z|u|\tau} G_i(\tau) , \quad (7.47)$$

where we define the functions  $G_i(\tau) = \text{Im } F_i(-i\tau)$ . At small  $\tau$ ,  $G_i(\tau) = \mathcal{O}(\tau^2)$ , while for Schwarzschild spacetime with  $\alpha_1 = \frac{1}{5}, \alpha_2 = \frac{7}{5}$ , we find for large  $\tau$ ,

$$\begin{aligned} G_1(\tau) &\rightarrow -\sqrt{\alpha_1^3 \alpha_2} \sin\left(\frac{\pi q_1}{4}\right) \tau^{\frac{q_1}{2}} = -\frac{\sqrt{7}}{25} \sin\left(\frac{\pi}{4}\right) \tau^{\frac{1}{2}} < 0 \\ G_2(\tau) &\rightarrow -\sqrt{\alpha_1 \alpha_2^3} \sin\left(\frac{\pi q_2}{4}\right) \tau^{\frac{q_2}{2}} = \frac{7\sqrt{7}}{25} \sin\left(\frac{\pi}{20}\right) \tau^{-\frac{1}{10}} > 0 . \end{aligned} \quad (7.48)$$

The small  $|u|$  behaviour of the integral in (7.47) depends on the form of the functions  $G_i(\tau)/\tau^2$ . These are plotted in Fig. 9. Crucially, the asymptotic forms (7.48) show that these go to zero at large  $\tau$  fast enough, and we can define

$$\begin{aligned} c_1 &= \int_0^\infty \frac{d\tau}{\tau^2} G_1(\tau) = -0.155 , \\ c_2 &= \int_0^\infty \frac{d\tau}{\tau^2} G_2(\tau) = 0.105 . \end{aligned} \quad (7.49)$$

This is in contrast to  $A\phi^2$  theory where the corresponding integral is divergent. As we now see, this produces quite different small  $|u|$  behaviour for the refractive index. Note also the difference in sign for the two polarizations. This can be inferred from (7.48)

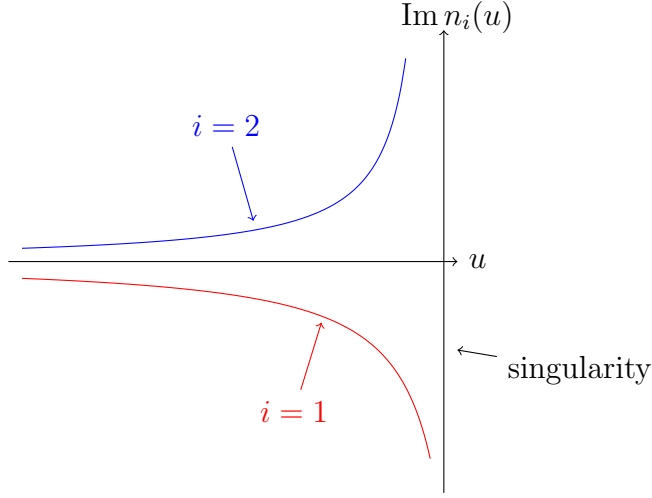


**Figure 10.** Plot of the imaginary part of the refractive index  $\text{Im } n(u; \omega)$  for the two polarizations in QED in a Schwarzschild background as  $u$  approaches the singularity at  $u = 0$  from  $u < 0$ .

and is determined by the properties of the VVM matrix, depending critically on the  $\alpha_i$  parameters. It now follows that the magnitude of the integrals in (7.47) will increase as  $|u|$  becomes smaller and the exponential decays less rapidly with  $\tau$ , until in the limit  $|u| \rightarrow 0$  we find

$$\text{Im } \mathcal{F}_i(u; z) \longrightarrow -\frac{1}{|u|} \int_0^\infty \frac{d\tau}{\tau^2} G_i(\tau) = -\frac{c_i}{|u|}. \quad (7.50)$$

We therefore find the following results for the small  $|u|$  behaviour of the imaginary part of the refractive index in QED (see Fig. 10):

$$\begin{aligned} \text{Im } n_1(u; \omega) &= \frac{\alpha}{6\pi} \frac{1}{2\omega} \frac{c_1}{|u|} < 0, \\ \text{Im } n_2(u; \omega) &= \frac{\alpha}{6\pi} \frac{1}{2\omega} \frac{c_2}{|u|} > 0. \end{aligned} \quad (7.51)$$

$\text{Im } n(u; \omega)$  diverges as  $\frac{1}{|u|}$  in the near singularity limit for both polarizations, but with opposite signs: polarization 2 is being dressed while polarization 1 is being undressed by the gravitational tidal forces.

The most illuminating way to see the effect on the amplitudes is to compare  $\mathcal{A}(u)$  with the amplitude  $\mathcal{A}(u_1)$  for some fixed  $u_1$  sufficiently far into the near singularity

region that the above approximations hold, then let  $|u| \rightarrow 0$ . From

$$\frac{|\mathcal{A}_i(u)|}{|\mathcal{A}_i(u_1)|} = 1 - \omega \int_{u_1}^u du'' \operatorname{Im} n_i(u''; \omega) , \quad (7.52)$$

we find

$$\frac{|\mathcal{A}_i(u)|}{|\mathcal{A}_i(u_1)|} = 1 + \frac{\alpha}{12\pi} c_i \log \frac{u}{u_1} , \quad (7.53)$$

for the two polarizations. These are both logarithmically divergent, but we can use the dynamical renormalization group to exponentiate to give

$$\frac{|\mathcal{A}_i(u)|}{|\mathcal{A}_i(u_1)|} = \left( \frac{u}{u_1} \right)^{\frac{\alpha}{12\pi} c_i} . \quad (7.54)$$

Recalling (7.49) for the coefficients  $c_i$ , we finally find the small  $|u|$  behaviour:

$$\begin{aligned} |\mathcal{A}_1(u)| &\sim |u|^{-0.155 \frac{\alpha}{12\pi}} , \\ |\mathcal{A}_2(u)| &\sim |u|^{0.105 \frac{\alpha}{12\pi}} , \end{aligned} \quad (7.55)$$

so in fact only  $|\mathcal{A}_1(u)|$  diverges, while for the second polarization  $|\mathcal{A}_2(u)| \rightarrow 0$  as  $|u| \rightarrow 0$ . The diverging case is for the polarization along the direction  $z^1$  for which the geodesics focus.

We see therefore that the evolution of the field amplitude as the singularity is approached is determined by the properties of the VVM matrix, which is encoded in the signs of the coefficients  $c_i$  and differs for the two polarizations. For polarization 2, which correspond to the direction  $z^2$  along which the geodesics diverge and for which  $\operatorname{Im} n(u; \omega)$  is positive, the photon becomes increasingly dressed – the screening increases and the amplitude falls to zero. For polarization 1, however, for which the geodesics focus, the gravitational tidal forces near the singularity strip away the vacuum polarization cloud of virtual  $\phi$  pairs and the photon becomes undressed, the screening is reduced and the amplitude increases. In the purely scalar  $A\phi^2$  theory, this process is bounded and the amplitude rises to a limiting value. In QED, however, we see the consequence of the theory requiring wave function renormalization. As the singularity is approached, the renormalized, dressed photon is being restored in real time to its bare state, but since for QED the ratio of bare to renormalized fields is UV divergent, in this case the amplitude rises without bound as  $|u| \rightarrow 0$  for one of the polarization states.

## 8 Conclusions

This work was motivated by the apparent paradox that, when vacuum polarization is taken into account, photons propagating in curved spacetime can experience a refractive index with a negative imaginary part, corresponding to an amplification of the amplitude. This is in direct contradiction to the conventional flat-spacetime optical theorem, which relates  $\text{Im } n(\omega)$  to a decay rate and is necessarily positive or zero.

In this paper, we have addressed this issue from the point of view of an initial value problem, tracing the evolution of a renormalized (dressed) quantum field as it propagates through curved spacetime. Different initial conditions were used, corresponding to an initially bare or dressed field, and renormalization issues carefully addressed. The simplifications following from being able to replace the background spacetime by its Penrose plane-wave limit were fully exploited, allowing in many cases a very detailed analysis of the field evolution using a Laplace transform solution of the one-loop equation of motion.

The physical picture that emerges is that in a curved spacetime background, gravitational tidal forces act on the virtual  $e^+e^-$  cloud which dresses a renormalized photon field in such a way as to increase or decrease the degree of dressing. In particular, gravity can “undress” a renormalized photon, returning the field towards its bare state. As the degree of dressing is reduced, so is the level of screening and in consequence the amplitude increases. This effect can therefore produce a negative  $\text{Im } n(u; \omega)$ , though the effect is constrained to be local, and bounded (with the exceptions above of theories with UV-divergent wave function renormalization taken at the limit of the initial-value surface or a spacetime singularity). Indeed, the propagation of a renormalized photon through a time-dependent curved background resembles in many ways the initial transient phase of propagation in flat spacetime when an interaction is abruptly turned on.

In addition, in studying scalar  $A\phi^2$  theories, as well as QED, we found many examples of below-threshold decays which would be kinematically forbidden in flat spacetime. These decay rates are non-perturbative in the curvature. In particular, the analytic structure and nature of the thresholds was studied in detail in the class of symmetric plane waves, where a rich pattern of curvature-dependent thresholds emerged. It is probable that these can be interpreted in terms of group representations, since this class of homogeneous plane waves admits an enhanced symmetry described by a Heisenberg algebra.

The central result of this paper, which provides the formal framework for all of these phenomena, is the formulation of a generalised optical theorem valid in curved spacetime. In a plane-wave spacetime, this has the form:

$$P_{A \rightarrow \phi\phi}(u) = 4\omega \int_{u_0}^u du'' \operatorname{Im} n(u''; \omega) = -\frac{2}{\omega} \int_{u_0}^u du'' \int_{u_0}^{u''} du' \operatorname{Im} \tilde{\Pi}_{\text{SK}}(u'', u'; \omega, p) , \quad (8.1)$$

and relates the total  $A \rightarrow \phi\phi$  decay probability to the integral of the imaginary part of the vacuum polarization. The key point is that while this allows  $\operatorname{Im} n(u; \omega) < 0$  *locally*, when integrated over the entire trajectory from the surface  $u = u_0$  at which the interaction is turned on,  $\int_{u_0}^u du'' \operatorname{Im} n(u''; \omega)$  must be positive to ensure consistency with unitarity.

This confirms the theme of our earlier work that, despite the many novel and unexpected effects due to vacuum polarization, quantum field theories in curved spacetime indeed respect the fundamental principles of causality and unitarity. However, in so doing, many of the basic and widely-assumed theorems of QFT in flat spacetime, notably dispersion relations, the analytic structure of Green functions and scattering amplitudes, as well as the optical theorem, must be reformulated in curved spacetime.

\*\*\*\*\*

This research was supported in part by the STFC grant ST/G000506/1. We would like to thank the TH Division, CERN for hospitality while much of this work was carried out.

## Appendix A: Weak Curvature Expansions

In this appendix, we quote the results for the weak coupling expansions of the refractive index for scalar and spinor QED generalizing the case of massless scalar fields (3.43)

$$n(u; \omega) = 1 - \frac{e^2}{(4\pi)^2} \frac{1}{360m^4} R_{uu}(u) - \frac{e^2}{(4\pi)^2} \frac{i\omega}{840m^6} \dot{R}_{uu}(u) + \dots , \quad (A.1)$$

The case for scalar QED follows from (7.17):

$$\begin{aligned} n_{ij}(u; \omega) = & \delta_{ij} - \frac{\alpha}{360\pi m^2} (R_{uu}(u)\delta_{ij} + 2R_{iuju}) \\ & - \frac{i\alpha\omega}{1680\pi m^4} (\dot{R}_{uu}(u)\delta_{ij} + 2\dot{R}_{iuju}(u)) + \dots , \end{aligned} \quad (A.2)$$

Here,  $R_{uu} = R_{1u1u} + R_{2u2u}$  is a component of the Ricci tensor. The result for (spinor) QED can be extracted from [4]

$$n_{ij}(u; \omega) = \delta_{ij} - \frac{\alpha}{180\pi m^2} (13R_{uu}(u)\delta_{ij} - 4R_{iuju}(u)) - \frac{i\alpha\omega}{1260\pi m^4} (25\dot{R}_{uu}(u)\delta_{ij} - 6\dot{R}_{iuju}(u)) + \dots, \quad (\text{A.3})$$

The first correction here is the original Drummond-Hathrell result [10]. The higher corrects are then non-linear in the curvature.

These expansions allow us to extract the leading order behaviour of the amplitude generalizing the expression for the scalar field in (3.44). For scalar QED

$$\mathcal{A}_i(u_1) = \mathcal{A}_j(u_2) \exp \left[ \frac{\alpha\omega^2}{1680\pi m^4} (\dot{R}_{uu}(u_1)\delta_{ij} + 2\dot{R}_{iuju}(u_1) - \dot{R}_{uu}(u_2)\delta_{ij} - 2\dot{R}_{iuju}(u_2)) \right] \quad (\text{A.4})$$

and (spinor) QED

$$\mathcal{A}_i(u_1) = \mathcal{A}_j(u_2) \exp \left[ \frac{\alpha\omega^2}{1260\pi m^4} (25\dot{R}_{uu}(u_1)\delta_{ij} - 6\dot{R}_{iuju}(u_1) - 25\dot{R}_{uu}(u_2)\delta_{ij} + 6\dot{R}_{iuju}(u_2)) \right]. \quad (\text{A.5})$$



## Appendix B: Penrose limit and de Sitter space

A key element of our analysis of field propagation in curved spacetimes has been the simplification brought about by the Penrose limit. It is remarkable that a highly non-trivial validation of this method can be found using the symmetric plane waves of the third type considered in section 6.

To see this, consider the spacetime  $dS_3 \times \mathbb{R}$ , with metric

$$ds^2 = -dt^2 + \cosh^2(\alpha t) (d\theta^2 + \sin^2 \theta d\phi^2) + dz^2, \quad (\text{B.1})$$

The three-dimensional de Sitter space metric is given in global coordinates where  $(\theta, \phi)$  are the coordinates on  $S^2$ . A congruence of null geodesics consists of  $t = z$  with  $\theta = \theta_0$  and  $\phi = \phi_0$  fixed. The associated null coordinates are

$$u = \frac{1}{\sqrt{2}}(z + t), \quad v = \frac{1}{\sqrt{2}}(z - t). \quad (\text{B.2})$$

The Penrose limit is now trivial to take: we identify  $x^1 = \theta - \theta_0$  and  $x^2 = \sin^{-2}(\theta_0)(\phi - \phi_0)$  and expand in powers of  $v$  and  $x^a$  keeping terms of order 2 with  $v$  having weight 2 and  $x^a$  weight 1:

$$ds^2 \Big|_{\text{Penrose limit}} = 2du dv + \cosh^2(\sigma u) dx^a dx^a. \quad (\text{B.3})$$

with  $\sigma = (\sqrt{2}\alpha)^{-1}$ . In this case, the Penrose limit is the symmetric plane wave of the ‘wrong sign’ kind with  $\sigma_1 = \sigma_2 = i\sigma$ . This geometry violates the null energy condition since in Brinkmann coordinates  $R_{uu} = -2\sigma^2 < 0$ , but we can nevertheless consider this, as in section 6, as a valid fixed background.

The remarkable feature that allows the test of the Penrose limit method is that the Green functions and spectral density are known exactly in this case for the original spacetime  $dS_3 \times \mathbb{R}$ , as well as its symmetric plane wave Penrose limit, due to the high degree of symmetry of the de Sitter space. In particular, the Green functions admit a Källén-Lehmann representations from which the spectral density  $\rho(M)$  can be extracted. In the limit  $M \rightarrow 0$ , we will show how this exact result reproduces the spectral density (6.34) already found in the plane wave background.

Using the notation of [38, 39], the Källén-Lehmann representation is

$$\tilde{G}_+(\nu; \tilde{x}, \tilde{x}') \tilde{G}_+(\mu; \tilde{x}, \tilde{x}') = \alpha^{-1} \int_0^\infty d\kappa^2 \rho_{\nu,\mu}(\kappa) \tilde{G}_+(\kappa; \tilde{x}, \tilde{x}'). \quad (\text{B.4})$$

Here,  $\tilde{G}_+(\nu; \tilde{x}, \tilde{x}')$  is the Wightman function and for a (minimally-coupled) field of mass  $m$

$$\nu^2 = \frac{m^2}{2\sigma^2} - 1, \quad (\text{B.5})$$

where  $\tilde{x}$  are coordinates on  $dS_3$ . The Källén-Lehmann weight-function for three-dimensional de Sitter space is explicitly<sup>19</sup>

$$\rho_{\nu,\mu}(\kappa) = \frac{\sinh^2(\pi\kappa)}{2^5 \pi \kappa \cosh \frac{\pi(\kappa+\nu+\mu)}{2} \cosh \frac{\pi(\kappa-\nu+\mu)}{2} \cosh \frac{\pi(\kappa+\nu-\mu)}{2} \cosh \frac{\pi(\kappa-\nu-\mu)}{2}}. \quad (\text{B.6})$$

The Green functions for a field of mass  $m$  on the product space  $dS_3 \times \mathbb{R}$  follows in a simply way by noticing that momentum along the  $z$  direction acts as an effective contribution to the three-dimensional de Sitter mass. Splitting the coordinates as  $x = (z, \tilde{x})$ , we have

$$G_+^{(m)}(x, x') = \int \frac{dp}{2\pi} e^{ip(z-z')} \tilde{G}_+(\sqrt{\frac{m^2+p^2}{2\sigma^2} - 1}; \tilde{x}, \tilde{x}'). \quad (\text{B.7})$$

Taking the Fourier transform along the  $z$  direction, we have

$$G_+^{(m)}(p; \tilde{x}, \tilde{x}') = \tilde{G}_+(\sqrt{\frac{m^2+p^2}{2\sigma^2} - 1}; \tilde{x}, \tilde{x}'). \quad (\text{B.8})$$

The vacuum polarization for the scalar  $A\phi^2$  theory is

$$\Pi(x, x') = ie^2 G_+^{(m)}(x, x')^2. \quad (\text{B.9})$$

Using the Källén-Lehmann representation for  $dS_3$  in (B.4), we therefore find

$$\begin{aligned} \int dz e^{-ip(z-z')} \Sigma(x, x') &= e^2 \int \frac{dq}{2\pi} G_+^{(m)}(q; \tilde{x}, \tilde{x}') G_+^{(m)}(p-q; \tilde{x}, \tilde{x}') \\ &= \int_0^\infty dM^2 \rho(M) G_+^{(M)}(p; \tilde{x}, \tilde{x}'), \end{aligned} \quad (\text{B.10})$$

where the weight function is

$$\rho(M) = \frac{e^2}{\sqrt{2}\sigma} \int \frac{dq}{2\pi} \rho_{\nu,\mu}(\kappa), \quad (\text{B.11})$$

with

$$\nu^2 = \frac{m^2 + q^2}{2\sigma^2} - 1, \quad \mu^2 = \frac{m^2 + (p-q)^2}{2\sigma^2} - 1, \quad \kappa^2 = \frac{M^2 + p^2}{2\sigma^2} - 1. \quad (\text{B.12})$$

---

<sup>19</sup>This follows directly from equations (4) and (38) of [39].

In particular,  $\rho(M)$  is precisely the spectral density for the vacuum polarization on  $dS_3 \times \mathbb{R}$  and the decay rate for  $A \rightarrow \phi\phi$ , for massless  $A$ , is given by  $\frac{\pi}{\omega}\rho(0)$ .

Now we carefully take the “geometric optics” and “weak curvature” limits described in section 2.1, which led to the use of the Penrose limit. First of all, we identify the external momentum as  $p = \frac{\omega}{\sqrt{2}}$ , where  $\omega$  is the light-cone momentum. In the geometric optics limit, due to the form of the function  $\tilde{\rho}_{\nu,\mu}(\kappa)$ , the integrand in (B.11) only has support in the neighbourhood of  $q = \frac{p}{2}$ , *i.e.* where the external momentum is shared equally by the two particles in the final state. Consequently the arguments of all the hyperbolic functions in (B.6), except the one involving  $\kappa - \nu - \mu$ , are large and therefore may be replaced by exponentials. This means we can approximate

$$\rho_{\nu,\mu}(\kappa) \simeq \frac{1}{2^3 \pi \kappa (1 + e^{\pi(\nu+\mu-\kappa)})} . \quad (\text{B.13})$$

In particular, we can parameterize  $q = \frac{\omega\xi}{\sqrt{2}}$  and restrict the  $\xi$  integral to the interval  $[0, 1]$  and then expand for large  $\omega$

$$\begin{aligned} \nu + \mu - \kappa &= \frac{\omega}{2\sigma} (\xi + (1 - \xi) - 1) + \frac{m^2}{2\omega\sigma\xi(1 - \xi)} + \dots \\ &= \frac{m^2}{2\omega\sigma\xi(1 - \xi)} + \dots . \end{aligned} \quad (\text{B.14})$$

It is important for the validity of these expansions that the support of the integrand lies away from the points  $\xi = 0, 1$ . Finally, putting all this together gives the spectral density at  $M = 0$ :

$$\rho(0) = \frac{e^2}{(4\pi)^2} \int_0^1 d\xi \frac{1}{1 + e^{\frac{\pi m^2}{2\omega\sigma\xi(1-\xi)}}} . \quad (\text{B.15})$$

This is precisely equal to (6.34) for  $M = 0$ . This confirms that the results we have obtained directly from the Penrose limit spacetimes are indeed the correct approximations to those of the full background spacetime when we impose the physically-motivated conditions described in section 2.

## References

- [1] T. J. Hollowood and G. M. Shore, Phys. Lett. B **655** (2007) 67 [arXiv:0707.2302 [hep-th]].
- [2] T. J. Hollowood and G. M. Shore, Nucl. Phys. B **795** (2008) 138 [arXiv:0707.2303 [hep-th]].
- [3] T. J. Hollowood and G. M. Shore, JHEP **0812** (2008) 091 [arXiv:0806.1019 [hep-th]].
- [4] T. J. Hollowood, G. M. Shore and R. J. Stanley, JHEP **0908** (2009) 089 [arXiv:0905.0771 [hep-th]].
- [5] T. J. Hollowood and G. M. Shore, Phys. Lett. B **691** (2010) 279 [arXiv:1006.0145 [hep-th]].
- [6] G. M. Shore, Nucl. Phys. B **460** (1996) 379 [arXiv:gr-qc/9504041].
- [7] G. M. Shore, “*Causality and Superluminal Light*”, in ‘Time and Matter’, Proceedings of the International Colloquium on the Science of Time, ed. I. Bigi and M. Faessler, World Scientific, Singapore, 2006. [arXiv:gr-qc/0302116].
- [8] G. M. Shore, Contemp. Phys. **44** (2003) 503 [arXiv:gr-qc/0304059].
- [9] G. M. Shore, Nucl. Phys. B **778** (2007) 219 [arXiv:hep-th/0701185].
- [10] I. T. Drummond and S. J. Hathrell, Phys. Rev. D **22** (1980) 343.
- [11] R. Penrose, “*Any space-time has a plane wave as a limit*”, in: Differential geometry and relativity, Reidel and Dordrecht (1976), 271-275.
- [12] M. Blau, M. Borunda, M. O’Loughlin, G. Papadopoulos, JHEP **0407** (2004) 068. [hep-th/0403252].
- [13] M. Blau, D. Frank and S. Weiss, Class. Quant. Grav. **23** (2006) 3993 [arXiv:hep-th/0603109].
- [14] J. Schwinger, J. Math. Phys. **2** (1961) 407.
- [15] K. T. Mahanthappa, Phys. Rev. **126** (1962) 329.
- [16] L. V. Keldysh, JETP **41** (1965) 1018.
- [17] S. Weinberg, Phys. Rev. D **72** (2005) 043514 [arXiv:hep-th/0506236].
- [18] D. Boyanovsky and H. J. de Vega, Annals Phys. **307** (2003) 335 [arXiv:hep-ph/0302055].
- [19] M. Cahen and N. Wallach, Bull. Am. Math. Soc. **76** (1970) 585-591.
- [20] D. Boyanovsky, R. Holman and S. Prem Kumar, Phys. Rev. D **56** (1997) 1958 [arXiv:hep-ph/9606208].
- [21] D. Boyanovsky, H. J. de Vega, Phys. Rev. **D70** (2004) 063508. [astro-ph/0406287].

- [22] D. Boyanovsky, H. J. de Vega, N. G. Sanchez, Phys. Rev. **D71** (2005) 023509. [astro-ph/0409406].
- [23] M. Blau, J. M. Figueroa-O’Farrill, C. Hull and G. Papadopoulos, JHEP **0201** (2002) 047 [arXiv:hep-th/0110242].
- [24] M. Blau, J. M. Figueroa-O’Farrill, C. Hull and G. Papadopoulos, Class. Quant. Grav. **19** (2002) L87 [arXiv:hep-th/0201081].
- [25] J. C. Plefka, “Lectures on the plane wave string / gauge theory duality,” Fortsch. Phys. **52** (2004) 264 [arXiv:hep-th/0307101].
- [26] G. W. Gibbons, Commun. Math. Phys. **45** (1975) 191.
- [27] D. Brecher, J. P. Gregory, P. M. Saffin, Phys. Rev. **D67** (2003) 045014. [hep-th/0210308].
- [28] D. Marolf, L. A. Pando Zayas, JHEP **0301** (2003) 076. [arXiv:hep-th/0210309 [hep-th]].
- [29] J. A. Hutasoit, S. P. Kumar and J. Rafferty, JHEP **0904** (2009) 063 [arXiv:0902.1658 [hep-th]].
- [30] R. D. Jordan, Phys. Rev. D **33** (1986) 444.
- [31] E. Calzetta and B. L. Hu, Phys. Rev. D **35** (1987) 495.
- [32] E. Calzetta, B. L. Hu, Phys. Rev. **D40** (1989) 656-659.
- [33] A. Mironov, A. Morozov and T. N. Tomaras, arXiv:1108.2821 [gr-qc].
- [34] P. Szekeres and V. Iyer, Phys. Rev. D **47** (1993) 4362.
- [35] M.N. Celerier and P. Szekeres, Phys. Rev. D **65** (2002) 123516 [arXiv:gr-qc/0203094].
- [36] O. Nachtmann. Osterr. Akad. Wiss., Math.-Naturw. Kl., Abt. II **176** (1968) 363.
- [37] N. P. Myhrvold, Phys. Rev. D **28** (1983) 2439.
- [38] J. Bros, H. Epstein and U. Moschella, arXiv:0812.3513 [hep-th].
- [39] J. Bros, H. Epstein, M. Gaudin, U. Moschella and V. Pasquier, arXiv:0901.4223 [hep-th].